ALTERNATE COMPUTER MODELS OF FIRE CONVECTION PHENOMENA FOR THE HARVARD COMPUTER FIRE CODE

by Douglas K. Beller

A Thesis
Submitted to the Faculty
of the
WORCESTER POLYTECHNIC INSTITUTE
in partial fulfillment of the requirements for the
Degree of Master of Science
in
Fire Protection Engineering
by

Douglas K Beller

August 1987

APPROVED:

Dr. Craig L. Beyler, major Advisor

Prof. David A. Lucht, Director, Center for Firesafety Studies

ABSTRACT

Alternate models for extended ceiling convection heat transfer and ceiling vent mass flow for use in the Harvard Computer fire Code are developed. These models differ from current subroutines in that they explicitly consider the ceiling jet resulting from the fire plume of a burning object. The Harvard Computer fire Code (CFC) was used to compare the alternate models against the models currently used in CFC at Worcester Polytechnic Institute and with other available data. The results indicate that convection heat transfer to the ceiling of the enclosure containing the fire may have been previously underestimated at times early in the fire. Also, the results of the ceiling vent model provide new insight into ceiling vent phenomena and how ceiling vents can be modeled given sufficient experimental data. this effort serves as a qualitative verification of the models as implemented; complete quantitative verification requires further experimentation. Recommendations are also included so that these alternate models may be enhanced further.

ACKNOWLEDGEMENTS

I would like to thank my advisors: Prof. W. H. Kistler for providing guidance concerning some of the more rigorous mathematics, Prof. B. J. Savilonis for helping me improve my "intuitive feel" for the phenomena being modeled, Prof. J. R. Barnett for helping me overcome program debugging problems and for useful information regarding CFC, and, my major advisor, Prof. C. L. Beyler for having that extra bit of knowledge and insight, into both the phenomena and the modeling, that added to the quality of this thesis.

I would also like to acknowledge the support of Gary Hartley and Sal Vella of General Dynamics' Electric Boat Division: without their support this project would have been that much more difficult.

Thanks are also extended to J. Muldoon, WPI computer center nighttime operator, for being that rare operator who is actually helpful.

And a very special thanks to Joanne for putting up with me for the duration of it all.

This work is dedicated to my parents, without whom which. . .

TABLE OF CONTENTS

TABLE OF CONTENTS (cont.)

TABLE OF CONTENTS (cont.)

TABLE OF CONTENTS (cont.)

LIST OF FIGURES

LIST OF FIGURES (cont.)

LIST OF FIGURES (cont.)

LIST OF TABLES

ALTERNATE COMPUTER MODELS FOR FIRE CONVECTION PHENOMENA

1.0) INTRODUCTION

Historically, modeling enclosure fires with computers has fallen into two categories: field models and zone models. Field models tend to be global in nature in that they explicitly consider all regions of space within the enclosure. This is accomplished by solving the equations of motion at a large number of points representing the space inside the enclosure. The heat transfer to the enclosure walls is also calculated at a number of points through the thickness of the wall. The exact number of points both for the space of the room and the walls, which comprise the mesh or grid, are determined in part by the problem at hand, part by available computational ability and part by user input. Field models can thus provide a fairly realistic representation of enclosure fire phenomena. However, the price to be paid for this realism is greatly increased computation time, which may be undesirable from a design or production point of view. Zone models, on the other hand, are not quite so time intensive because, instead of considering individual points within the enclosure, the enclosure is modeled as if it were a conglomeration of regions. In these models, a small number of regions is required and entails a control volume approach. Typically the number of regions is on the order of ten or less. In the

past these regions have consisted of the burning object (and any other target objects), the combustion zone and plume above the burning object, a lower gas layer and an upper gas layer. However, zone models are typically referred to as two-zone models; i.e., the upper and lower gas layers are the two zones of interest.

1.1) DISCUSSION

The implication of a two-zone enclosure fire model is that the hot, upper and cold, lower layers are homogeneous, i.e., assumed to be well-mixed and of a uniform temperature. Both assumptions are probably more valid for the lower layer than for the upper layer, especially early in the fire (see Fig. 1.1(A), Ref. 14). The upper layer, prior to flashover, has different zones of mixing and exhibits thermal stratification (see Fig. 1.1(B), Ref. 14) as well as radial temperature variations. However, the upper layer as presently modeled does not account for the dynamics associated with the upper part of the fire plume and the resultant ceiling jet, which causes some of these nonhomogenous effects. The ceiling jet is significant for the following reasons: the convective heat transfer between the extended ceiling of the enclosure and the ceiling jet can be a significant fraction of the fire's total heat release (especially during the early stages of the fire) and because the mass flow rate out of a ceiling vent or wall

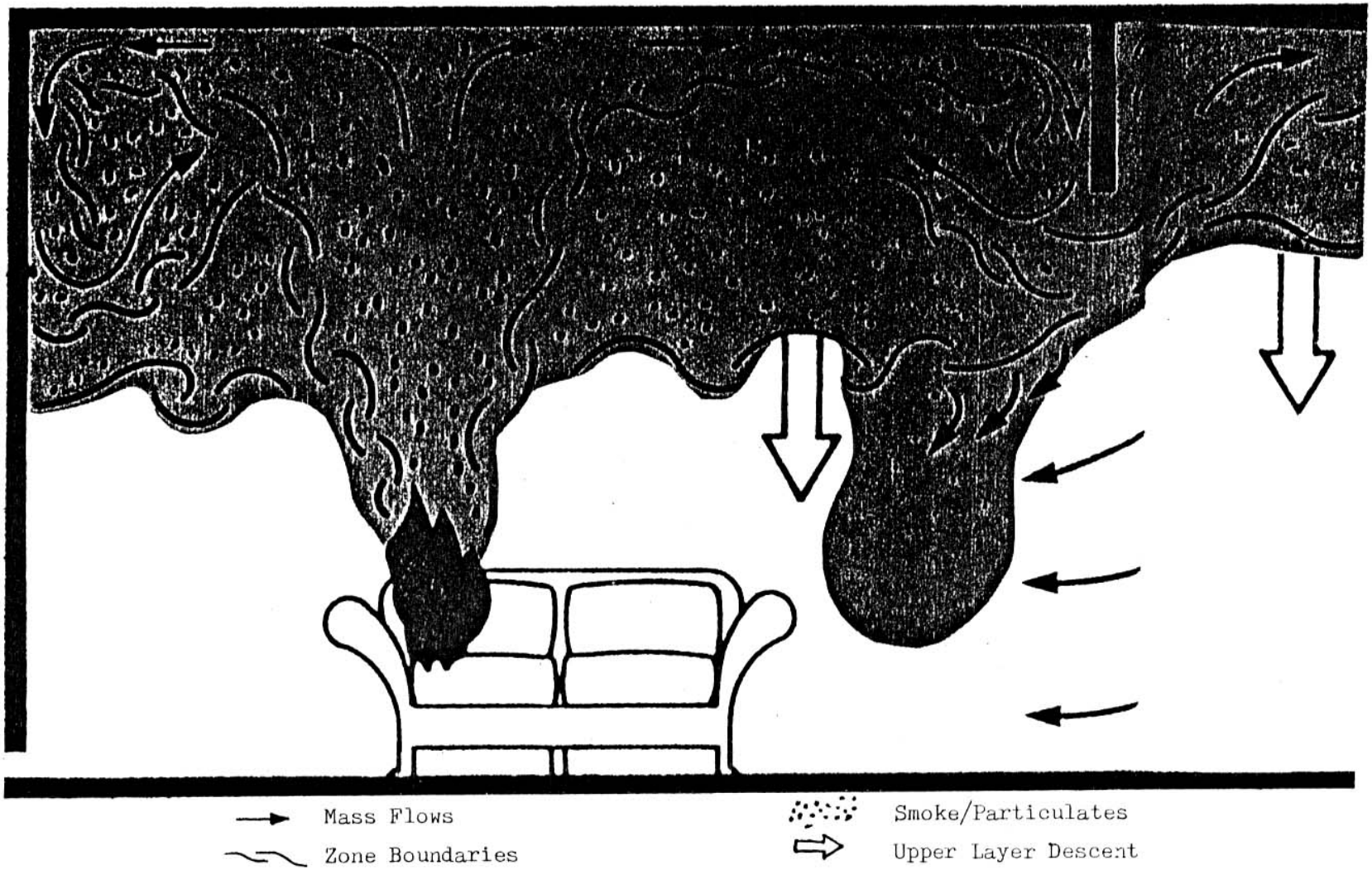

Figure 1.1(A) Fire Transport Phenomena: Room w/ Open Door (Ref. 15)

Figure 1.1(B)

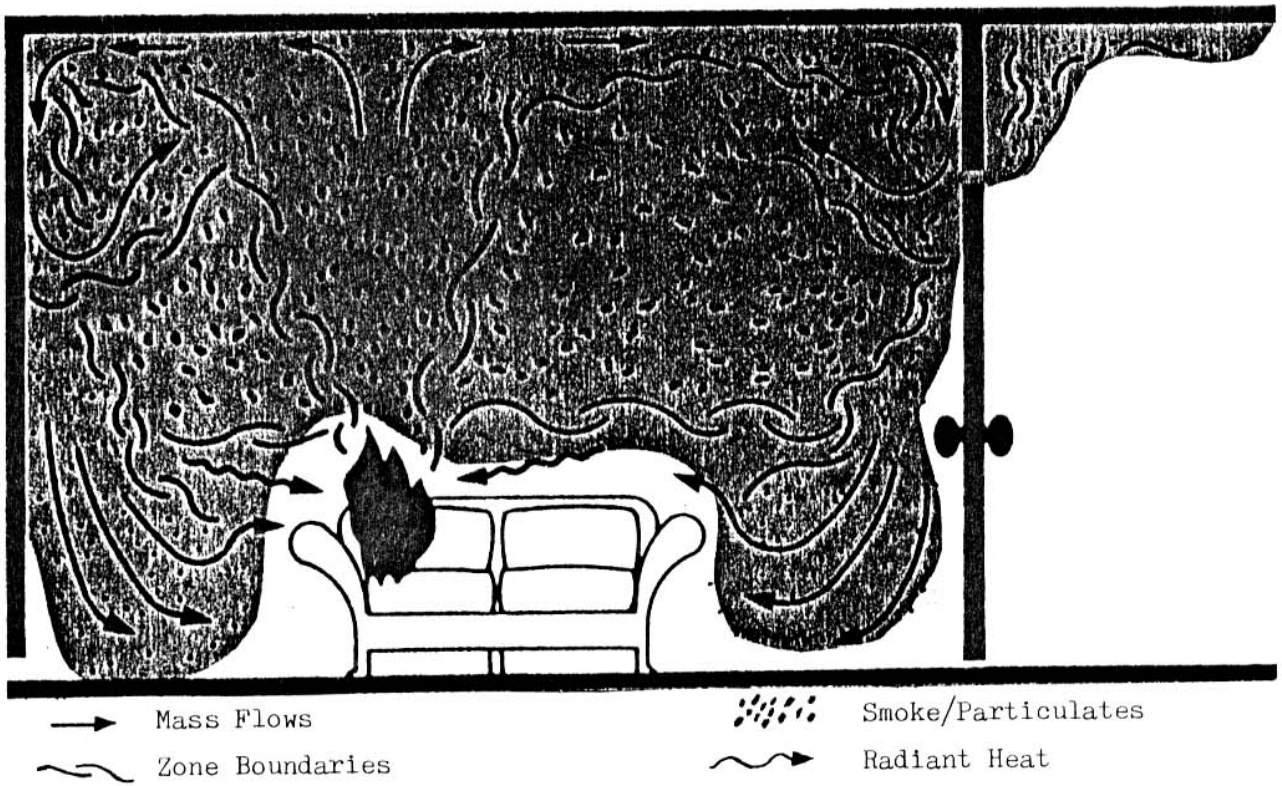

Fire Transport Phenomena: Nearly Closed Room (Ref. 15)

vent with a small soffit depth may be significantly affected by the momentum of the ceiling jet. The alternative models described herein attempt to overcome these inadequacies

1.2) PURPOSE

The purpose of this endeavor is to provide a description of alternate computer models characterizing extended ceiling convection heat transfer (ECCHTX) and ceiling vent mass flow rate (CVMFR) which consider the existence of a plume and ceiling jet in their formulation.

Essentially, these are two different models, describing different phenomena, which can be used alone or together and which also share several subroutines. The extended ceiling is defined to be those enclosure surfaces exposed to the hot upper layer gases. As such these alternate models represent a departure from current modeling techniques. The ceiling jet is produced by the impingement of the fire plume on the ceiling. In existing models the fire plume is assumed to be "cut off" at the interface between the upper and lower layers within the enclosure. With this assumption, certain aspects of ECCHTX and CVMFR are not included. The alternative models discussed here are an attempt to alleviate some of the restrictions imposed by cutting off the fire plume at the layer interface.

The alternate models described herein have been

incorporated into the Worcester Polytechnic Institute (WPI) version of the Computer Fire Code (CFC). This program was originally developed at Harvard University, and described in Ref. 16.

2.0) EXTENDED CEILING CONVECTION HEAT TRANSFER

In order to fully appreciate the differences between the alternate model and those currently employed, a brief description of the existing model, along with the assumptions upon which it is based, is presented next. This section also discusses some of the shortcomings of the existing models and suggests improvements to overcome them. Section 2.2 is a description of some of the models available which were considered as a possible basis for an alternative to the existing model. And finally, a more complete description of the alternate model which was actually implemented is discussed in Sect. 2.3. A description of the subroutines this model requires is included in Sect. 2.4.

2.1) CURRENT CFC MODEL

The extended ceiling convection heat transfer (ECCHTX) model currently used by CFC assumes that the ECCHTX is a function of uniform extended ceiling surface temperature, instantaneous upper layer temperature, and a heat transfer coefficient. This heat transfer coefficient is defined as (Ref. 16):

$$h = \min\left[50, 5 + \frac{(50 - 5)\,(T_L - T_A)}{100}\right] \; (W/m - K)$$

In other words, the heat transfer coefficient has a minimum value of 5 W/m-K and rises linearly with temperature over

a temperature rise of 100K up to 50W/m-K; T_L is the upper layer temperature and T_A is the ambient temperature. These two values (5 and 50) are used as the max/min values of the heat transfer coefficient used as input by CFC. Therefore, these values can be user defined.

In view of our latest understanding of enclosure fires, the existing model is inadequate in several ways. First of all, although not stated above, the instantaneous upper layer temperature is assumed to be uniform throughout the layer. This is not necessarily the case due to the presence of the fire plume and the resultant ceiling jet. Indeed, the ceiling jet will exhibit a radial temperature distribution (decreasing with increasing distance from the fire plume axis). Also, it is this ceiling jet which would tend to drive the convection heat transfer to the ceiling more than the uniform hot layer temperature. Furthermore, the extended ceiling surface temperature will not be uniform since it is induced by the impingement of the plume on the ceiling and the resultant ceiling jet. Specifically, the ceiling surface will exhibit a radial temperature distribution while the surface temperature distribution of the portion of the wall exposed to hot gases will be monotonically decreasing with increased distance from the ceiling. Therefore, both the adjacent surface gas temperature and the extended ceiling surface temperature are functions of distance from the plume axis and the

model should incorporate this phenomena. While it is true that the heat transfer coefficient is an indirect function of temperature, it seems likely that it is a stronger function of the velocity of the gases adjacent to the ceiling surface and the radial distance from the plume axis. The observed behavior of fire plumes impinging on ceilings has been: high radial gas velocities near the ceiling impingement point which decrease as the jet approaches the enclosure walls. In view of this, the alternate model should be based on (at least) a spatially dependent heat transfer coefficient. Optimally the ECCHTX model should also incorporate the phenomena detailed above and have provision for: convective heat transfer to the entire ceiling and all parts of the heated wall, upper layer effects (i.e., increased ambient temperatures), disruption of the ceiling jet (and, therefore, a change in ECCHTX) due to increased hot layer turbulence attributable to an open ceiling vent or other obstructions, and the (presumed) increase in ECCHTX due to more than one burning object. However, the state-of-the-art does not allow the formulation of such a complete model: therefore, the intent is to provide as comprehensive model as our current understanding allows.

2.2) AVAILABLE MODELS

Reference 2 provides a review of available ceiling jet and ceiling heat transfer models. From that reference, the following models were considered: Alpert (Ref. 1), Cooper (Ref. 5), Evans (Ref. 9), Heskestad and Delichatsios (Ref.

11), and You and Faeth (Ref. 18). Of these, References 5, 9 and 18 are for ceiling convection heat transfer, while 1 and 11 are for ceiling jets (i.e., from which an ECCHTX model could subsequently be developed).

Alpert (Ref. 1) is concerned with the actuation of fire detectors, which may or may not be suitable for an alternate ECCHTX model. His model has the limitation of being unable to account for the heated portion of the wall. Therefore, Alpert's model will not be considered as an alternate ECCHTX model.

Cooper (Ref. 5 and 7) devises a method to calculate the heat transfer to the entire ceiling as well as the heated part of the walls (Ref. 8) which is based on data accumulated from the available literature. Cooper also considers the effect of the hot upper layer, which results from confined ceilings, by preserving the average temperature of the plume and the mass flux across the layer interface.

Evans (Ref. 9) is also interested in detector actuation. He modifies Cooper's method by maintaining the plume width and gas velocity to develop the correlations for hot layer effects. These variables are less important than those considered by Cooper when modeling ECCHTX and thus Evans' method will not be considered.

Upon initial inspection, the model of Heskestad and Delichatsios (Ref. 11) appears to be adequate: it is an experimental validation of the modeling relations for convective flow generated by "power-law" fires and it applies to the entire ceiling. However, it does not consider heat transfer to the heated parts of the walls nor does it apply to the general fire case. Therefore, the Ref. 11 formulation is not considered.

The model of You and Faeth (Ref. 18) is also a heat transfer model which applies to the entire ceiling. However, it does not explicitly account for hot layer effects or heat transfer to the heated part of the walls.

After weighing the advantages and disadvantages, Cooper's model was chosen as the basis for the alternate ECCHTX model. It should be pointed out that the choice of Cooper's model is somewhat pragmatic and not necessarily optimal in all aspects. There are three components to consider: ceiling jet flow, ceiling jet heat transfer and hot layer effects. Conceivably each of these components could be provided by three different sources and then combined into the desired model. This approach was thought to be unnecessary since Cooper's model already combines these three components into a single, comprehensive whole. Thus the problem of developing consistent interfaces between the individual, and possibly disparate, components is

avoided. No improvements to Cooper's basic formulation were discerned.

2.3) ALTERNATE MODEL

The model proposed by Cooper in Refs. 5, 7, and 8 was chosen as the basis for an alternate ECCHTX model since it fulfills most of the requirements previously stated. The original model of Ref. 5 was revised and enhanced in Ref. 7 and 8. These second two references serve to expand the geometric applicability of the model and to incorporate heated wall heat transfer. Therefore, this model has the advantage of calculating the heat transfer to all points on the ceiling as well as to the heated walls. Cooper also includes the effect of the hot upper layer which results from confined ceilings. In this context, confined is defined to mean that the enclosure is small enough such that a hot upper layer will form. Alternately the enclosure could be so large that an appreciable upper layer may not form. Cooper's model is based on the review of other researcher's experiments. This is not to be construed as a shortcoming, however, since Ref. 2 states that even though Cooper did not include the data of Heskestad and Delichatsios (Ref. 11), i.e., the correlation recommended in Ref. 2, his correlations "are in good agreement" with the data of Ref. 11.

This alternate ECCHTX model is broken into two parts: one for the convection heat transfer to the ceiling proper and one for the convection to the heated portion of the wall, i.e., wall area covered by the hot, upper layer. Ref. 5 and 7 will provide the basis for the former and Ref. 8 for the latter. These models are described in Sect. 2.3-2 and 2.3-3. The next section details the assumptions required by the model.

2.3-1 ASSUMPTIONS

This model requires several assumptions. Most of these assumptions are made to simplify the modeling and/or programming and all are subject to change pending available experimental data. The assumptions for the ECCHTX model are:

1) Model is applicable to smooth ceilings only. This assumption eliminates any ceiling jet flow changes due to open ceiling vents and ceiling obstructions. This may decrease the model's applicability. However, for the purpose of this model, if the model is in effect, then the ceiling jet is also present.

2) The flame axis is the geometrical center of horizontally burning objects and is not affected by ambient conditions, i.e., it does not migrate in the presence of wind or drafts
caused by ventilation systems.

3) When more than one object is burning, only the object with the highest heat release rate is considered, i.e., contributions of smaller fires are assumed insignificant. (Note: As described in a later section, this assumption may neglect the geometry of the scenario if the object with the highest heat release rate is not the initially burning object.) If this assumption is not made, then the interaction of individual plumes would determine the ceiling jet characteristics. This interaction has not been studied to date so that no information exists as to how it should be modeled. This is a gross oversimplification and requires further investigation.

4) To simplify the programming, an equivalent vent radius is needed to locate the ceiling vent relative to the fire plume axis.

5) No definition has been supplied for the layer depth at which increased ambient temperatures should be considered to be significant, as discussed in Sect. 2.1 and 2.3-2(A). Therefore, this "significant" layer depth is assumed to be

twice the ceiling jet thickness or 0.24 times the floor to ceiling height. This is an arbitrary choice as to "significant" fraction of room height (see page 30 of Ref. 17 for this definition of ceiling jet thickness = 0.12 times the floor-to-ceiling height). Presumably the value of "significant" fraction of room height is critical to the subsequent computer output and its effect should be more extensively investigated.

6) Radial temperature gradients of the problem are assumed to be small enough so that in the ceiling is quasi-one dimensional in space, i.e., the in-depth ceiling coordinate (Ref. 6).

2.3-2 CEILING PROPER

From Ref. 7, the ceiling convection heat flux can be estimated by:

Eq. 2.3-2

$$\dot{q}''c = h(T_{ad} - T_s)$$

where T_{ad} is the gas temperature distribution at the surface of an adiabatic ceiling established by the ceiling jet flow from the plume of a given fire with a given fire-to-ceiling distance; T_s is the instantaneous lower (i.e., exposed)

surface ceiling temperature distribution; and h is the heat transfer coefficient based on the (T_{ad} - T_s) temperature difference. All three of these parameters must be modeled in order for this model to be consistent and complete.

This formulation was originally developed for confined ceiling scenarios by Cooper in Ref. 5. However, the basis for that work is supplied by Ref. 4. In Ref. 4 Cooper incorporated the work of several researchers investigating heated turbulent ceiling jet flows and unheated turbulent wall jets into a model describing the scenario of Fig. 2.3-2(A). This was accomplished by modeling the fire's combustion zone as a point source of energy and by drawing equivalence between the momentum and mass fluxes of the free jet and of a buoyant plume at the position of their respective impingement with the ceiling surface (Ref. 4). The resultant model consisted of correlations for T_{ad} and h as functions of fire parameters and a geometric parameter, r/H, where r is the radial distance from fire plume axis and H is the plume source-to-ceiling distance.

Figure 2.3-2(A) depicts the scenario near the plume axis at early times in the fire or at later times for large, expansive ceilings. If vertical surfaces are sufficiently distant (i.e., expansive smooth ceiling with large r/H), then the ceiling jet loses most of its momentum far out in its trajectory. However, if the enclosure has a low aspect

Figure 2.3-2(A)

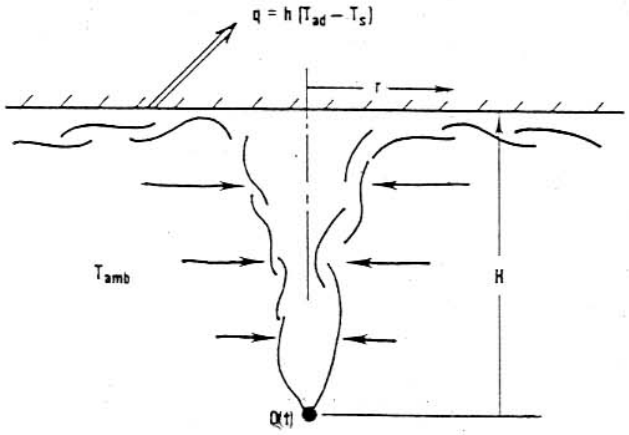

Heat transfer to an unconfined ceiling.

(Ref. 4)

Figure 2.3-2(B)

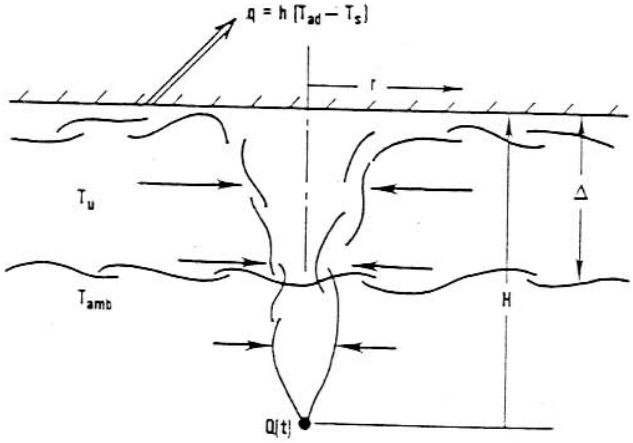

Heat transfer to a confined ceiling with an upper layer.

(Ref. 4)

ratio, then the ceiling jet flow is blocked by the bounding vertical surfaces (i.e., walls) and forms a downward overturning wall jet flow which is eventually turned back inward and upward by its own buoyancy (Ref. 5), see Fig. 1.1-(A), 1-1(B), and 2.3-3(A). The blocked ceiling jet gases eventually redistribute themselves horizontally across the cross section of the enclosure. This tends to form a relatively quiescent, stably stratified upper layer, below the ceiling jet (Ref. 4), which also defines the layer interface. This layer interface defines the demarcation between the cooler, ambient air below and the hotter products of combustion and entrained air above. This layer interface drops with increasing time, see Fig. 1.1(A), while the average absolute temperature, T_u, of the upper layer rises with time, i.e., as the fire continues to burn. Figure 2.3-2(B) depicts the near plume scenario as just discussed. Therefore, in Ref. 5 Cooper reformulates the Ref. 4 correlations to account for Fig. 2.3-2(B) scenario, i.e., to account for hot, upper layer effects.

2.3-2(A) HEAT TRANSFER COEFFICIENT

The formulation for the heat transfer coefficient used in the alternate ECCHTX model was originally developed in Ref. 4 for unconfined ceiling scenarios. Heat transfer

coefficient data from several researchers were curve fit using a least squares approach. The resultant formulation is a function of r/H for the heat transfer coefficient. Also, in order to incorporate the data from wall jet heat transfer measurements with that from plume driven heat transfer measurements, an equivalence between these two phenomena was required. A relationship was established between the measured properties of a wall jet and the properties of its equivalent buoyant plume at their respective points of impingement (Ref. 4) by developing an equivalent Reynolds number. This equivalent Reynolds number, Re_H, differs from the traditional formulation by a constant, if Re_H is cast in terms of the fire heat release rate and the plume source-to-ceiling distance as presented below. As stated previously, Ref. 5 enhanced the Ref. 4 model by including hot layer effects. In Ref. 7 Cooper and Woodhouse increased the range of r/H to 2.2 for which the Ref. 5 correlations are applicable.

The heat transfer coefficient, h, is defined by Eq. 6, Ref. 7 to be:

Eq. 2.3-2(A)1a

$$\frac{h}{\tilde{h}} \begin{cases} \{8.82 Re_H^{-1/2} Pr^{-2/3}[1 - (5 - 0.284 Re_H 0.2)(r/H)], 0 \le (r/H) \le 0.2 \\ 0.283\, Re_H^{-0.3}\, Pr^{-2/3} (r/H)^{-1.2} \dfrac{(r/H - 0.0771)}{(r/H + 0.279)}, 0.2 \le (r/H) \end{cases}$$

where: $\tilde{h} = \rho_{amb} c_{pg}^{1/2} H^{1/2} Q_H^* \dfrac{1}{3}$

$$Re_H = (g^{1/2} H^{3/2} Q_H^* \frac{1}{3}) / \nu$$

$$Q_H^* = (1 - \lambda_r)\dot{Q} / (\rho_{amb} c_p T_{amb} g^{1/2} H^{5/2})$$

ρ_{amb} = ambient density

c_p = ambient specific heat

T_{amb} = " temperature

ν = " kinematic viscosity

Pr = Prandtl number = 0.7

g = acceleration of gravity

H = plume source-to-ceiling distance

r = distance from fire plume axis

$\dot{Q}$ = energy release rate of the fire

λ_r = fraction of Q lost by radiation

Note: since CFC does not currently calculate λ_r, coding is included to calculate it as the radiant energy loss of the flames divided by the energy release rate of the fire (TEPZR / TEOZZ) and is calculated every time step.

As the fire progresses, the upper layer depth increases and the phenomena governing the heat transfer becomes more complex. From Fig. 2.3-2(B), two additional parameters are required, T_u and Δ (upper layer thickness) (Ref. 4). In Ref. 5 Cooper develops the correction factors that allow the Ref. 4 formulations to be used for the scenarios shown in Fig. 2.3-2(B). In this scenario, the temperature of the gases entrained by the plume above the interface is greater than that of the gas entrained below the interface. Cooper submits "that once the depth of the upper layer becomes a significant fraction of H (room height)...the impact of the

now elevated upper layer temperatures on the temperature and mass flux of the upper portion of the plume will also be significant" (Ref. 5). However, Cooper does not define "significant fraction". Thus, when assumption five of Sect. 2.3-1 holds, the ambient environment will be the hot upper layer, not that outside the room. Three correction factors are calculated to account for elevated upper layer temperatures: T_u/T_{amb}, and the two factors defined by Eq. 2.3-2(A)2 and 2.3-2(A)3. Therefore, h is modified as per Ref. 5 as follows:

Eq. 2.3-2(A)1b

$$\frac{h'}{\tilde{h}'} \begin{cases} \{8.82 Re_{H'}^{-1/2} Pr^{-2/3} [1 - (5 - 0.284 Re_{H'}^{0.2})(r/H')], 0 \le (r/H') \le 0.2 \\ 0.283\, Re_{H'}^{-0.3}\, Pr^{-2/3} (r/H')^{-1.2} \dfrac{(r/H' - 0.0771)}{(r/H' + 0.279)}, 0.2 \le (r/H') \end{cases}$$

where: $\tilde{h}' = (H'/H)^{-1/3}(Q'/Q)^{1/3}(T_{amb}/T_u)\tilde{h}$ (Eq. 18, Ref. 5)

Eq. 2.3-2(A)2

$$\frac{H'}{H} = \frac{\Delta}{H} + \frac{(1 - (\Delta/H))(T_u/T_{amb})}{\left[\dfrac{0.201(1 - T_u/T_{amb})}{Q_{Zi}{}^{*2/3}} + 1\right]^{1/5}}$$ (Eq. 21, Ref. 5)

Eq. 2.3-2(A)3

$$\frac{Q'}{Q} = \frac{0.201(1 - T_u/T_{amb})}{Q_{Zi}{}^{*2/3}} + 1$$ (Eq. 22, Ref. 5)

Q_{Zi}* = Q* evaluated at interface elevation, Z_I

T_u = temperature of upper layer (K)

Δ = upper layer thickness

$$Re_{H'} = \frac{(H'/H)^{2/3}(Q'/Q)^{1/3}[(T_{amb}/T_u) + (110.4/T_{amb})]}{(T_u/T_{amb})^{5/2}(1 + 110.4/T_{amb})(1/Re_H)}$$

(Eq. 20, Ref. 5)

2.3-2(B) GAS TEMPERATURE

In addition to the heat transfer coefficient, Cooper also curve fit small scale buoyant plume driven ceiling jet experimental data (Ref. 4) to arrive at an expression for T_{ad}. This formulation was also enhanced in Ref. 5 and 7 as previously discussed. T_{ad} represents the maximum temperature possible for the times of interest. T_{ad} is determined by the characteristics of the plume immediately prior to impingement. In other words, the maximum gas temperature of the entire distribution is at the impingement point, and, therefore, all "downstream" temperatures are dependent on this temperature. The impingement point ceiling surface temperature is a function of the fire plume conditions just prior to impingement. The (T_{ad} - T_{amb}) temperature difference is a function of r/H and is shown in Eq. 2.3-2(B)1 and 2.3-2(B)2 The adiabatic gas temperature, T_{ad}, is defined by Eq. 9, Ref. 7:

Eq. 2.3-2(B)1a

$$\Delta T_{ad}^* = \begin{cases} 10.22 - 14.9(r/H), & 0 \le (r/H) \le 0.2 \\ 8.39f(r/H), & 0.2 \le (r/H) \end{cases}$$

where: $$\Delta T_{ad}^{*} = \frac{T_{ad} - T_{amb}}{T_{amb} Q_H^{*2/3}}$$

$Q_H^{*2/3}$ = Q* evaluated at H

Eq. 2.3-2(B)2

$$f(r/H) = \frac{1 - 1.1(r/H)^{0.8} + 0.808(r/H)^{1.6}}{1 - 1.1(r/H)^{0.8} + 2.2(r/H)^{1.6} + 0.69(r/H)^{2.4}}$$

(Eq. 7, Ref. 7)

As in Sect. 2.3-2(A), an increased temperature environment also affects the resultant gas (i.e., ceiling jet) temperature in a manner similar to the affect on the heat transfer coefficient. Therefore, correction factors are required when assumption five of Sect. 2.3-1 holds. These are the same correction factors discussed in Sect. 2.3-2(A). Tad is modified as per Ref. 5 as follows:

Eq. 2.3-2(B)1b

$$\Delta T_{ad}^{*'} = \begin{cases} 10.22 - 14.9(r/H'), 0 \le (r/H') \le 0.2 \\ 8.39 f(r/H'), 0.2 \le (r/H') \end{cases}$$

where: $$\Delta T_{ad}^{*'} = \frac{T_{ad}' - T_{amb}}{T_{amb} Q_H'^{*2/3}}$$

$$Q'H^{*} = (Q'/Q)(H'/H)^{5/2} Q_H^{*} \quad \text{(Eq. 19, Ref. 7)}$$

$f(r/H')$ = $f(r/H)$ evaluated at H'

2.3-2(C) SURFACE TEMPERATURE

The ceiling surface temperature for this model is calculated in a similar manner to what is currently done in CFC. The only difference is that, instead of only one bulk condition (i.e., one

surface temperature, one gas temperature, and one heat transfer coefficient), between, typically, three and ten local conditions may be used, depending on the
size of the room. The process for selecting these local points is discussed in Sect. 2.3-4(A) For further information, see subroutine TMPW01 as described in Ref. 16.

2.3-3 HEATED WALL

From Ref. 8, the heated wall convection heat flux can be estimated by:

Eq. 2.3-3:

$$\dot{q}'' = h(T_{ad} - T_w)$$

where T_{ad} is the gas temperature distribution adjacent to an adiabatic wall upon which a plane jet from an elevated temperature plume is impinging; T_w is the wall temperature which "would generally vary with position from the stagnation point" (Ref. 8); and h is the heat transfer coefficient at the stagnation point of the ceiling jet where it impinges on the wall and is equivalent to h_s. All three of these parameters must be modeled in order for this model to be consistent.

In Ref. 8, Cooper draws an analogy "between the flow dynamics and heat transfer at ceiling jet-wall impingement and at the line impingement of a wall and a two-dimensional, plane, free jet". To accomplish this, Cooper developed a correlation for Nusselt number,

based on the small scale, experimental plane jet impingement data he reviewed. In order to apply this (small scale) formulation to ceiling

jet-well impingement, i.e., by analogy, Cooper chose the distance from the jet's virtual origin, X, and the momentum flux per unit width, M_o', so that they simulate the ceiling jet flow immediately upstream of (i.e., near) the wall impingement point at r = D shown in Fig. 2.3-3(A). The results are some "readily available estimates for the heat transfer from, and the mass, momentum, and enthalpy fluxes of the turned compartment fire ceiling jet [i.e., downward wall jet] as it begins its initial descent as a negatively buoyant flow along the compartment wall" (Ref. 8). This is shown in Fig. 2.3-3(A) (Ref. 8). The "equivalence" method used in Ref. 8 is analogous to that used in Ref. 4 and is discussed briefly in Sect 2.3-2.

When the upper layer is a "significant fraction" (Sect. 2.3-2(A)) of the room height, two scenarios are possible, as shown in Fig. 2.3-3(B). The scenario shown in Fig. 2.3-3(B)1 is not considered in this alternate ECCHTX model. Instead, the negative wall flow is assumed to not penetrate the layer interface, as shown in Fig. 2.3-3(B)2. Also, the front of the negative wall flow is assumed to descend at the same rate as the layer interface. Thus, the heated wall area becomes the heat transfer area for the negative wall flow.

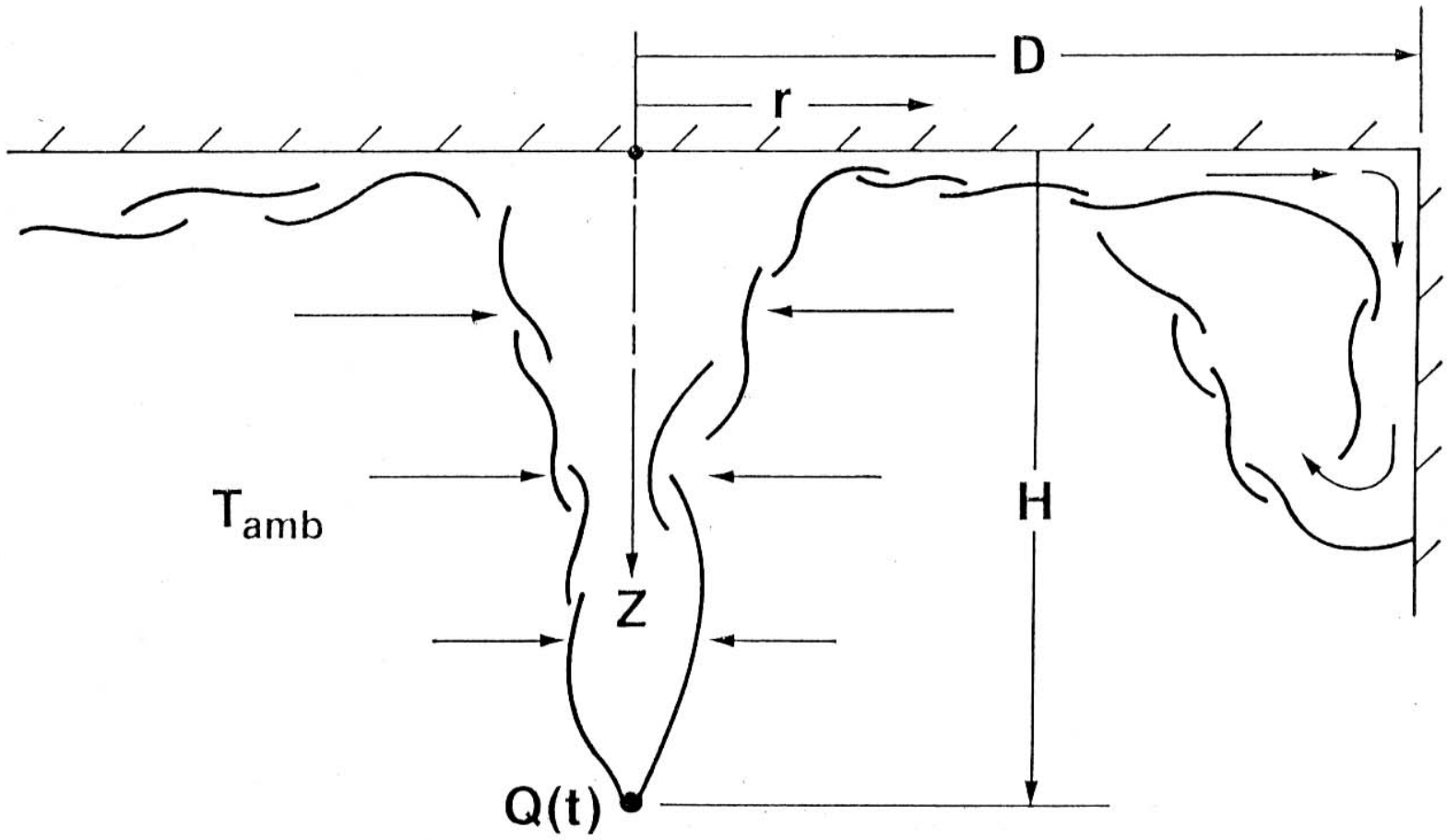

Figure 2.3-3(A) Early Time Ceiling Jet-Wall Impingement (Ref. 8)

Figure 2.3-3(B)

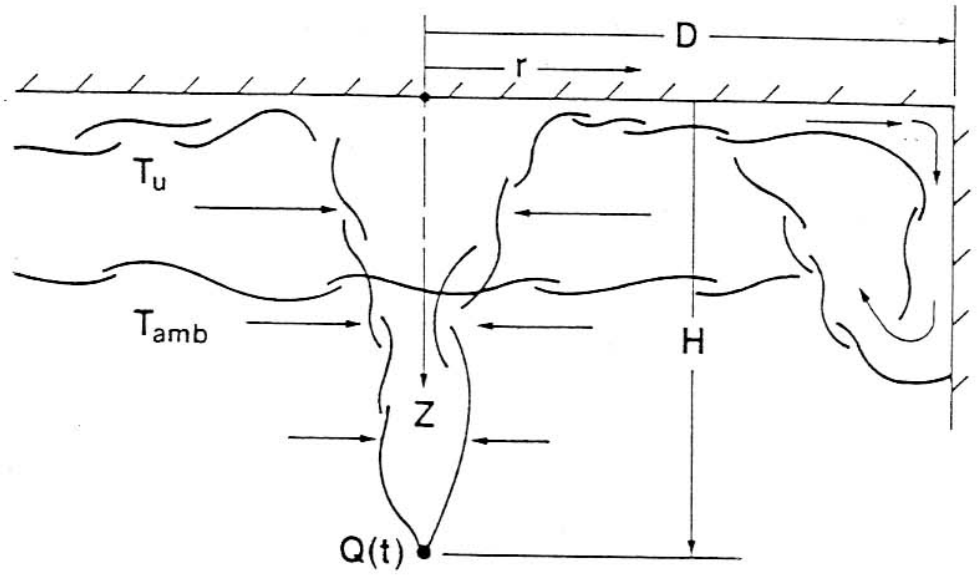

1) penetration of interface

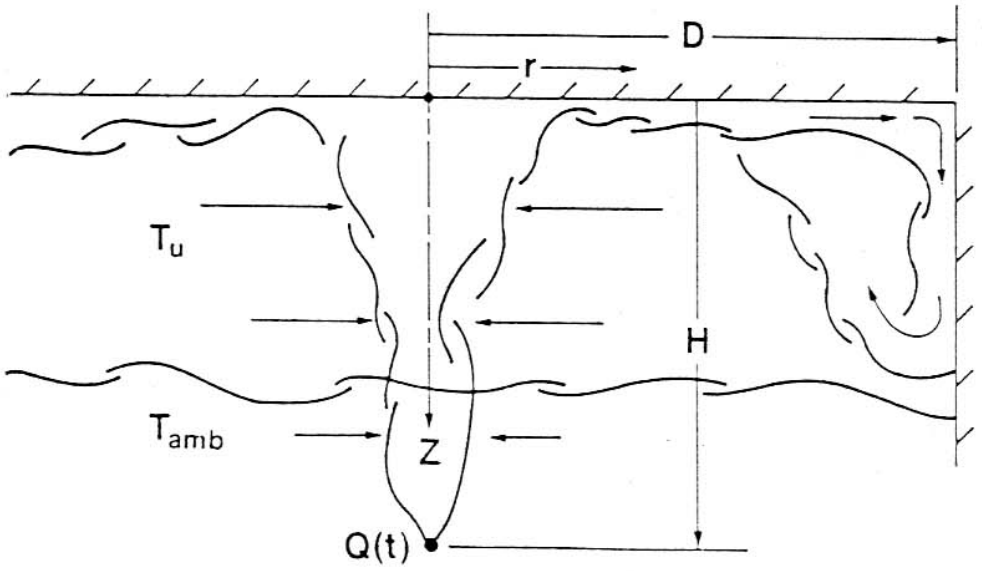

2) no penetration of interface

Ceiling jet-wall interaction with upper layer

(Ref. 8)

2.3-3(A) HEAT TRANSFER COEFFICIENT

In Ref. 8, Cooper uses experimental data of heat transfer from an ambient temperature plane jet to an isothermal wall to arrive at the required expressions for the stagnation point heat transfer coefficient. A curve fit to the data resulted in a Nusselt number formulation for this heat transfer coefficient. Cooper then extends this result to "estimate heat transfer rates, q, from elevated temperature jets to non-uniform temperature walls" in a manner analogous to that discussed in Sect. 2.3-2. This result is then recast in terms of enclosure fire parameters and is discussed below.

The heat transfer coefficient, h_s, is defined by Eq.15, Ref. 8:

Eq. 2.3-3(A)1a

$$\frac{h_s}{h} \equiv \frac{h_s}{\tilde{h}} = 0.89\,Re_H^{-0.42}\,Pr^{-1}(D/H)^{-1.02}$$

where: D= wall-to-fire distance: Fig. 2.3-3(A)

When assumption five of Sect. 2.3-1 holds, i.e., as discussed in Sect. 2.3-2(A), the ambient environment will be the hot upper layer, not that outside the room and the three correction factors discussed in Sect. 2.3-2(A) are used. The heat transfer coefficient is defined (as per Ref. 5) by:

Eq. 2.3-3(A)1b

$$\frac{h_s'}{h} \equiv \frac{h_s'}{\tilde{h}} = 0.89\,Re_H'^{-0.42}\,Pr^{-1}(D/H')^{-1.02}$$

2.3-3(B) GAS TEMPERATURE

The heat transfer coefficient described in Sect. 2.3-3(A) requires T_{ad}. That is to say, in order to use Eq. 2.3-3(A)1 in Eq. 2.3-3, the $(T_{ad} - T_w)$ temperature difference must be known. Thus, T_{ad} is defined by Eq. 2.3-2(B)1 with r = D.

2.3-3(C) SURFACE TEMPERATURE

As stated in Ref. 8, the wall temperature, T_w "would generally vary with (vertical) position from [the] stagnation point". However, for this model the vertical surface temperature profile along a line down the wall a given radial distance from the fire axis, will be considered to be a constant. In other words, this assumption does not require multiple points, vertically spaced down the heated portion of the wall. Instead, only four points are needed: one for each wall. This assumption is made for two reasons: one, because h_s is based on conditions just upstream of the stagnation point (i.e., where the ceiling and wall meet) and two, because at larger values of r/H, h, T_{ad}, and T_w do not vary significantly. In other words, the magnitudes of these variables tend to reach a fairly uniform value a given

distance outside the impingement zone, see Fig. 2.3-4(A)5. Therefore, the error introduced by this assumption is not expected to be large.

The heated wall surface temperature is calculated in a manner similar to what is currently done by CFC. The only difference is that, instead of only one bulk condition, four local conditions are used. These are the conditions present at the distances, D, as defined in Eq. 2.3-3(A)1a. Therefore, a total of seven to fourteen points may be used to characterize the convective heat transfer to the entire extended ceiling. The selection of these points is described in Sect. 2.3-4(A).

2.3-4) MODEL FORMULATION

The correlations provided by Cooper in Ref. 5 and 7 are intended to evaluate local conditions along the ceiling proper. The correlations of Ref. 8 are intended to evaluate the local conditions just upstream of the stagnation point of the ceiling jet before it contacts the wall. Thus, the local conditions at any point of the extended ceiling can be determined, subject to the assumptions of Sect. 2.3-1 and 2.3-3. However, for this alternate ECCHTX model, the interest is in the convective heat transfer to the extended ceiling as a whole. The crux of the problem is choosing the points along the extended ceiling which, taken in combination, yield a fairly accurate estimate of the energy convected to extended ceiling.

2.3-4(A) POINT SELECTION PROCESS

Essentially, the problem is how to apply equations which describe local conditions i.e., those of Cooper, in a global manner. The solution is to integrate the equations over the range of interest. If this can be done analytically then an accurate solution can be obtained. However, if done numerically, then the associated error must be taken into consideration, as well as which points, and how many of them, to use. First the point

selection process for the ceiling proper will be discussed and then for the heated wall.

Start with the governing equations: expressions are available which describe the heat transfer coefficient (Eq. 2.3-2(A)1) and near surface gas temperature (Eq. 2.3-2(B)1) as functions of heat release rate and geometry. It is assumed that these two effects are separable and that it is sufficient to deal with only the geometric dependency for this abstraction. Furthermore, since convection is predominant at the beginning of a fire, when the ceiling temperature rise is small, $T_{surf} \div T_{amb}$, the model is more concerned with making its most accurate prediction at that time. That is to say that, in the beginning of a fire, the radial temperature gradient across the ceiling surface is small enough to be ignored. So, since the ceiling surface temperature is essentially constant at this time, another assumption is made: that

Eq. 2.3-4(A)1

$$\dot{q}'' = h * (T_{gas} - T_{surf})$$

can be replaced with

Eq. 2.3-4(A)2

$$\dot{q}'' \propto h * T_{gas}$$

Thus, the difference between these two formulations (Eq. 2.3-4(A)1 and 2.3-4(A)2) is assumed to be a constant of proportionality. Also, this point selection process

only, the emphasis is on the trend of the heat flux with varying r/H, not necessarily the absolute magnitude of it. The local values of the heat flux will be calculated at the locations resulting from this abstraction process. Therefore, both h and T_{gas} now become functions of r/H so that the total convection heat transfer to the ceiling proper is:

Eq. 2.3-4(A)3

$$\dot{q} = \int_0^{(r/H)_{max}} 2\pi h(T_{gas})dr$$

which with a change of variable, r = (r/H)H, becomes:

Eq. 2.3-4(A)4

$$\dot{q}/H^2 = \int_0^{(r/H)_{max}} 2\pi r/H)h(T_{gas})d(r/H)$$

The functions for h and T_{gas} are composed of expressions for the impingement zone ($0 \leq r/H < 0.2$) and for the region outside the impingement zone ($0.2 \leq r/H \leq (r/H)_{max}$). Therefore, the above integral is actually the sum of two integrals:

Eq. 2.3-4(A)5

$$\dot{q}/H_2 = \int_0^{0.2} 2\pi(r/H)h(T_{gas})d(r/H) + \int_{0.2}^{(r/H)_{max}} 2\pi(r/H)h(T_{gas})d(r/H)$$

As it turns out, the integral between 0 and 0.2 (first term of Eq. 2.3-4(A)5) can be found analytically. Therefore, there is no

error associated with this region. A point at r/H = 0.0 and another at r/H = 0.2 are required to

characterize the heat transfer in the impingement region. However, the expression for $0.2 \leq r/H \leq 2.2$ (i.e., 2.2 is the limiting $(r/H)_{max}$ for Cooper's expressions) is not so well behaved and requires a numerical technique.

The numerical integration of the second term of Eq. 2.3-4(A)5 was done with a Simpson's rule algorithm taken from Ref. 3. 36 evenly spaced intervals were used to calculate the solution correct to four decimal places and thus this is considered to be the "correct' solution. The problem now becomes how to arrive at the "36 interval" solution using a finite number of not necessarily evenly spaced intervals and then where (i.e., at which values of r/H) to place the interval boundaries. Typically, a minimum of three points are required to span the entire space between r/H = 0 and $(r/H)_{max}$: r/H = 0.0, 0.2 and $(r/H)_{max}$. In other words, the emphasis is placed on the heat transfer associated with the impingement zone while accepting the error associated with outer region. So, for the region outside the impingement zone at least one point is required. If the error associated with the outer region is to be reduced, then more points are required. The maximum number of outer region intervals is arbitrarily set to six. In order to size the intervals appropriately, a variable interval generator is required.

The error associated with a variable interval generator is proportional to the fourth derivative (f^{iv}) of the function being integrated (Eq. 2.3-4(A)5). This is comparable to the error associated with the Simpson's rule numerical integration subroutine provided by Ref. 3. For example, in Ref. 3, this error is shown to be:

Eq. 2.3-4(A)6

$$E^{S}_{N} = -\frac{f^{iv}(\in)(h/2)(b-a)}{180}, \quad a < \in < b$$

where: h = interval size

a = lower bound

b = upper bound

This equation indicates that knowledge of the fourth derivative is required to estimate the error associated with the procedure described below. Therefore, by evaluating the fourth derivative, the order of magnitude of the error can be estimated.

The required fourth derivative was also found numerically and the algorithm employed was taken from Ref. 14. Double precision was used and a smooth fourth derivative resulted, as shown in Fig. 2.3-4(A)1.

The fourth derivative is employed as follows: since the fourth derivative may represent the error associated with the interval h_i.

Figure 2.3-4(A) 1

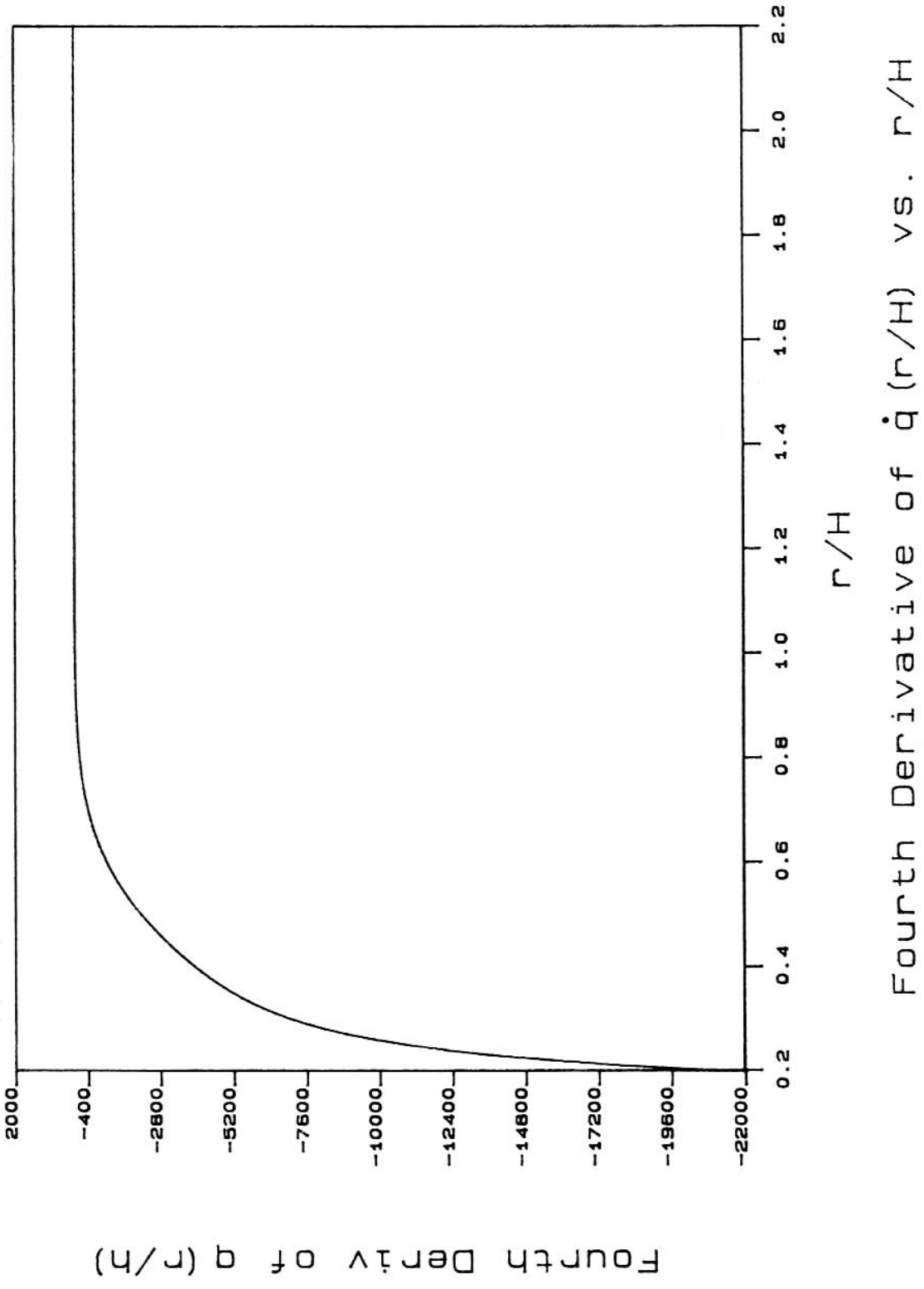

One way to minimize the error is to find: min $\{|f_i^{iv}| * h_i^4(\in)\}$ (or, as shown by Eq. 2.3-4(A)8, min $\{|f_i^{iv}|^{1/4} * h_i(\in)\}$, subject to:

Eq. 2.3-4(A)7

$$\sum_{i=1}^{n} h(\in) = (r/H)_{max} - 0.2$$

where f_i^{iv} is the "error" associated with $h_i(\in)$ at some $r/H = \in$. In order to do this, set

Eq. 2.3-4(A)8a

$$\left|f_i^{iv}\right| * h_i^4 = \text{constant, K.}$$

By setting this product equal to a constant, the error associated with any interval is no greater than that for any other. This constant is actually a function of $(r/H)_{max}$ and the number of intervals, n:

Eq. 2.3-4(A)9

$$K = C * \Delta r_n$$

where: C = $c(n, (r/H)_{max})$
= function to account for the number of intervals, n, and the total area involved represented by $(r/H)_{max}$: to be developed below
Δr_n = $(r/H)_{max} / n$

Now, from Eq. 2.3-4(A)8a we have

Eq. 2.3-4(A)8b

$$h_i = K / (f_I^{iv})^{1/4}$$

The next step is to plug in for K and Δr_n and then to sum over the intervals. This results in:

Eq. 2.3-4(A)10

$$\sum_{i=1}^{n} h_i = \sum_{i=1}^{n} \frac{C * \Delta r_n}{\left|f_i^{iv}\right|^{1/4}} = \sum_{i=1}^{n} \frac{C * \{(b-a)/n\}}{\left|f_i^{iv}\right|^{1/4}} = b - a$$

where: $b - a \equiv (r/H)_{max} - 0.2$

Solving for C results in:

Eq. 2.3-4(A)11a

$$C = n / \sum_{i=1}^{n} (1/\left|f_i^{iv}\right|^{1/4}) \quad \text{or}$$

Eq. 2.3-4(A) 11b

$$C \approx n / \int_{0.2}^{(r/H)_{max}} (1/\left|f_i^{iv}\right|^{1/4}) d(r/H)$$

Now plugging into the expression for a single interval, Eq. 2.3-4(A)8b, $h_i = \Delta(r/H)$ results in:

Eq. 2.3-4(A)12a

$$\Delta(r/H) = \frac{C * \{[(r/H)_{max} - 0.2]/n\}}{\left|f_i^{iv}\right|^{1/4}}$$

or

Eq. 2.3-4(A)12b

$$\Delta(r/H) = \frac{\{n / \int_{0.2}^{(r/H)_{max}} (1/\left|f_i^{iv}\right|^{1/4}) d(r/H)\} * \{[(r/H)_{max} - 0.2]/n\}}{\left|f_i^{iv}\right|^{1/4}}$$

Before finding the interval sizes, and ultimately the points where the local conditions are to be calculated, values for $\left|f_i^{iv}\right|^{1/4}$ and $1/\left|f_i^{iv}\right|^{1/4}$ are required as functions of r/H. These functional relationships are shown in Fig. 2.3-4(A)2 and 2.3-4(A)3. The curve of Fig. 2.3-

4(A)2 asymptotically approaches x = 0. The spike shown in Fix 2.3-4(A)3 is caused by the function of Fig. 2.3-4(A) crossing the X axis at approximately r/H = 0.92. The data of Fig. 2.3-4(A)2 were coded into a function subroutine that returns a value of $\left|f_i^{iv}\right|^{1/4}$ given r/H. Also, it is the integral of the data of Fig. 2.3-4(A)3 between r/H = 0.2 and $(r/H)_{max}$ that is required. Therefore, the values of X, given by:

Eq. 2.3-4(A)13

$$X = \int_{0.2}^{(r/H)_{max}} (1/\left|f_i^{iv}\right|^{1/4}) d(r/H)$$

for a range of $(r/H)_{max}$ were found using a Simpson's rule algorithm and then tabulated in a DATA statement to provide values for the term in the numerator of Eq. 2.3-4(A)12b.

An algorithm was devised to iteratively find the local r/H's at the interval boundaries. The required input for this algorithm is the maximum value of r/H and the number of intervals (i.e., points) to be considered. The algorithm then tried to calculate a variable mesh by starting at r/H = 0.2 and ending at $(r/H)_{max}$ by "spanning the space" between these two points. A flowchart of this algorithm is shown in Fig. 2.3-4(A)4.

Unfortunately, this approach did not yield usable results. The fourth derivative is recognized to be important when determining the error, as shown by Eq. 2.3-

Figure 2.3-4(A)2

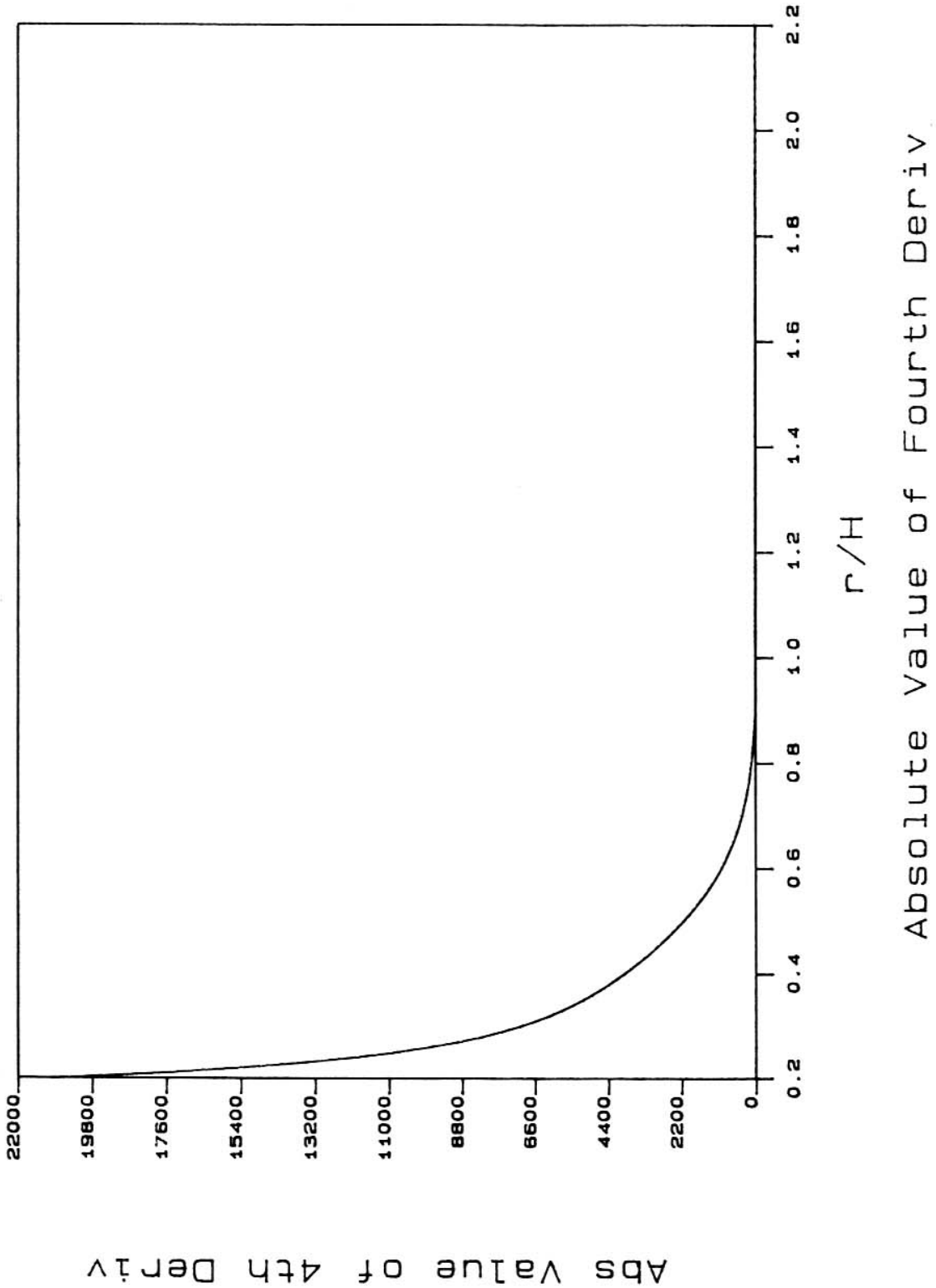

Figure 2.3-4(A)3

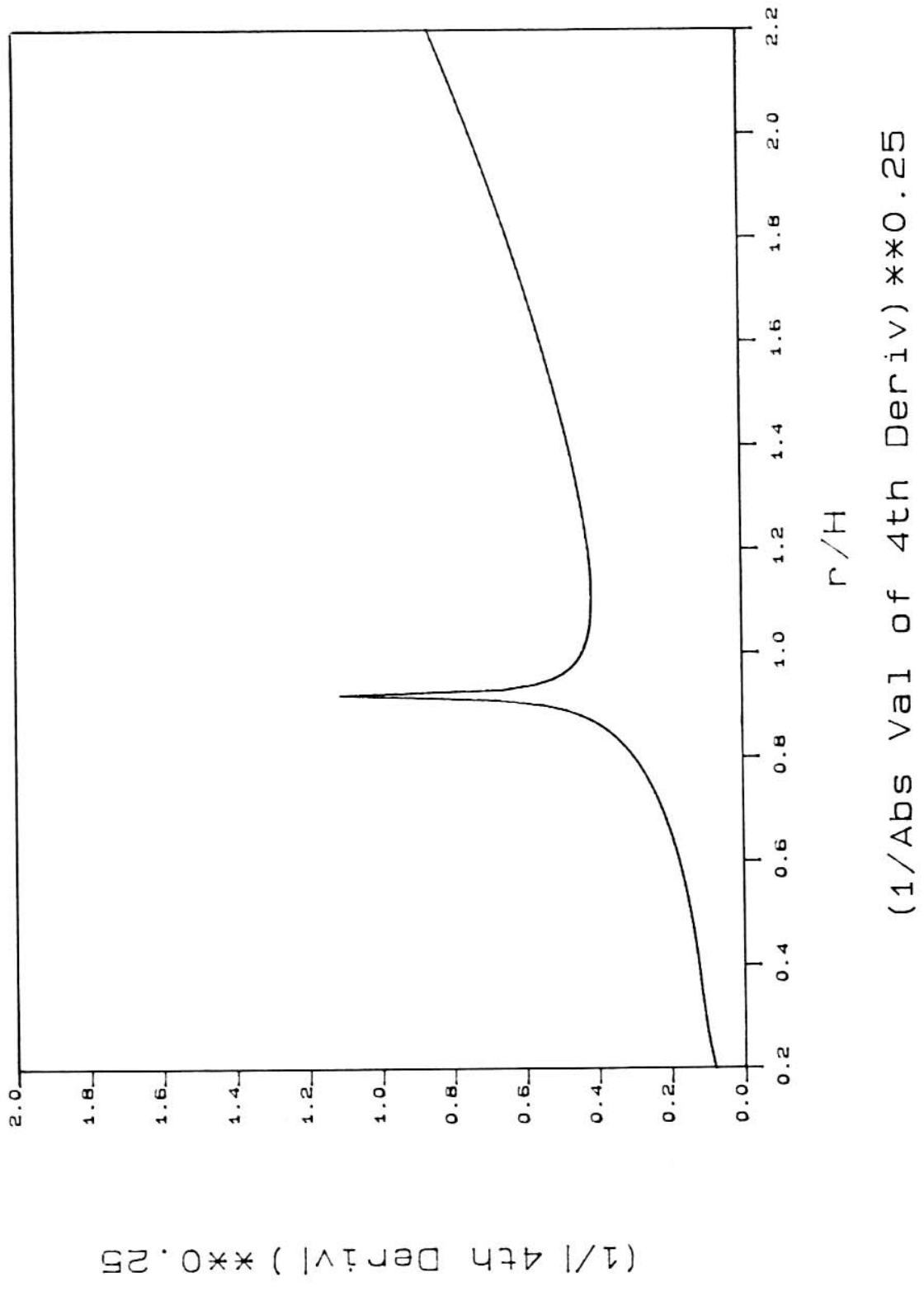

(1/| 4th Deriv|)**0.25

Figure 2.3-4(A)4

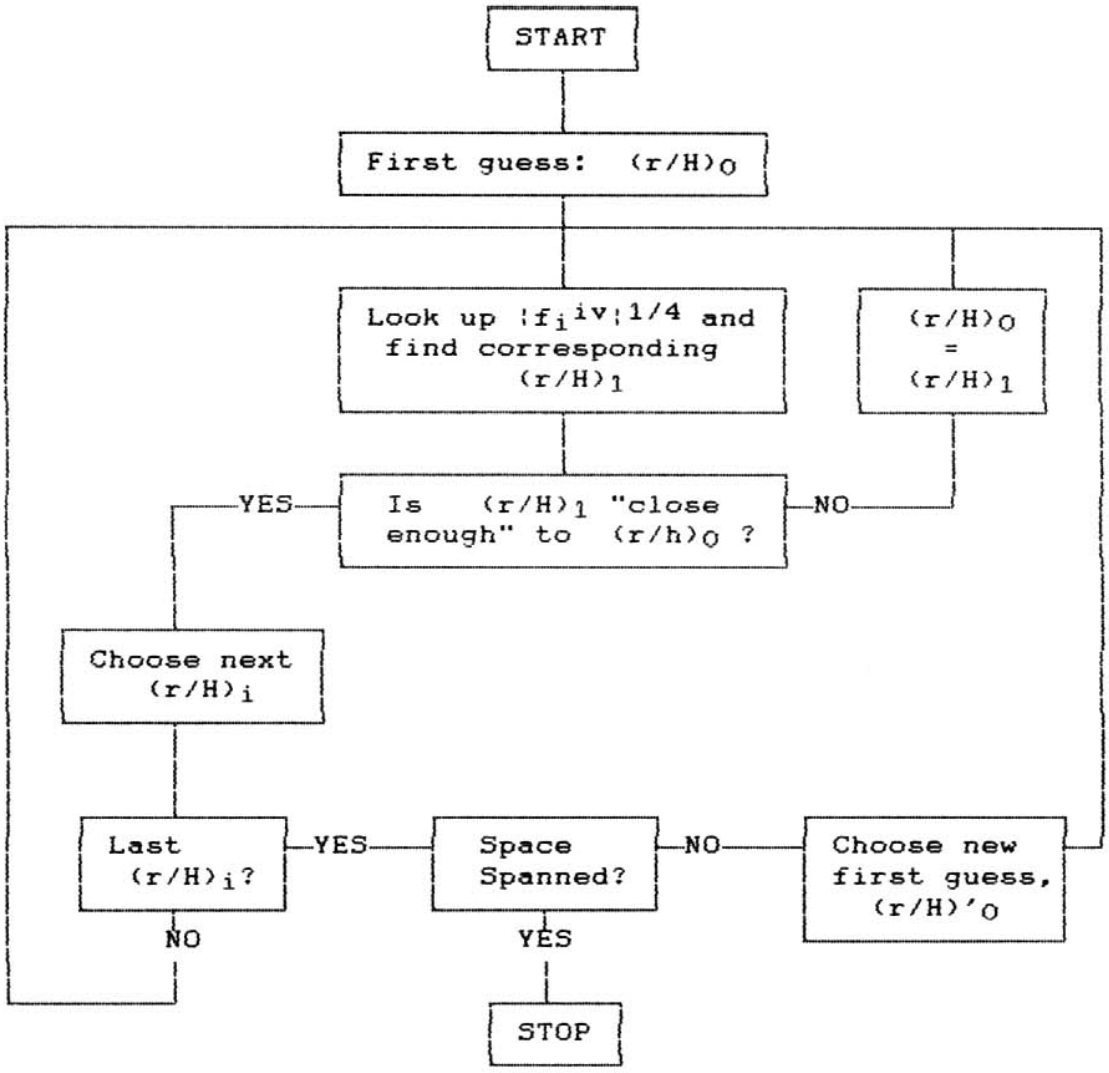

New first guess chosen in a variety of ways: twice original first guess, half original first guess and fraction of original first guess. None were successful: see text.

Variable Mesh Generation Algorithm Flowchart

4(A)6. However, the fourth derivative used in this algorithm is not numerically well behaved. It appears that the upper bound on the problem, $(r/H)_{max} \leq 2.2$, in conjunction with the wide range of values for $\left|f_i^{iv}\right|^{1/4}$, 34 - 21000, is too restrictive to provide a rigorous solution. This algorithm would continually calculate interval sizes greater than r/H = 2.2 and/or consistently find the maximum value and nothing else. The problem seems to be numerical in nature. Therefore, a less rigorous approach will be used.

It appears that one road leading to a spacing scheme involves some intuition. From the rigorous scheme detailed above, and from Fig. 2.3-4(A)2, it seems that the region between r/H = 0.2 and 1.1 would be the region of greatest concern since the fourth derivative is largest there. In other words, the region where the error (i.e., the fourth derivative of the function in question) is largest is where the majority of the points should be located: large error, small intervals. Based on this observation, three spacing schemes were considered: (A) evenly spaced between r/H = 0.2 and $(r/H)_{max}$; (B) evenly spaced between 0.2 and 1.1, with one point at $(r/H)_{max}$ (number of points in outer region ≥ 2 and $(r/H)_{max} > 1.1$); and (C) evenly spaced between 0.2 and 1.1, one point at $(r/H)_{max}$ and another halfway between 1.1 and $(r/H)_{max}$ (number of points ≥ 3 and $(r/H)_{max} > 1.1$). Each of these schemes (where applicable) is employed in

conjunction with six different values for $(r/H)_{max}$ as shown in Table 2.3-4(A)1. Since these "intuitive" schemes are assumed to be linear between successive points, a modified trapezoid rule was used to evaluate the integral between 0.2 and the various values of $(r/H)_{max}$. The trapezoid rule was modified so that only two intervals between successive points are used: this implies that the functional relationship between adjacent values of $h * T_{gas}$ is linear. Thus, a number of estimates for the integral in question, second term of Eq. 2.3-4(A)5, are obtained for the three different spacing schemes and six different values of $(r/H)_{max}$. In addition, Simpson's rule was also used with the six values of $(r/H)_{max}$ to provide the basis for the comparison. The results of this comparison are also presented in Table 2.3-4(A)1.

From this table it appears that an even spacing between 0.2 and $(r/H)_{max}$ is adequate for characterizing the convection heat transfer from the ceiling jet to the ceiling proper, for all values of $(r/H)_{max}$. The "non-even" schemes tended to overpredict $h * T_{gas}$: this is not conservative since too much heat would be convected. An even spacing doesn't appear to be unreasonable when a plot of $(h * T_{gas})$ vs. r/H, as shown in Fig. 2.3-4(A)5, is seen. From this figure it can be seen that, although the function is complicated, its plot vs. r/H is not.

Table 2.3-4(A)1

$(r/H)_{max}$	Simpson's Rule N = 40	Spacing* Scheme	Trapezoid Rule Number of intervals = 1	2	3	4	5	6
0.6	2.5569	A	2.4658	2.5333	2.5464	2.5510	2.5531	2.5543
		B						
		C						
1.1	4.6095	A	4.3036	4.5152	4.5659	4.5846	4.5935	4.5983
		B						
		C						
1.7	6.2526	A	5.7963	6.0401	6.1466	6.1905	6.2120	6.2241
		B		6.2747	6.2728	6.2726	6.2722	6.2718
		C			6.3095	6.2868	6.2742	6.2681
2.2	7.4020	A	6.9810	7.0883	7.2296	7.2977	7.3330	7.3531
		B		7.5926	7.5277	7.5037	7.4914	7.4838
		C			7.5464	7.4956	7.4673	7.4524
2.5	8.0452	A	7.7069	7.6806	7.8302	7.9119	7.9560	7.9817
		B		8.3611	8.2518	8.2111	8.1903	8.1777
		C			8.2526	8.1822	8.1431	8.1222
5.0	12.683	A	13.903	12.395	12.245	12.308	12.390	12.456
		B		14.423	13.856	13.640	13.529	13.462
		C			13.651	13.353	13.195	13.107

*Spacing schemes:

A = evenly spaced from 0.2 to $(r/H)_{max}$

B = evenly spaced from 0.2 to 1.1 w/ 1 point at $(r/H)_{max}$

C = evenly spaced from 0.2 to 1.1 w/ 1 point at $(r/H)_{max}$ and 1 point halfway between 1.1 and $(r/H)_{max}$

Preliminary Spacing Scheme Results

Figure 2.3-4(A)5

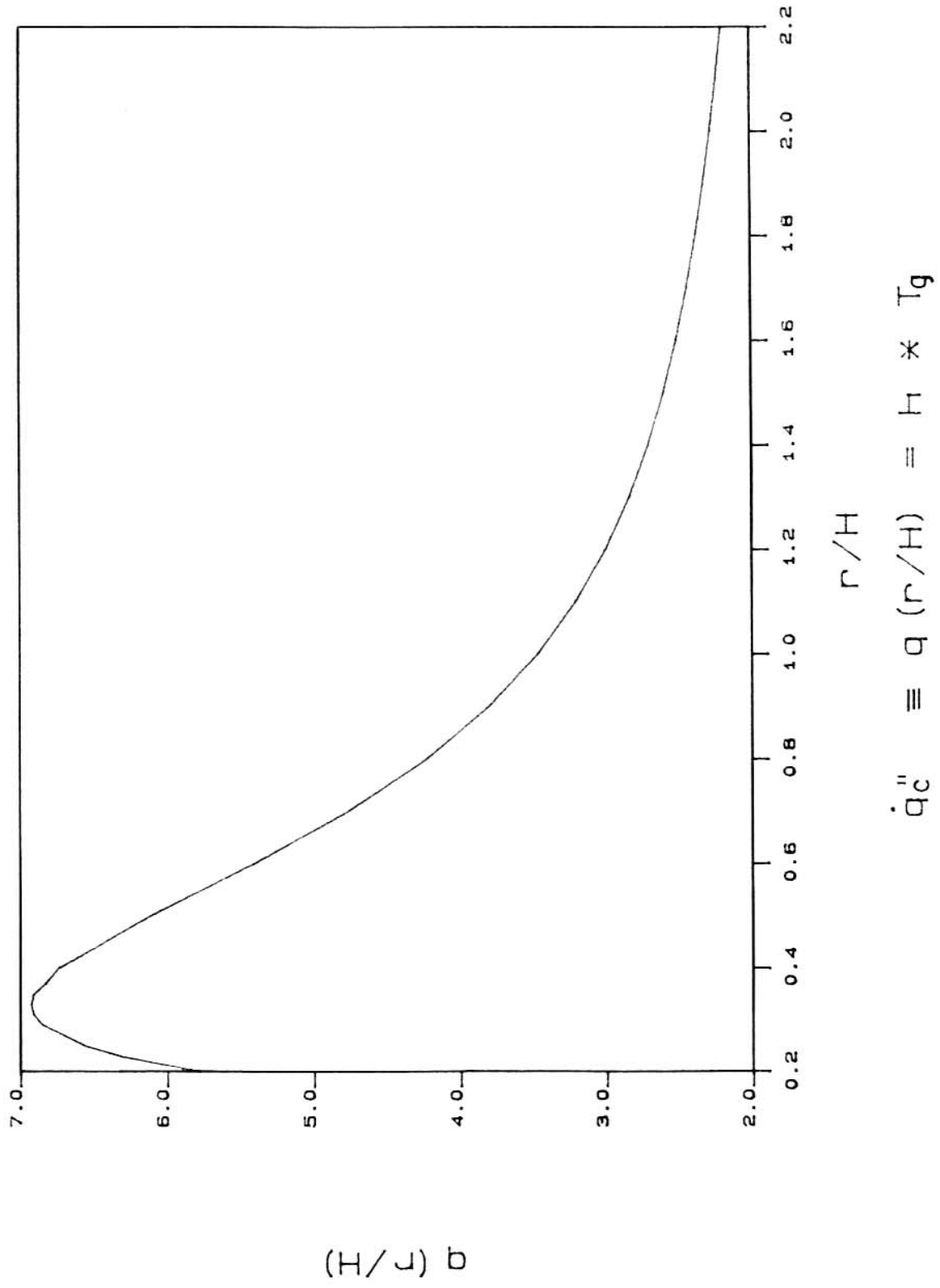

Upon closer examination of Fig. 2.3-4(A)5, the effect of different spacing schemes (when used in conjunction with various values of $(r/H)_{max}$) can readily be seen. An even spacing scheme should be the best fit since it tends to reduce the error associated with any given interval and thereby minimize the overall error. On the other hand, schemes B and C result in one interval having an error relatively larger than the others in the scheme. For example, scheme C with $(r/H)_{max} = 2.2$ has points at 0.2, 0.35, 0.5, 0.65, 0.8, 1.65, 2.0 and 2.2. The interval between 0.8 and 1.65 has a much larger error associated with it because the curve (Fig. 2.3-4(A)5) is concave up in that region (indeed, the curve is concave up between, roughly, 0.5 and 2.2). Therefore, the trapezoid rule over predicts in this region. This also explains the results presented in Table 2.3-4(A)1.

Based on Fig. 2.3-4(A)5, another spacing scheme that might reduce the overall error was considered. This scheme is unevenly spaced and linearly approximates the curve shown in Fig. 2.3-4(A)5. The local points (values of r/H) are chosen as follows: in this scheme the number of points to be used depends on $(r/H)_{max}$ for the problem. That is to say

that the larger $(r/H)_{max}$ is, the more points that will be used. This will be accomplished by prescribing that certain points are always used, depending on $(r/H)_{max}$. More explicitly, to minimize the error associated with assuming a linear relationship between adjacent points, the following points will always be used: 0.33, 0.53, 0.8, 1.1, 1.5, 1.9, and 2.2. If, for example, $(r/H)_{max} = 0.9$, then four points outside the impingement zone are used: 0.33, 0.53, 0.8 and 0.9. Similarly, if $(r/H)_{max} = 1.8$, then six points are used: 0.33, 0.53, 0.8, 1.1, 1.5, and 1.8. If $(r/H)_{max} > 2.2$ then a total of eight points would be used: the seven specified above and $(r/H)_{max}$. This should ensure that the "trapezoids" chosen fit the curve fairly well. A comparison of this latest scheme and Simpson's rule is provided in Table 2.3-4(A)2. Please note that the four place decimal accuracy shown in this table is based on $T_s = T_{amb}$ and only of importance from a numerical standpoint. These results may not fully represent the accuracy of the more general case.

Upon comparison with Table 2.3-4(A)1, the results of Table 2.3-4(A)2 are no worse, and in some cases better, than those of Table 2.3-4(A)2. Therefore, this uneven, predetermined spacing scheme is used in the alternate ECCHTX model. It provides acceptable results (all results within 1% of Simpson's rule) while speeding up the input processing. In other words, the argument is that this

Table 2.3-4(A)2

Final Spacing Scheme Results

$(r/H)_{max}$	Simpson's Rule	Modified Trapezoid Rule	Number of Points *
0.3	0.6487	0.6448	1
0.6	2.5569	2.5394	3
0.9	3.9140	3.8888	4
1.1	4.6095	4.5887	4
1.3	5.2101	5.1900	5
1.6	6.0058	5.9895	6
1.92	6.7731	6.7584	7
2.2	7.4020	7.3876	7
2.5	8.0452	8.0309	8
5.0	12.684	12.702	8

* i.e., outside the impingement zone

uneven, predetermined scheme provides acceptably accurate results without user intervention and thus relieves the user of making a decision that the program can make just as easily. In this way a (typical) minimum of three and a maximum of ten points are used to characterize the ceiling proper, depending on $(r/H)_{max}$.

Because of the assumption of Sect. 2.3-3, four points are required to characterize the heat transfer to the heated portion of the walls. Specifically these points are located at the radial distances from the axis of the burning object to each of the four walls as defined by Eq. 2.3-3(A)1a. (As discussed in the Recommendations, this is not necessarily the only scheme for placing the four points used to represent the walls). These four points are numbered one through four in Fig. 2.3-4(A)6 which depicts the ceiling of the CFC standard case (center of burning object is located at point five). The local conditions at these four points are then considered to act upon/through the corresponding heated wall area. These four wall points represent the least distance traveled by the ceiling jet to a given wall. Therefore, this point of the wall will experience the highest gas temperature and is conservative from the wall's point of view. Table 2.3-4(A)3 summarizes the point locations for the alternate ECCHTX model.

Figure 2.3-4(A)6

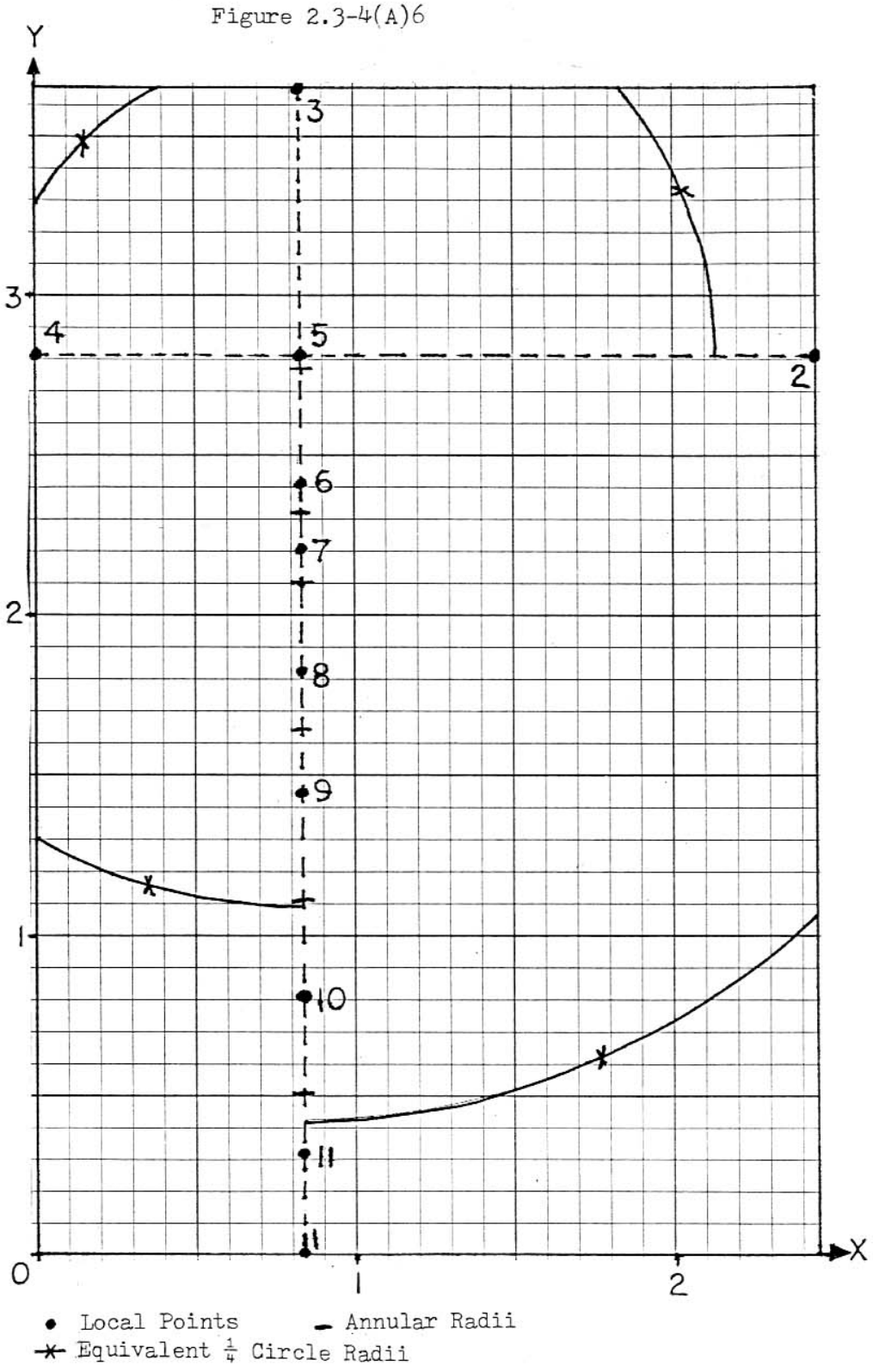

Ceiling Representation of the Standard Case

Table 2.3-4(A)3

Point Locations for Ceiling Calculations

Point Number	r/H
7	0.33
8	0.53
9	0.8
10	1.1
11	1.5
12	1.9
13	2.2
14	50.0

Points 1 - 4 are for the heated walls, points 5 and 6 are for the plume axis and the impingement zone boundary (at r/H = 0 and r/H = 0.2). Point 14 is an arbitrarily large maximum value, greater than the imposed maximum value of 2.2, which allows the model to be used "out of bounds". A warning message is printed should this condition be detected.

2.3-4(B) Averaging Calculations

When numerics and output are considered, the data structure of CFC is currently not equipped to handle up to 14 points for ECCHTX calculations. In other words, the numerics and output deal with a single value of wall temperature as well as one value for the resultant ceiling convective heat flux and one value for the ceiling convective energy transfer. Therefore, a method that condenses or averages the (up to) 14 values of these parameters provided by the alternate ECCHTX model into a single number is required. An area weighted averaging scheme is used to average the local wall temperatures, convective heat fluxes, and convective energy transfer of the ceiling proper and the heated portion of the walls. As shown in Fig. 2.3-4(A)6, the ceiling is divided into four quadrants, with the plume axis at the origin. Each quadrant is then converted to an equivalent quarter circle. The radii of these four quarter circles then determine the value for $(r/H)_{max}$ and the four equivalent quarter circle ceiling areas. A more thorough discussion of this averaging algorithm is presented in Sect. 2.4-1.

2.4 Required Programming

In order to incorporate the alternate ECCHTX model discussed in Sect. 2.3 into CFC, a total of ten subroutines and two (new) function routines are required. These routines are similar in function to subroutines CNVW, CNVL, and TMPW01, which are currently used by CFC. Figure 2.4(A) presents a flowchart of the alternate ECCHTX model. A description of each routine is now provided.

2.4-1 CNVW02

This is the controlling subroutine for the alternate ECCHTX model. The physical basis for this subroutine is identical to that of subroutine CNVW of CFC: CNVW02 effectively applies CNVW at each of the local points. Subroutine CNVW02 calculates the plume source-to-ceiling height: H = room height - object one height. NOTE: The room height of room one and the height of object one are hardwired into this subroutine. At the current time, CFC is limited to the room of origin and object one is always the initially burning object. Because of this, object one is the object with the highest heat release at the start of the fire ad determined by subroutine BIGHRR. CNVW02 then calculates the plume source-to-layer interface (HZ = H - layer thickness) distances, and the radial distances from the plume axis to the points where the local conditions are

Figure 2.4(A)

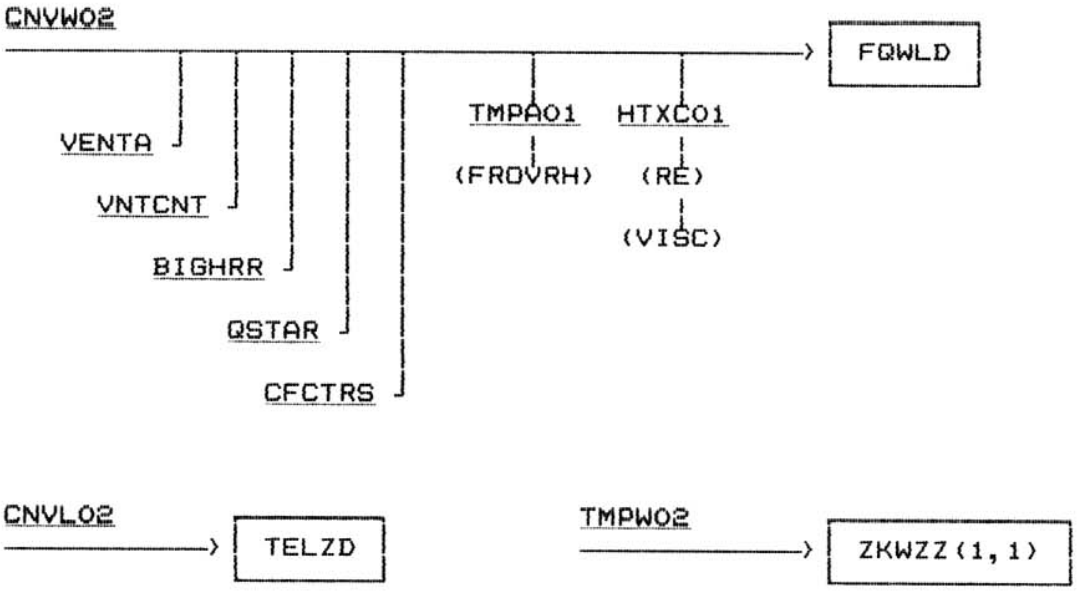

Underlined parameters are subroutine names and those in parentheses are function names as described in Section 2.4. Subroutines CNVL02 and TMPW02 are based on the existing CFC subroiutines CNVL and TMPW01. Function VISC also exists in the current version of CFC. All other subroutines/functions have been developed for the alternate ECCHTX model except CNVW02. CNVW02 is based on the existing subroutine CNVW, however, more extensive modifications were required for this routine than for CNVL02 and TMPW02.

Parameters in boxes are output variables: FQLWD = convective heat flux at the ceiling, TELZD = convective energy at the ceiling, and ZKWZZ(1,1) = inside ceiling surface temperature.

Alternate ECCHTX Model Flowchart

to be determined. These are the seven to fourteen points described in Sect. 2.3-4(A). Subroutines VENTA and VNTCNT are called to calculate all vent areas and to locate the centers of the ceiling vents. The four equivalent quarter circular radii and areas (see Sect. 2.3-4(B) for a description) as well as $(r/H)_{max}$ are calculated only once (for the room) at the beginning of this routine.

Next, function QSTAR is called to calculate the dimensionless heat release rate of each object. After that, subroutine BIGHRR determines which object has the highest heat release rate. At the present time this subroutine is somewhat moot because only the geometry associated with object one is calculated (see above). This is not viewed as a serious restriction: for the times of interest, the fire of object one generally has not caused ignition of other objects. If this is not the case, then either only one object should be modeled when using the growing fire algorithm or a burner fire should be used which effectively models all combustible items of interest in the room (i.e., considers the ignition of additional objects to be an increase in the "total" gas flow rate of the burner). Making this subroutine sophisticated enough to always use the correct geometry of the object with the highest heat release rate would be onerous but not impossible.

If hot layer effects are significant (i.e., assumption

five of Sect. 2.3-1 applies), subroutine CFCTRS is called to provide the appropriate correction factors. Subroutines HTXC01 and TMPA01 are called to provide local heat transfer coefficients and near surface gas temperatures. These are used in conjunction with the output from TMPW02 to calculate the local convective fluxes according to Eq. 2.3-2.

Before a single value for the convective heat flux between the upper layer and the extended ceiling can be determined (and output), the appropriate heat transfer areas for each point must be found. The radii for the equivalent quarter annuli ceiling surface areas have been predetermined, based on information presented in Sect. 2.3-4. The max/min radii for the annular ceiling surface areas are shown in Table 2.4-1(A). The points shown in this table correspond to those of Table 2.3-4(A)3. Points seven through thirteen are located at the approximate centers of their respective annuli (see Fig. 2.3-4(A)6). If so desired, logic could be implemented to calculate the centroid of the annuli and place the point there. However, because of time constraints, the more expedient approach was taken. The error thus introduced is assumed to be acceptable when the program as a whole is considered. (Point fourteen in Table 2.3-4(A)3 is essentially a dummy point and not considered for the heat transfer areas. If a maximum radius of a quadrant of the room is greater than r/H = 2.35, then the maximum quarter radius becomes the $(r/H)_{max}$

Table 2.4-1(A)

Annular Heat Transfer Area Max/Min Radii

Point Number	$(r/H)_{min}$	$(r/H)_{max}$
5		0.05
6	0.05	0.265
7	0.265	0.4
8	0.4	0.65
9	0.65	0.95
10	0.95	1.3
11	1.3	1.7
12	1.7	2.05
13	2.05	2.35

for that quadrant). Points five and six are at r/H = 0 and 0.2. The radius for the center circle was arbitrarily set to an r/H of 0.05. This value appears to strike a balance between the impingement point heat transfer area and the annulus it is encircled by: once again, an alternate method or balance can readily be obtained. Therefore determining these annular radii is simply a matter of a table lookup, based on a given maximum radius for a given quadrant. Figure 2.3-4(A)6 shows the relationship and placement of the annuli radii relative to the points where the local conditions are determined. (These annuli apply to the ceiling only; Sect. 2.3-4(A) describes the areas used for the heated wall). Figure 2.3-4(A)6 shows a representation of the default/standard room used in CFC. The location of the center of the burning object is at the intersection of the dashed lines. The local points and annular radii are shown on the lower portion of the vertical dashed line. The equivalent radii for each quadrant are also shown. These equivalent radii are the radii of the quarter circles whose areas are equal to each of the quadrants. These represent the maximum radius used for a given quadrant and may be used as an alternative distance for D of Fig. 2.3-3(A). For each quadrant the appropriate number of annular areas are calculated up to the maximum radius for the quadrant. The net heat transfer areas are found by subtracting the ceiling vent area from the annulus containing the center of the vent. If the vent center falls outside the maximum radius

for a quadrant, the vent area is subtracted from the outermost annulus. If the vent area is larger than the annulus its center is in, then the excess vent area is subtracted from the next larger annulus. (For the heated walls, all wall vent areas covered by the upper layer are subtracted from wall number one. These vents are not assigned locations within CFC. Therefore, this choice is arbitrary and based on CFC designating wall one to be the wall with the door in it.)

Finally, with the local net heat transfer areas calculated, the average convective heat flux to the extended ceiling is the sum of the area weighted average heat flux to the heated wall and the area weighted average heat flux to the ceiling proper:

$$\dot{q}''w = \sum_{i=1}^{n} (A_i / A_{TOT,w}) * \dot{q}''i$$

$$\dot{q}''c = \sum_{m=1}^{n} (A_m / A_{TOT,c}) * \dot{q}''m$$

$$\dot{q}''_{TOT} = \frac{(A_{TOT,w} * \dot{q}''_w) + (A_{TOT,c} * \dot{q}''c)}{(A_w + A_c)}$$

where: A_i, A_m =local areas for heated wall, ceiling

$A_{TOT,w}$, $A_{TOT,c}$ = total heated wall and ceiling areas

$\dot{q}''i$, $\dot{q}''m$ = local heat fluxes for heated wall, ceiling

However, if any local ceiling jet temperature as calculated by TMPA01 rises above the maximum, actual flame

temperature (1300K) then the alternate ECCHTX model is no longer used. (This average flame temperature was obtained by time averaging the flame temperature measurements of experimental burner fires). At that point, CFC switches to the CVNW subroutine for the remainder of the run.

2.4-2 VENTA

This subroutine calculates the vent areas at time = 0.0 and after an initially closed vent opens. This routine also calculates the total wall vent area and total ceiling vent area required by the alternate CVMFR model.

2.4-3 VNTCNT

This subroutine calculates the equivalent ceiling vent radii of all ceiling vents (assumption five, Sect. 2.3-1) and the distances from the plume axis to the center of the ceiling vent.

2.4-4 BIGHRR

This subroutine finds the object with the highest heat release rate by employing a simple sort algorithm. See assumption three of Sect. 2.3-1 for the reasoning behind this subroutine.

2.4-5 QSTAR

This function calculates the dimensionless heat release rate defined by Cooper in Ref. 5 (and shown in Sect. 2.3-2(A) as Q_H^*) that is required by the routines which calculate the heat transfer coefficient and the adiabatic near-surface gas temperature. This function also calculates the fraction of the heat release rate of the fire that is lost by radiation.

2.4-6 CFCTRS

This routine calculates the correction factors to use when upper layer effects are significant, i.e., when the upper layer depth is approximately 1/4 of the room height (assumption five, Sect. 2.3-1). These correction factors are applied to the plume source-to-ceiling distance, the heat release rate and the temperature values used in calculating the heat transfer coefficient and the near surface gas temperature. See Eq. 2.3-2(A)1b for an example of how these correction factors may be applied.

2.4-7 TMPA01

This subroutine calculates the local, near-surface gas temperature of the ceiling jet, i.e., just under the ceiling. This local temperature is a function of r/H,

dimensionless heat release, and the ambient temperature. This routine also calculates a dimensionless temperature as defined in Ref. 7. These equations are shown in Sect. 2.3-2(B).

2.4-8 FROVRH

This function accepts a value of r/H and uses it to evaluate Eq. 2.3-2(B)2. This function is called by subroutine TMPA01 and provides the functional variation in near-surface gas temperature outside the impingement zone, r/H > 0.2.

2.4-9 HTXC01

This subroutine calculates the local heat transfer coefficient at a point adjacent to the ceiling, as given by Eq. 2.3-2(A)1. The value of the heat transfer coefficient depends on the radial distance across the ceiling divided by the plume source-to-ceiling distance of the burning object (r/H), a Reynolds number, and a normalizing heat transfer coefficient. This routine determines the correct value of the Prandtl number to use, and also calculates r/H and the normalizing heat transfer coefficient ($\tilde{h}$ of Eq. 2.3-2(A)1). This subroutine relies on function RE to calculate the required Reynolds number. The output is the local heat transfer coefficient and r/H which is used in subroutine

TMPA01.

2.4-10 RE

This function calculates the Reynolds number, as defined by Cooper in Ref. 5 (and shown in Sect. 2.3-2(A) as Re_H) of the plume/ceiling jet resulting from a burning object. It calls function VISC (currently in CFC) which calculates the temperature dependent kinematic viscosity of the gases in question.

2.4-11 CNVL02

This routine calculates the time rate of change of convective energy of the upper layer. The method used is identical to that of CNVL (Ref. 15) but, instead of considering only one temperature difference, between seven and fourteen points are used in the calculation. Basically all this routine does is multiply the local heat flux (q''_i) at each of the points with the area (A_i) that corresponds to that point:

$$\dot{q}_i = A_i * \dot{q}''_i$$

And it also finds the average time rate of change of convective heat flow to the extended ceiling:

$$\dot{q} = \sum_{i=1}^{n} (A_i * \dot{q}''_i)$$

where A_i and $\dot{q}''_i$ are the local extended ceiling areas and

heat fluxes.

2.4-12 TMPW02

This routine calculates the ceiling temperature profiles for seven to fourteen different points representing the extended ceiling. The method this routine uses is identical to that already found in TMPW01 (Ref. 16), except that more than only one bulk condition (i.e., not a local condition) is used. This routine uses the local net heat fluxes at the inside surface as the driving force behind the temperature profile.

2.5 Model Verification - "Unconfined Ceiling"

Originally, these scenarios were intended to reproduce the computational results described by Cooper in Ref. 6. In Ref. 6, Cooper used algorithms taken from CFC to model the scenario shown in Fig. 2-5(A). He calculated impingement point temperature increases and radial surface temperature profiles. In other words, he developed an algorithm intended only for ceilings so expansive that a hot upper layer would not form within the "enclosure", i.e., the convective heat transfer to the ceiling is driven only by the unconfined ceiling jet. Unfortunately this configuration is not entirely possible with the current version of CFC. In CFC, numerical instabilities result if

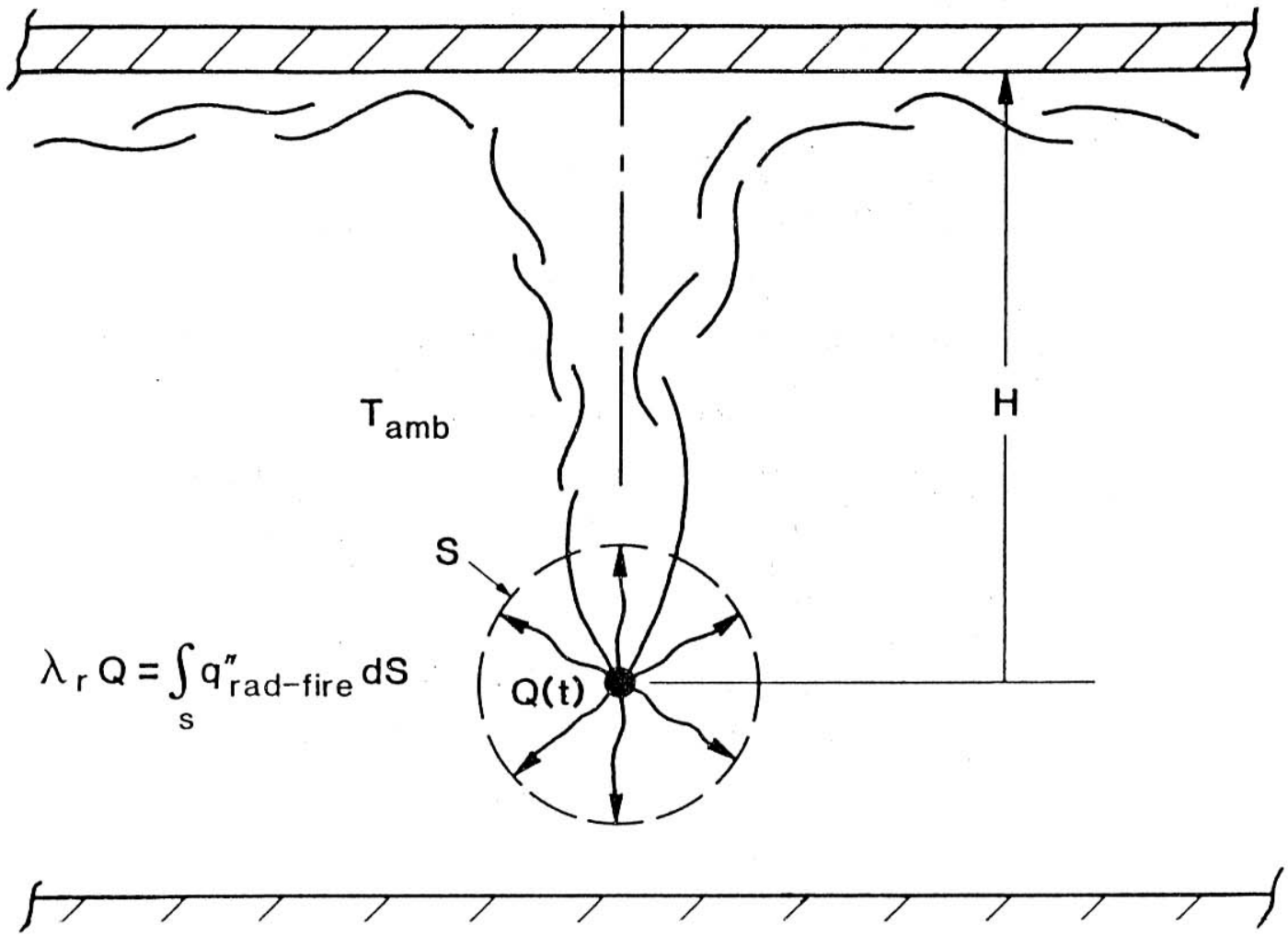

Figure 2.5(A) The Unconfined Ceiling Scenario (Ref. 6)

the wall vents are too large. That is to say that attempting to use a value larger than the maximum vent size, as determined by trial and error, resulted in either non-convergence at time zero and/or a very small time step size. This problem was encountered only when trying to verify this alternate ECCHTX model.

Several fundamental differences also exist between the Ref. 6 procedure and that employed by the alternate ECCHTX model. First, the alternate model contains coding that, essentially, calculates a time varying function of λ_r, fraction of energy release rate of the fire lost as radiation, while Ref. 6 assumes this quantity to be constant (= 0.35) over time. Visual inspection of CFC output for the alternate ECCHTX model cases indicates that the time-varying function is close to the constant value and appears to present a minor difference. However, the value of Q* is affected by this parameter and a slightly different value was used by the alternate ECCHTX model than that of Ref. 6.

In Ref. 6, Cooper specifies a problem end time of 300 seconds or terminates the run if the ceiling temperature at the impingement point (r/H = 0) exceeded 1300°K. For the alternative ECCHTX model verification, the problem end time was also set to 300 seconds. However, the program was not stopped if the temperature at r/H = 0 exceeded 1300K. Instead, for this verification only (not for general use),

the area weighted average ceiling jet and peak surface temperatures were limited to 2500K and 1300K. These values were chosen to facilitate the extrapolation calculations CFC performs at the beginning of a time step, while providing some reflection of reality.

Another difference between the Ref. 6 model and the alternate ECCHTX model addresses the spacing scheme used to locate the points where the local conditions are calculated. In Ref. 6, "the ceiling response was computed at 28 values of r, where the r/H for these were r/h =0., 0.1, 0.2, 0.3, 0.4, 0.5, 0.6, 0.7, 0.8, 0.9, 1.0, 1.25, 1.5, 1.75, 2.0, 2.25, 2.5, 2.75, 3.0, 3.5, 4.0, 4.5, 5.0, 6.0, 7.0, 8.0, 9.0, and 10.0. This is in sharp contrast to the maximum of 14 used by the alternate ECCHTX model as described in Sect. 2.3-4.

Yet another difference between these two models is how the radiation from the combustion zone to the ceiling is calculated. In Ref. 6, Cooper calculates the local incident radiation similar to that of the convective energy: as a function of fire heat release and radial distance from the fire axis. Thus, the radiation from the combustion zone is not attenuated by an upper gas layer and it increases with increasing fire strength. In CFC, this radiation is attenuated by the upper layer. Also, for radiation purposes at least, the fire plume/combustion zone is assumed to be

cut off at the interface of the two layers. Therefore, the combustion zone decreases with increasing upper layer depth and thus the radiant energy from the combustion zone to the extended ceiling is decreased further. Because of this, the net energy flux should be significantly different for these two models.

The total heat transfer areas of these two models are not equal. The area used by the alternate ECCHTX model is larger than that of Ref. 6: the heated part of the walls are considered by the alternate ECCHTX model. This is consistent with a "confined" scenario.

Two rooms were considered: a small one (2.4m x 3.6m x 2.4m, high) and a large one (5.0m x 4.0m x 5.4m, high). As in Ref. 6, three fires were used, for each of the four different ceiling materials of Table 2-5(A), in each of the two rooms. A burner fire algorithm was used to model a T-squared fire, a small steady fire, and a large steady fire. The steady fires were sized and calculated to correspond to the heat release rates and Q_H^* (see Eq. 2.3-2(A)1a) values used in Ref. 6. The "fuel" of the burner is the urethane mattress of the standard CFC case. The scenarios considered are identified by the "x'ed" pairs of Q and H of Table 2.5(B) (Ref. 6).

Thus, a total of 24 cases were run, more than half of

Table 2.5(A)

Ceiling Material Physical Properties

	Material			
	Concrete	**FIB**	**Gypsum**	**Steel**
Thickness (m)	0.0508	0.0127	0.0127	0.003175
k (W/m-°K)	0.92	0.04	0.134	46.0
α (m^2/s)	4.2E-7	1.2E-7	1.577E-7	120.0E-7
Density (kg/m^3)	2000	240	240	7800
cp (J/kg-°K)	1095	1389	3540	491
# of Nodes	20	19	16	2

Thickness, thermal conductivity, and thermal diffusivity from Ref. 2. Density and specific heat values are typical: not used individually, only their product is used.

Table 2.5(B)

H (m) = Q (kW) =	101.2	1000.	9883.	$0.1054\ (t/s)^2$ (t in seconds)
2.0	(2) x $Q_H^* = 0.01048$	(3) x $Q_H^* = 0.1035$		(1) x
5.0		(3) x $Q_H^* = 0.01048$	(4) x $Q_H^* = 0.1035$	(1) x

Description of Six Fire Scenarios
(Ref. 6)

them failed to converge before the problem end time of 300 seconds. One reason for this non-convergence problem may be attributable to the formulation of the model itself. The ceiling jet temperatures calculated by Eq. 2.3-2(B)1 have no apparent limitations: they increase as the heat release rate of the fire increases. However, there is a physical, upper limit on the ceiling jet temperature. No temperature within the enclosure should be higher than the flame temperature, otherwise the first law of thermodynamics is violated. Therefore, program logic was included to switch to the original ECCHTX model when the ceiling jet temperature rises above 1300K. Presumably, had this logic been implemented, CFC would have switched sooner than the end times shown in Table 2.5(C) and 300 seconds would have been obtained. Instead, the area weighted average ceiling jet temperature was limited to 2500K and the peak ceiling surface temperature was limited to 1300K. (When the logic was implemented, the switch occurred too early in the fire to provide meaningful results. Therefore, it was not used.)

As shown later in Fig. 2.5(D), 2.5(G), and 2.5(H), the FIB ceiling cases show an impingement point surface temperature of 1300K (equal to a rise of 1000K) and they appear to exhibit a numerical instability. This non-convergence problem may be traceable to where CFC accounts for the radiative energy loss of the extended ceiling. This calculation involves the difference of two

Table 2.5(C)

Calculation Information: "Unconfined" Cases

Case *	Total # of Time Steps	Total # of Iterations	CPU Time (sec)	End Time (sec)
A1C	55	2758	4:26.50	100
A2F	27	1939	6:05.46	40
A1G	100	3453	5:50.34	100
A1S	360	6855	10:59.18	90
A2C	155	5742	7:16.71	300
A2F	155	6005	7:40.21	300
A2G	155	5232	6:38861	300
A2S	1200	17762	23:11.81	300
A3C	610	26583	34:00.72	300
A3F	32	3042	4:41.03	50
A3G	565	25667	32:42.01	300
A3S	1200	28088	35:59:84	300

* Naming convention is:

First Character: A = small room, B = large room

Second Character: Fire number in parentheses shown in Table 2.5(B).

Third Character: Ceiling type = Concrete, FIB, Gypsum, Steel

Table 2.5(C) (cont.)

Calculation Information - "Unconfined" Cases

Case	Total # of Time Steps	Total # of Iterations	CPU Time (sec)	End Time (sec)
B1C	131	5711	6:44.07	200
B1F	200	10516	12:12.64	250
B1G	143	6154	7:37.03	220
B1S	7675	14487	18:08.41	190
B3C	181	6478	6:42.83	300
B3F	181	6337	6:33.53	300
B3G	181	6511	6:47.35	300
B3S	1205	24854	27:19.28	300
B4C	20	912	2:04.93	48
B4F	62	3174	5:43.60	49
B4G	23	1217	2:44.26	49
B4S	160	2900	4:54.58	44

very large numbers of similar magnitude and this condition has been known to lead to numerical instabilities in the past. The switching logic mentioned above is intended to eliminate this problem.

The scenario differences mentioned previously, do not facilitate a one-to-one comparison with the Ref. 6 data. However, one reasonable comparison is that between unconfined and confined ceiling scenarios, i.e., considering (or not) the presence and effect of elevated upper layer temperatures on ECCHTX. This being the case, higher temperature predictions are expected from the alternate ECCHTX model than the data of Ref. 6. These two formulations are expected to be qualitatively similar, however.

In Ref. 6, Cooper presents plots of normalized radial surface temperature distributions vs. r/H. Since this data is not normally available when using the alternate ECCHTX model, only one of these distributions will be considered for this verification. Figure 2.5(B) shows the normalized surface temperature at ten seconds for the small room, small steady fire, FIB ceiling case (A2F). The small inset figure is taken from Ref. 6 to provide the comparison. That these results are qualitatively similar is evident: both behave as expected. Upon close examination, it can be seen that the temperature gradient across the impingement zone,

Normalized Surf Temp
1.0
0.9
0.8
0.7
0.6
0.5
0.4
0.3
0.2
0.1
0.0
0.0
0.2
0.4
0.6
0.8
1.0
1.2
1.4
1.6
1.8
2.0
r/H
(T-T(AMB))/(T(R/H=0)-T(AMB))
R/H
Typical Radial Surface Temp Dist

Figure 2.5(B)

r/H < 0.2, is greater for the alternate ECCHTX model than for that of Ref. 6. This can be attributed to the points chosen in Sect. 2.3-4(A). Whether or not this is an acceptable error remains to be seen. If so, the point selection process can be easily changed to provide closer agreement.

Figures 2.5(C) through 2.5(H) present plots of the impingement point temperature rise above ambient and are constructed in a similar manner to Fig. 2.5(B): larger curves from the alternate ECCHTX model, inset from Ref. 6. The legends for the ceiling constructions for Fig. 2.5(C) through 2.5(H) are as follows:

Alt ECCHTX Model	**Ceiling Material**	**Ref. 6 Data**
+	Concrete	_____.
x	Fiber Insul Board	_____
□	Gypsum	.....
■	Steel	_.._.._.._.

Overall these figures provide verification of the alternate ECCHTX model. The temperatures predicted by the alternate ECCHTX model are indeed higher than the unconfined ceiling data predicted in Ref. 6 and thus illustrate the difference between confined/unconfined scenarios. Figures 2.5(C) and 2.5(D) present the small room data for the small and large steady fires. These data indicate that for a small steady fire in a small room (as defined above), the

Temperature Rise (deg K)
200.0
180.0
160.0
140.0
120.0
100.0
80.0
60.0
40.0
20.0
0.0
0
30
60
90
120
150
180
210
240
270
300
Time (sec)
Imp Pnt Temp Rise: Sm Rm, Sm Stdy Fire
(T(R/H=0)-T(AMB)), DEGS K
125
100
75
50
25
0
0
50
100
150
200
250
300
TIME (s)

Figure 2.5(C)

Temperature Rise (deg K)
1200.0
1000.0
800.0
600.0
400.0
200.0
0.0
0
30
60
90
120
150
180
210
240
270
300
Time (sec)
Imp Pnt Temp Rise: Sm Rm, Lrg Stdy Fire
(T(R/H=0)-T(AMB)), DEGS K
500
400
300
200
100
0
0
50
100
150
200
250
300
TIME (s)

Figure 2.5(D)

impingement point temperature rise is roughly 25-40% greater for the confined scenario than for the unconfined scenario, depending on the ceiling material.

For the large steady fire case in the small room, Fig. 2.5(D) indicates that the confined scenario predicts impingement point temperature rises more between approximately 1.5 and 2 times the impingement point temperature rises predicted by the unconfined scenario of Ref. 6. However, the qualitative comparison between the two models is good, i.e., up to the point where the prediction becomes unreasonable. (The ten second offset at the beginning of the ECCHTX model data is the result of the burner curve used: if the initial slope is too steep, convergence problems result). The FIB case failed to converge after 60 seconds. These results are readily explained when the ceiling properties and fire size are considered. FIB is a good insulator. Therefore, it conducts very little heat through its thickness. Because of this, the surface experiences a larger temperature rise than a poorer insulator (e.g., concrete or steel). Put simply, most of the "large steady" fire's convective energy goes into raising the surface temperature of the FIB.

In other words, relatively little of the fire's heat is lost through the enclosure surfaces by convection and conduction. However, in order to provide a stable solution

it seems that some (as yet undetermined) given fraction of the fire's total heat may be lost through enclosure surfaces. If this heat is not transferred, then the ceiling surface temperature increases very rapidly. The result is that the heat is contained within the enclosure, thus increasing the effective heat release rate of the fire to the point where the equations/methodology used by the model are inadequate. Therefore, the enclosure can be thought of as being too small to "contain" the fire and numerical instabilities are the ultimate result.

The formulation for the gas temperature appears to be the reason the alternate ECCHTX model predicts ceiling surface impingement point temperature rises greater than that of Ref 6. Unlike the current formulation for the gas temperature (i.e., the upper layer temperature) which depends on the amount of energy deposited in the layer, the alternate ECCHTX model gas temperature is driven by the convective heat release rate of the fire. Therefore, it is possible that the gas temperature could (unrealistically) increase to a point where unexpectedly large ceiling surface temperatures are predicted. In this way, the temperature limitations as imposed by the coding logic are met and numerical problems are encountered. The FIB run failed to converge after 60 seconds. The maximum area-weighted average ceiling jet temperature for the FIB ceiling case was on the order of 1800K while the maximum upper layer

temperature was roughly 800K. Due to the ceiling jet temperature limitation of 2500K on the average ceiling jet temperature, the gas temperature is unreasonable. Unfortunately, Cooper did not provide hot gas temperatures in Ref. 6. Had he done so, a comparison could have been made regarding the hot gas temperatures to determine if radiation plays a bigger part in the alternate ECCHTX model than in the model developed in Ref. 6.

However, these results also tend to indicate the degree to which increased upper layer temperatures are significant. In the alternate model ECCHTX cases, the upper layer thickness was greater than 0.24 times the room height. Therefore, the correction factors given by Eq. 2.3-2(A)2 and 2.3-2(A)3 are employed and this effectively increases the heat transfer to the ceiling by raising the near surface gas temperatures. The end result is that the (confined scenario) alternate ECCHTX model predicts significantly higher (impingement point) ceiling surface temperatures than the (unconfined) model of Ref. 6.

Figures 2.5(E) and 2.5(F) present the same data as Fig. 2.5(C) and 2.5(D) for the large room. Once again the qualitative agreement between the two models is good for the small fire cases of Fig. 2.5(E). The quantitative difference, as in the small room cases, is roughly 40%, also.

Figure 2.5(E)

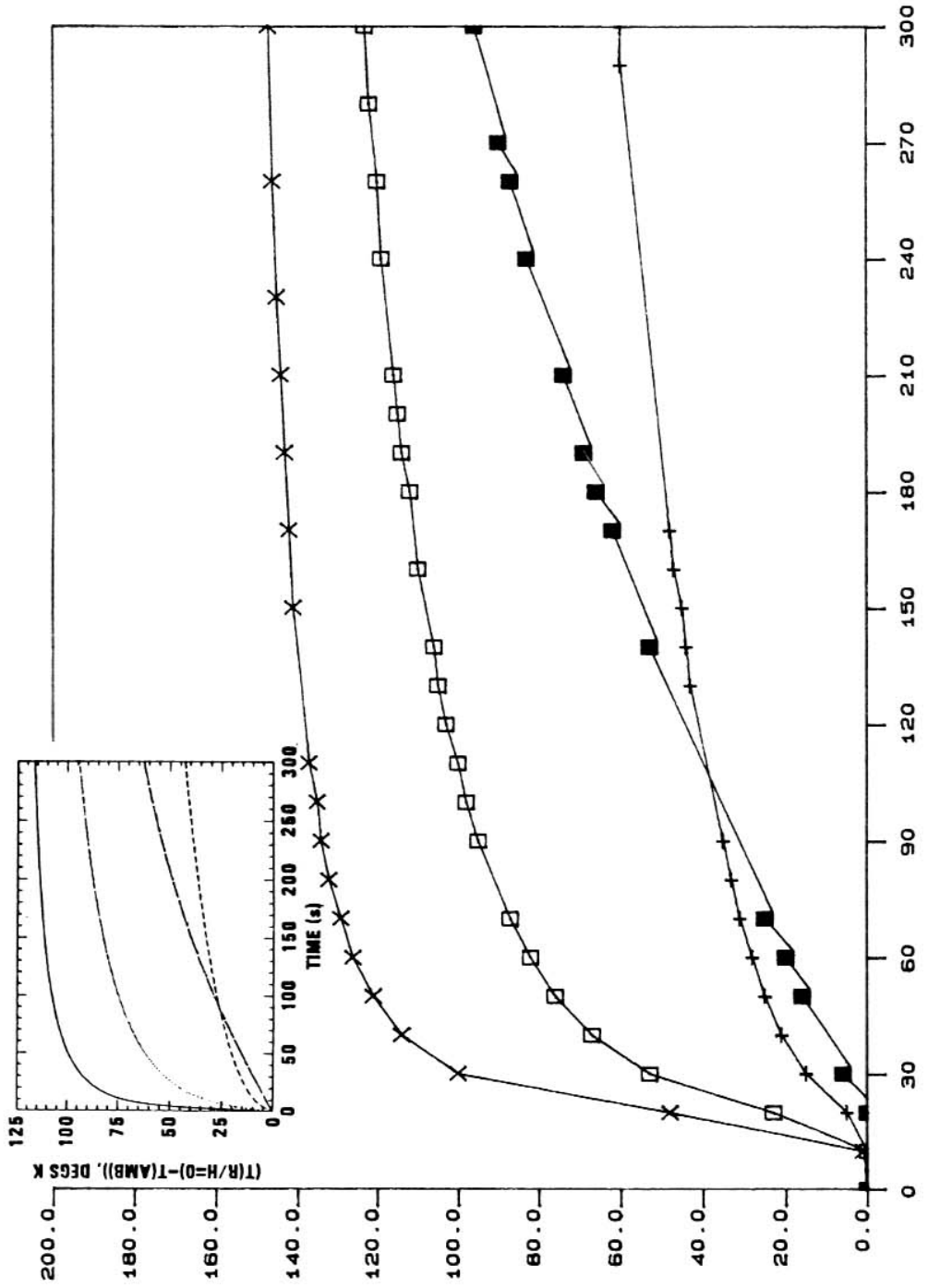
Imp Pnt Temp Rise: Lrg Rm, Sm Stdy Fire
Temperature Rise (deg K)
Time (sec)
0.0
20.0
40.0
60.0
80.0
100.0
120.0
140.0
160.0
180.0
200.0
0
30
60
90
120
150
180
210
240
270
300
(T(R/H=0)-T(AMB)), DEGS K
TIME (s)
0
25
50
75
100
125
0
50
100
150
200
250
300

Figure 2.5(F)

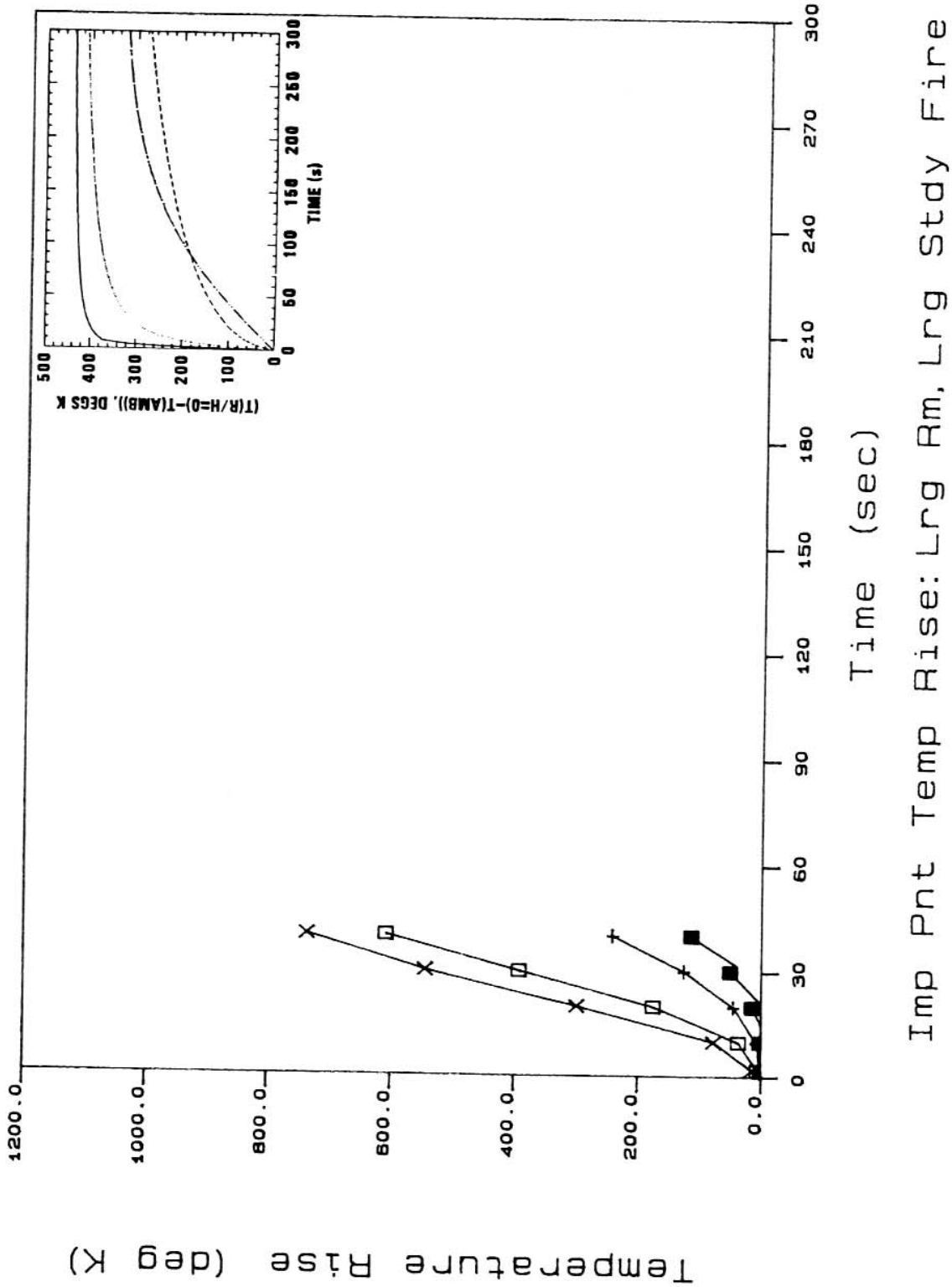
Temperature Rise (deg K)
1200.0
1000.0
800.0
600.0
400.0
200.0
0.0
0
30
60
90
120
150
180
210
240
270
300
Time (sec)
Imp Pnt Temp Rise: Lrg Rm, Lrg Stdy Fire
(T(R/H=0)-T(AMB)), DEGS K
500
400
300
200
100
0
0
50
100
150
200
250
300
TIME (s)

From Fig. 2.5(F) it would appear that the "large" fire is too large for the "large" room, as described above for the small room, large steady fire cases. Figure 2.5(F) appears to lend some credence to the fire being too large for an enclosure, from a numerical viewpoint. Up to about 40 seconds, the solution is well behaved, even for the FIB case (as compared to Fig. 2.5(D)). However, it would appear that the heat release rate at roughly 40 seconds is too severe to provide a stable solution.

Although the qualitative comparison between the two models for this scenario is not so good, at least the alternate ECCHTX model data is congruent with the expected, relative behavior of these materials. In the large steady fire cases for the large room, the results indicate that the heat release rate is severe enough to cause radiation effects to be significant. This would be contrary to the Ref. 6 model because in that model the layer would be thin, dispersed over a large area, and cooler than a confined model would predict. Therefore, Cooper's gas temperatures seem to be lower than those encountered in this verification.

Figures 2.5(G) and 2.5(H) present the impingement point temperature rise for the small and large room, T-squared fire cases. The alternate ECCHTX model data of Fig. 2.5(G) and Fig. 2.5(H) is somewhat inconclusive due to the "too

Temperature Rise (deg K)
1200.0
1000.0
800.0
600.0
400.0
200.0
0.0
0
30
60
90
120
150
180
210
240
270
300
Time (sec)
Imp Point Temp Rise: Sm Rm, T**2 Fire
(T(R/H=0)-T(AMB)), DEGS K
1000
800
600
400
200
0
0
50
100
150
200
250
300
TIME (s)

Figure 2.5(G)

Temperature Rise (deg K)
1200.0
1000.0
800.0
600.0
400.0
200.0
0.0
0
30
60
90
120
150
180
210
240
270
300
Time (sec)
(T(R/H=0)-T(AMB)), DEGS K
500
400
300
200
100
0
0
50
100
150
200
250
300
TIME (s)
Imp Point Temp Rise: Lrg Rm, T**2 Fire

Figure 2.5(H)

large" fire problem previously discussed, especially for the small room. The alternate ECCHTX model FIB data of these figures is noteworthy. Presumably the reason for the step increase in impingement point temperature rise for FIB in the small room case, Fig. 2.5(G), is similar to that for Fig. 2.5(D). However, from Fig. 2.5(H) it appears that after 170 seconds an incorrect root is being found for the FIB case. The reason for this is unknown and requires more extensive investigation. Other than that presented for the steady fire cases, no explanation for this prediction is given.

As with the other fire scenarios considered the T-squared scenario results indicate that the relative behavior of these materials is correct, which can be seen upon comparison with Cooper's data.

To illustrate that the lower ceiling surface convection heat transfer is significant in the ceiling surface temperature predictions, Cooper (Ref. 6) plots the convective heat flux divided by the total heat flux (at r/H = 0; the impingement point) as a function of time. In Ref. 6 the total net heat flux at the impingement point equals the local radiative flux from the fire to the ceiling plus the local convective heat flux minus the radiative flux from the ceiling to the ambient environment. Cooper uses data for the small room, T-squared fire scenario for this

calculation and the results are shown in Fig. 2.5(1), which uses the same legend as that of Fig. 2.5(C) through 2.5(H). Unfortunately, the alternate ECCHTX model does not provide this information for the impingement point. Instead, the area weighted average convective flux of the alternate ECCHTX model is added to the radiative flux from the plume to the ceiling and then the radiation from the ceiling to the upper layer is subtracted from the sum to arrive at the total net heat flux to the ceiling as a whole. The plot of this value vs. time is shown in Fig. 2.5(J) for the alternate ECCHTX model small room, T-squared fire scenario. This figure also uses the legend of Fig. 2.5(C) through 2.5(H). When comparing Fig. 2.5(J) to Fig. 2.5(I), the data of Fig. 2.5(J) are not entirely conclusive. It seems that the difference between these two figures is attributable to (1) the difference between comparing local conditions to bulk conditions, (2) the difference between the two models in how the radiation from the combustion zone to the ceiling is calculated, as mentioned above, and (3) instability problems on the part of the alternate ECCHTX model when using a steel or FIB ceiling. However, when considering the gypsum and concrete ceilings and the alternate ECCHTX model, it can be seen that the average convective heat flux is generally of the order of the total net heat flux.

From this viewpoint, the results indicate that ECCHTX within an enclosure is more severe when the upper layer is

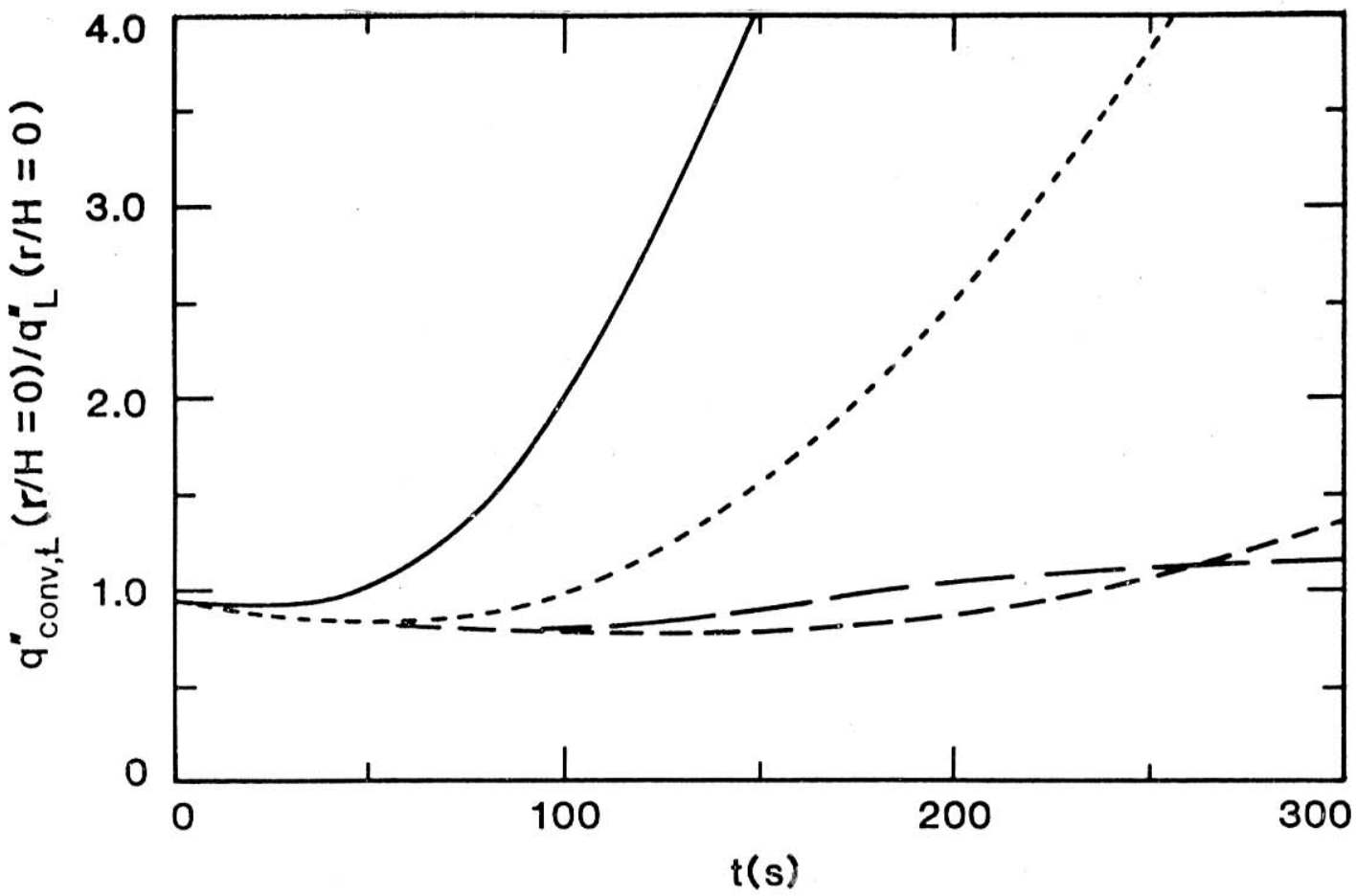

Figure 2.5(I) Ref. 6 Normalized Impingement Point Heat Flux

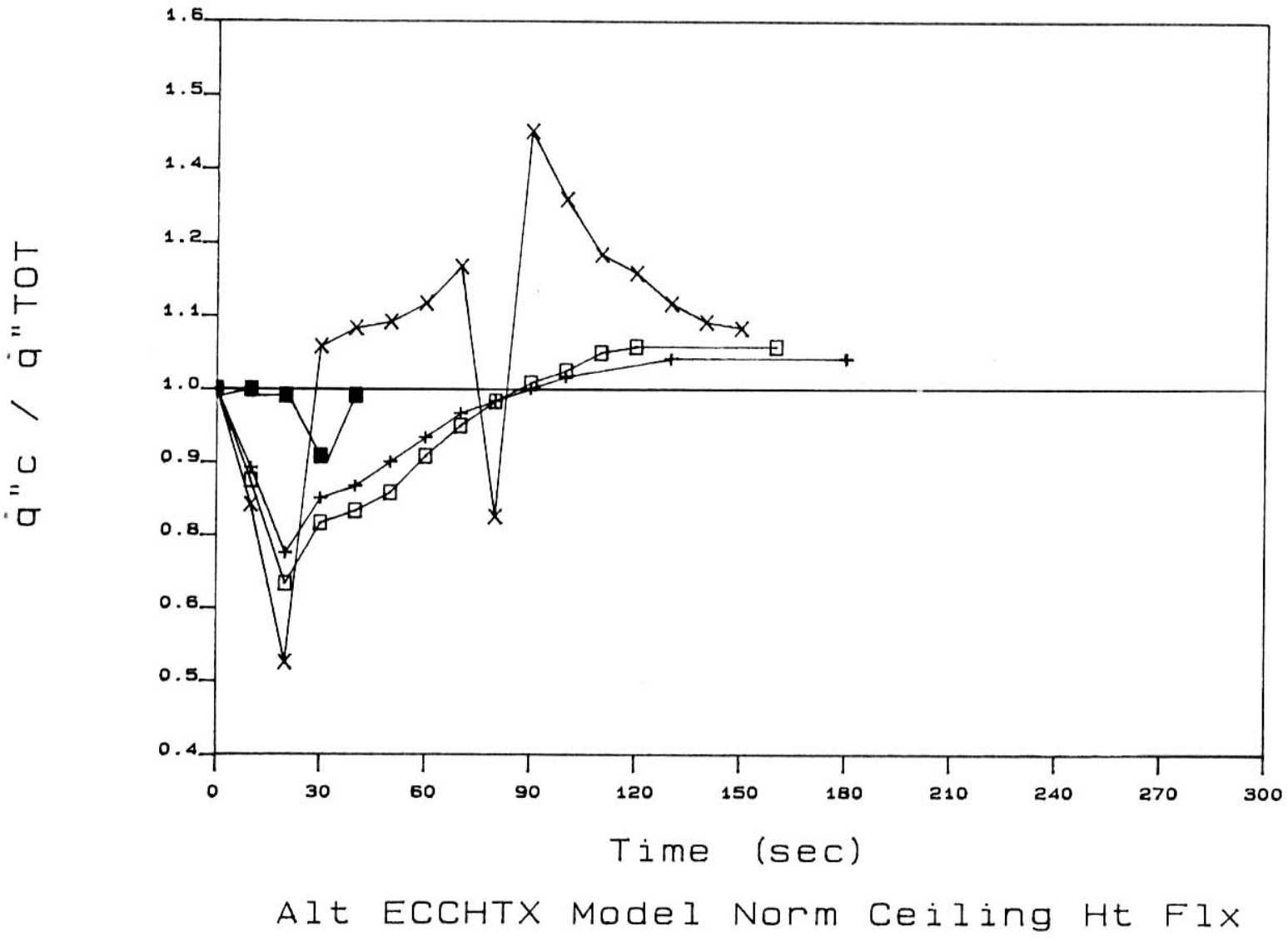
q"c / q"TOT
1.6
1.5
1.4
1.2
1.1
1.0
0.9
0.8
0.6
0.5
0.4
0
30
60
90
120
150
180
210
240
270
300
Time (sec)
Alt ECCHTX Model Norm Ceiling Ht Flx

Figure 2.5(J)

thicker than when the layer is at a minimal depth. Specifically, this severity is manifested in the form of increased gas temperatures which subsequently result in higher ceiling surface temperatures. This result is not unexpected since it is one of the major effects of increased upper layer thicknesses. However, the absolute value of the ceiling surface temperatures for some scenarios are questionable and require further verification: specifically the large room/large steady fire case and the T-squared fire cases. These results also indicate that knowledge of the radial surface temperature distribution of the extended ceiling during a particular case is desirable from a ceiling failure viewpoint. Specifically, these impingement point temperatures show that ceiling burn-through or combustion is an effect whose occurrence should be considered in enclosure fire computer models.

As indicated by Table 2.5(C), total number of time steps and iterations required for a given problem is highly dependent on the various components of the problem. In general steel ceilings will take longer and well insulated ceilings when used in conjunction with fires which are, or grow to be, large will most likely result in convergence or instability problems.

3.0 Ceiling Vent Mass Flow Rate

A brief description of the existing CFC/WPI ceiling vent mass flow rate model and its underlying assumptions will be presented first. This will be followed by a description of the available models that may be used as the basis for an alternate CVMFR model. Finally a description of the alternate CVMFR model itself will be discussed, followed by a description of the subroutines required by the alternate model.

3.1 Current CFC Model

The ceiling vent model currently employed by CFC/WPI ignores the presence of the fire plume and ceiling jet. In this model the pressure differential which drives the CVMFR is assumed to be attributable to the difference between the static pressure at the ceiling and the pressure at the floor of the enclosure. The upper and lower layers are assumed to be in static (i.e., quasi-steady) equilibrium and the pressure in the enclosure is hydrostatic. The pressure at the ceiling inside the enclosure is a function of the pressure at the floor and the densities and thicknesses of the two layers. See the appendix for a more detailed description of the current CFC/WPI CVMFR model. In this scenario, the pressure will decrease with increasing elevation because the weight

per unit cross sectional area of the two layers decreases with increasing height above the floor of the enclosure. The resulting vent flow then becomes a simple function of the buoyancy induced pressure differential, vent area, and the upper layer and ambient densities. Furthermore, the radial distance from the plume axis does not enter into the current model.

Since this model only addresses the general conditions in the upper portion of the fire enclosure, i.e., does not account for conditions directly below the vent, a more realistic model can be developed which considers the presence of a ceiling jet and the location of the fire plume relative to the vent. The ceiling jet is particularly significant for large fires where the momentum of the fire plume tends to be large. In other words, for large fires the inertial forces associated with the fire plume and ceiling jet are significant enough that they should be considered when determining the CVMFR, especially if the vent is near the fire plume axis. Optimally, the ceiling vent model should incorporate the phenomena detailed above and have provision for upper layer effects as described in Sect. 2.3-2(A), conditions at other ceiling vents which may be downstream of an open ceiling vent, and the possibility of entraining upper layer gases out through the ceiling vent; i.e., if the ceiling jet rises entirely through the vent, other gases will also be discharged through the

ceiling vent.

3.2 Available Models

Other than the model currently used by CFC/WPI, there appears to be only one other available model for CVMFR. This model is the result of the work of two independent research efforts: the second building upon the first. The first model, proposed by Thomas, et al., (Ref. 18), is a theoretical and experimental investigation of ceiling vent behavior. In this study the main concern was "the effects of various sizes of vent area and depths of roof screen upon the flow of heat and smoke from various sizes of fires in buildings of different height" (Ref. 18). The theory behind the experiments of Thomas, et al., was developed for flat roof ceiling vents and then extended to pitched roofs. This theory was based on four assumptions: (1) fire plume of hot gases originates at a virtual point source below the actual height of the burning object (thus the theory is restricted to the early stages of a fire, i.e., when it is small), (2) a relatively stagnant hot upper layer forms beneath the ceiling (within the confines of the roof screens) and no interlayer mixing is allowed, (3) uniform hot layer temperature due to perfect mixing, and (4) heat loss to walls by conduction and radiation is negligible. Bernoulli's theorem was then applied to develop an expression for the mass flow rate of gases through a ceiling

vent. No systematic differences between the experimental data and the results from the theoretical expression (to be discussed below) were observed (Ref. 18). The experimental apparatus was a scale model of a large, one story, pitched roof building having smoke curtains and ceiling vents.

The primary difference between the current CFC/WPI CVMFR model and Thomas, et al., is the pressure differential, Δp, used by the two formulations. Basically, these two formulations for vent flow take the form:

Eq. 3.2(A)

$$\dot{m}_v = C_v A_v \rho (2g)^{\frac{1}{2}} (\Delta p)^{\frac{1}{2}}$$

where: $\dot{m}_v$ = mass flow rate out the ceiling vent

C_v = ceiling vent discharge coefficient

A_v = ceiling vent area

ρ = density of vented gas

g = acceleration of gravity

Δp = pressure differential

In the current CFC/WPI model, Δp in Eq. 3.2(A) is given by:

Eq. 3.2(B)

$$\Delta p = p_f + \frac{(h_r - h_L)(\rho_a - \rho_L)}{\rho_a} + \frac{h_L(\rho_a - \rho_u)}{\rho_a}$$

where: p_f = pressure at the floor

h_r = room height

h_L = upper layer height

ρ_a = ambient density

ρ_L = lower layer density

ρ_u = upper layer density

and for Thomas, et al., this term is, effectively, Eq. 74 of Ref. 18:

Eq. 3.2(C)

$$\Delta p = h_L \frac{(T_c - T_a)}{T_a}$$

where: T_c = gas temperature at the ceiling vent

T_a = ambient temperature

Figures 3.2(A) and 3.2(B) present the scenarios modeled by these two approaches. In addition to the ceiling vent flow $\dot{m}_v$, Fig. 3.2(A) also shows the other mass flows of interest: $\dot{m}_{D,u}$ = upper door flow, $\dot{m}_{D,l}$ = lower door flow, $\dot{m}_m$ = mass of exiting upper layer gases entrained by and mixed with the inlet (lower door) flow, $\dot{m}_e \equiv$ mass of air entrained by the plume, and $\dot{m}_p$ = plume flow. Q(t) represents the heat output of the fire. Note: in Fig. 3.2(B), $d_b \equiv h_L$, $h_c \equiv h_r$. The temperatures required in Eq. 3.2(C), T_c and T_a, are taken to be the (uniform) temperature of the layer of hot gases, T_u, and the temperature at the floor of Fig. 3.2(B). The inlet area in Fig. 3.2(B) is assumed to be large.

Figure 3.2(A)

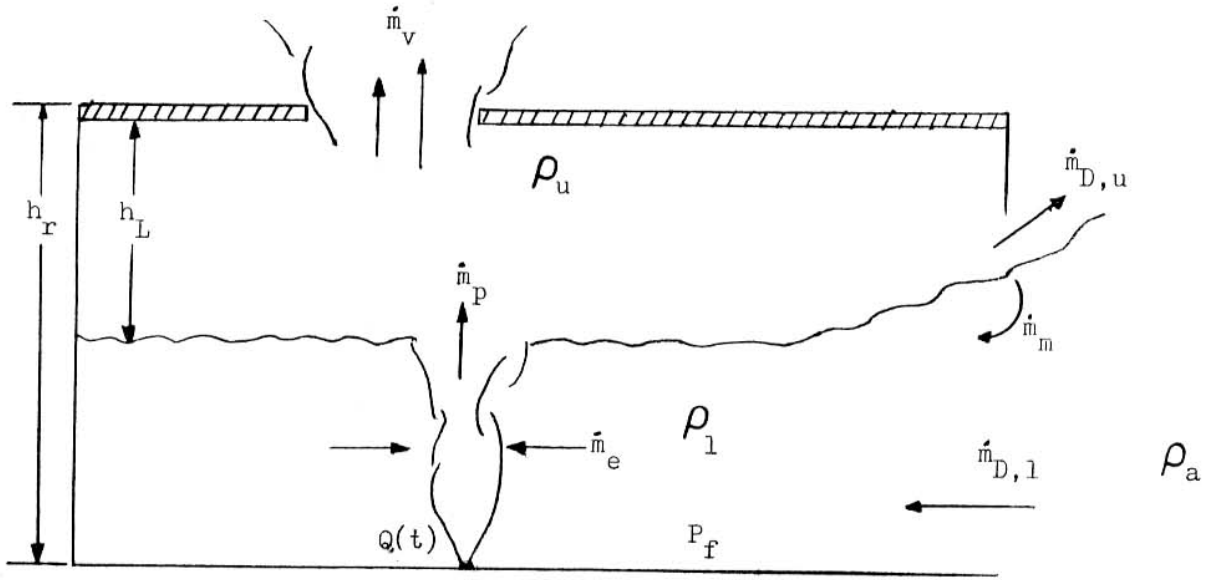

Current Model: Ceiling Vent Scenario

Figure 3.2(B)

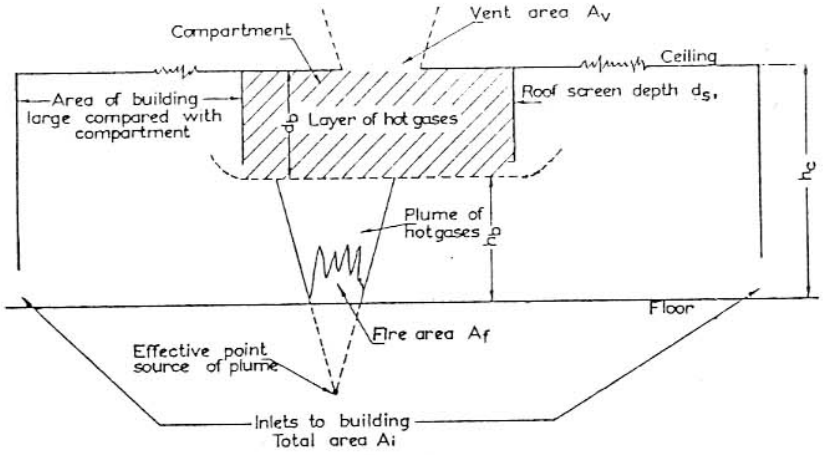

Thomas, et al, Model: Ceiling Vent Scenario

(Ref. 19)

The second model is that of Mitler (Ref. 17) which generalizes the theoretical formulation of Thomas, et al. Mitler's approach is strictly theoretical and there are no known data which might provide verification. Essentially, Mitler accomplished this by first deriving the same theoretical formulation as Thomas, et al., describing ceiling vent discharge; Eq. 3.2(A) and 3.2(C). Mitler then derives another expression which considers the inlet pressure drop ignored by Thomas, et al. In other words, the scenario of Fig. 3.2(B) no longer applies. Instead, the inlet for cold air flow is not appreciably larger than the ceiling vent area, the total inlet area in the external walls of the building is also small (in the case of CFC this is equal to the total inlet area to the enclosure), and the layer interface remains above the soffit. The would be similar to Fig. 3.2(A) except $\dot{m}_m = \dot{m}_{D,u} = 0.0$ because the layer would not be deep enough to make these flows greater than zero; i.e., the fire is small, early in its growth. Because of this, the fuel gas flow rate, $\dot{m}_f$, is assumed to be small when compared to other flows. The result is another expression for the pressure drop of Eq. 3.2(A) (Eq. 22, Ref. 17):

Eq. 3.2(D)

$$\Delta p = h_L \frac{T_a(T_u - T_a)}{T_u(T_u + T_a R_a^{\,2})}$$

where: T_u = upper layer temperature

$R_a = C_v A_v / C_i A_i$

C_i = inlet coefficient

A_i = inlet flow area

Mitler's next step is to allow the layer interface to drop below the soffit. This implies that the fire has grown to the point where the volume of its products of combustion is great enough to permit some mass of the upper layer to leave the enclosure, as shown in Fig. 3.2(A) by $\dot{m}_{D,u}$. In addition, the fuel flow rate, $\dot{m}_{py} = |\dot{m}_f|$, is also used in the steady state mass conservation expression for the upper layer that relates the inlet flow, $\dot{m}_I$ (= $\dot{m}_{D,l}$ of Fig 3.2(A)) to the ceiling vent flow, $\dot{m}_v$ (Eq. 26, Ref. 17):

Eq. 3.2(E)

$$\dot{m}_i + \dot{m}_{py} = \dot{m}_v + \dot{m}_{door}$$

where: $\dot{m}_{door}$ = rate of mass flow through other vents (i.e., doors and windows)

In this formulation, the area associated with the inlet flow, $\dot{m}_i$, is the actual area, of the doors/windows, through which fluid enters the enclosure. With some substitution Eq. 3.2(E) becomes (Eq. 27, Ref.16):

Eq. 3.2(F)

$$C_i A_i \rho_a u_i + \dot{m}_{py} = \dot{m}_{door} + C_v A_v \rho_u u_v$$

where: u_i, u_v = inlet and ceiling vent gas velocities

The final step is to find the Δp to be used in Eq. 3.2(A). This is obtained by employing Bernoulli's theorem and by solving Eq. 3.2(F) for u_i as a function of u_v. Thus, the pressure difference is found to be:

Eq. 3.2(G)

$$\Delta p = \frac{\{(1/\rho)[h(\rho_a - \rho) + H_d(\rho_a - \rho_d)](\rho_a^2 + \rho\rho_a R_a^2)\}^{\frac{1}{2}} - \beta R_a/(2g)^{\frac{1}{2}}}{\rho_a + \rho R_a^2}$$

where: h = upper layer depth

ρ = upper layer density

H_d = floor-to-layer interface distance

$\beta = (\dot{m}_{door} - \dot{m}_{py})/(C_i A_I)$

$R_a = (c_v A_v)/(c_i A_I)$

This formulation has the advantage of being able to accommodate the upper layer mass entrained by the inlet flow ($\dot{m}_m$ of Fig. 3.2(A)) by allowing the lower layer to increase in temperature. Thus Mitler has developed a generalization of Eq. 3.2(A), in combination with Eq. 3.2(G), "for the case where there is outflow through the "door(s)", and where lower layer temperature may not be ambient" (Ref. 17).

Up to this point Mitler, in Ref. 17, has generalized the theoretical formulation of Thomas, et al., (Ref. 18). In essence he has recast the Ref. 18 formulation in enclosure fire terms and slightly extended the range of applicable fire sizes. The next logical step is to

consider larger fires. To this end, Mitler states in Ref. 17, "when the fire in the burn room is very large, so that flames reach the ceiling or may emerge through the vent, these expressions (Eq. 3.2(A) used with 3.2(G)) must be modified." Thus, Mitler expects "that the momentum of the flames begin to play a role in the venting" (Ref. 17).

First Mitler considers the scenario in which a axisymmetric flame is centered below a ceiling vent. The presence of the vent is assumed to have negligible effect on the mean upward velocity of the plume. In this case, the mean vent flow corresponds to the sum of a dynamic pressure, associated with the plume, and the static pressure as previously described, i.e., the small fire case. This results in an equivalent expression, which relates the effective vent velocity, V, to the "small fire" vent velocity, u_v, and the upward flame velocity, u_f as (Eq. 35, Ref. 17):

Eq. 3.2(H)

$$V = (u_v^{\,2} + u_f^{\,2})^{\frac{1}{2}}$$

The velocity, u_v, is the result of multiplying Eq. 3.2(G) by $(2g)^{1/2}$ and is given by Eq. 3.3-2(B). The expression for u_f is based on work done by McCaffrey and is given by Eq. 43 and 44 of Ref. 17:

Eq. 3.2(I)a

$$u_f \approx 0.412 v_c(\text{tip})$$

Eq. 3.2(I)b

$$V_c(\text{tip}) \approx 2\dot{Q}^{\frac{1}{5}}$$

where: $\dot{Q}$ = heat release of the fire (kW)

v_c = centerline velocity

The vented gas velocity, V, can be used in conjunction with Eq. 3.2(A), to predict ceiling vent flow rates, by noting the following equivalence:

$$v \equiv (2g)^{1/2}(\Delta p)^{1/2}$$

Thus, Eq. 3.2(A) becomes:

Eq. 3.2(J)

$$\dot{m}_v = C_v A \rho_v$$

When the vent is not centered over the fire, the situation becomes more complex because the fire plume impinging on the ceiling creates a ceiling jet which becomes less energetic as radial distance from the fire plume axis increases. Mitler postulates two possibilities for the case where the vent is far from the plume axis "so that a ceiling jet of density, ρ_c, and thickness, Δ, flows past the vent with velocity u_c" (Ref. 16), see Fig. 3.2(C) (Ref. 16). In order to simplify the formulation, Mitler assumes "that the hot layer (of density ρ) which lies under the ceiling jet has the (constant) thickness h-Δ so that the layer and the jet rise together as shown" (Ref. 16) in Fig. 3.2(C).

Figure 3.2(C)

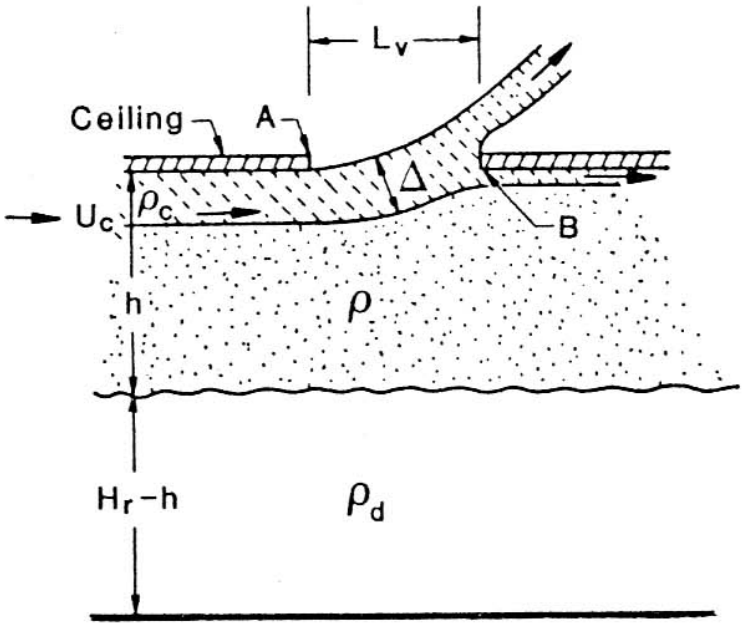

Ceiling Jet Rise Through a Ceiling Vent
(Ref. 18)

Mitler treats the problem from a trajectory viewpoint by considering the distance the layer (and ceiling jet) rises through the vent while the ceiling jet has moved across the plane of the open vent. He does this by first deriving an expression for the pressure difference between the top of (but inside) the ceiling jet and at the top of the ceiling jet, outside the room (Eq. 47, Ref. 17):

Eq. 3.2(K)

$$D \equiv p_f - p_a + g(\rho_a - \rho_d)(H + \delta) + gh(\rho_a - \rho) + g\Delta(\rho - \rho_c)$$

where: p_a = ambient pressure

H = floor-to-ceiling height

δ = distance ceiling jet rises in the vent as described below

a = acceleration as described below

L_v = vent length

u_c = ceiling jet velocity as described below

Δ = ceiling jet thickness

= 0.125H (Eq. 53', Ref. 17)

The ceiling jet and hot layer are assumed to rise together, with the ambient air above them, as a rigid sphere. The acceleration per unit area, attributable to the (buoyant force per unit area) pressure difference of Eq. 3.2(K) is given by (Eq. 49, Ref. 17):

Eq. 3.2(L)

$$a \approx \frac{D}{[\rho(h - \Delta) + \rho_c \Delta + \rho_a (h/2)]}$$

Two situations are now possible: if the ceiling jet velocity is large enough, the entire ceiling jet thickness will not rise through the vent, as shown in Fig. 3.2(C). If the ceiling jet velocity, u_c, is small, the ceiling jet momentum is also small and the entire ceiling jet plus some of the upper layer gases are discharged through the ceiling vent. Thus, the ceiling jet rises the distance δ through a vent of length L_v as (Eq. 51, Ref. 17):

Eq. 3.2(M)

$$\delta = (a/2)(L_v/u_c)^2$$

where the value of u_c is provided by (Eq. 53", Ref. 17):

Eq. 3.2(N)

$$u_c = 0.365^{u_f}$$

The ceiling jet velocity could also be a function of r/H (or r) as for the alternate ECCHTX model and not just the heat release rate of the fire, as in Eq. 3.2(N). However, this portion of Mitler's formulation was left intact so that the ceiling jet velocity is a function of heat release rate only for the alternate CVMFR model.

Therefore, when $\delta \leq \Delta$ the ceiling jet does not entirely rise through the vent, as shown in Fig. 3.2(C) and the vent mass flow rate is given by (Eq. 52, Ref. 17):

Eq. 3.2(O)

$$\dot{m}_v = (a\rho_c A_v L_v)/(2u_c)$$

This formulation neglects any effects caused by the

downstream vent lip and Mitler states "whether this is a justifiable simplification remains to be seen" (Ref. 17).

When the entire ceiling jet does rise through the vent, $\delta > \Delta$, some part of the ceiling vent area is available to discharge gases of the upper layer. The mass flow rate of the ceiling jet only is given by (Eq. 55, Ref. 17):

Eq. 3.2(P)

$$\dot{m}_{vJet} \approx B_v \rho_c \Delta \tilde{u}_c$$

where: B_v = vent width

$\tilde{u}_c$ = effective vented ceiling jet velocity

$$= [u_c^2 + (2C_d^2 D)/\rho_c]^{1/2}$$

C_d = appropriate efflux coefficient

The formulation for $\tilde{u}_c$ is intended to account for the indistinct dividing line between "large" and "small" fires, i.e., when u_c is large (comparable to the near axis case) and when u_c approaches zero.

The mass flow rate of the upper layer that leaves the vent concurrent with the ceiling jet is given by combining Eq. 3.2(A) with Eq. 3.2(D) with the efflux area for the upper layer as $B_v L_v'$. B_v is the vent width, normal to the ceiling jet flow and L_v' is the vent length available to discharge the upper layer gases. This length is determined by considering the trajectory of the ceiling jet and is given by (Eq. 57 and 58, Ref. 17):

Eq. 3.2(Q)

$$L_v' = Lv - \tilde{u}_c t$$

$$= L_v - \tilde{u}_c[(2\Delta)/a]^{1/2}$$

where: t = time (sec)

Therefore, to arrive at the vent flow due to the ceiling jet rising entirely through the vent along with a portion of the upper layer, these two flows are added to give (Eq. 59, Ref.18):

Eq. 3.2(R)

$$\dot{m}_v = B_v \rho_c u_c \Delta + C_v B_v L_v' \rho_a [2ghr(1-r)/\xi]^{1/2}$$

where: $r \equiv \rho/\rho_a = T_a/T$

$$\xi = 1 + rR_a^2$$

The final situation to be considered is an intermediate one: where the vent is neither over the fire nor far from it. Mitler states that this intermediate situation is "too complicated to handle" (Ref. 17). Although this does represent a shortcoming of this particular model, it does not detract from the model's usefulness as a theoretical tool.

Another alternate method for determining CVMFR was also considered. This method involved combining the static pressure results of Faeth (Ref. 10) and the ceiling pressure profile of Heskestad (Ref. 12). In order to use this approach, however, the Ref. 12 ceiling pressure profiles

must be assumed to apply to all fire enclosure scenarios and to all fires. There is no justification for this broad assumption, thus the approach's applicability is in doubt. In order to obtain a realistic model, suitable to production work, it seems desirable to include specific variables (e.g., ceiling jet thickness and velocity); this "combination" approach does not introduce these variables, whereas the alternate model previously discussed at least provides some of the requisite "hooks". In other words, the opportunity exists to include these variables now so why not take advantage of them. Also, of minor concern, is that the purpose of Ref. 12 is to arrive at the convective heat release rate of the fire; since it does not address ceiling vents, per se, its applicability is in question.

3.3 Alternate Model

The model proposed by Mitler in Ref. 17 was chosen as the basis for the alternate CVMFR model. Of the possibilities considered above, it is the most comprehensive. Due to the nature of Mitler's model, i.e., untried and unproved, the purpose of this alternate CVMFR model is to perform some numerical experiments to determine the plausibility of Mitler's model. This model is also broken into two parts: one for small fires and one for large fires. These models are described in Sect. 3.3-2 and 3.3-3. The next section details some additional assumptions

required by the model.

3.3-1 Assumptions

Assumptions one through six of Sect. 2.3-1 are also applicable to the alternate CVMFR model. In addition, the following assumptions are made:

1. The ceiling jet is assumed to have a constant thickness of 0.124 times the floor-to-ceiling height (as used in Ref. 17), and a velocity which is a constant fraction of the plume velocity, independent of distance from the plume centerline/ceiling height.
2. For CVMFR calculations, the ceiling jet flow will be equal to zero at the ceiling boundaries, i.e., the ceiling jet does not impinge on the wall and create a downward (or upward if possible) wall flow, see right hand side of Fig. 2.3-3(A). This avoids, at present, having to account for the change in flow direction at the wall and its associated ramifications. This assumption may be acceptable for all ceiling vents except those near the walls. Those ceiling vents near the wall can still use the alternate CVMFR model.

Yet again, this is another topic requiring theoretical and experimental verification.

3. The ceiling jet is a factor for ceiling vents "downstream" of other open ceiling vents. In other words, the CVMFR through these downstream vents will be calculated as though no other ceiling vents are present. It may be possible to model these downstream vents. If the equations derived by Mitler, concerning the ceiling jet rise through the vent, then the appropriate logic could be added to keep track of which vents are upstream and which are downstream.

3.3-2 Small Fires

The distinction between large and small fires is that flames of large fires touch the ceiling, whereas those of small fires do not. Therefore, the flame height, l, is required and is computed from the correlation presented by Heskestad (Ref. 13):

Eq. 3.3-2(A):

$$l = 0.23\dot{Q}_c^{\,2/5} - 1.02D$$

where: $\dot{Q}_c$ = rate of heat release (kW)

D = fuel bed diameter (m)

The CVMFR for the alternate CVMFR model's small fire is similar to the model used by CFC/WPI. From Eq. 3.2(J) this formulation is:

$$\dot{m}_v = C_v A \rho V$$

where: C_v = discharge coefficient

A = ceiling vent area

ρ= vented gas density

V = vented gas velocity = u_v of Eq. 3.2(H)

Eq. 3.3-2(B)

$$u_v = \frac{\{(2g/\rho)[h(\rho_a - \rho) + H_d(\rho_a - \rho_d)](\rho_a^2 + \rho\rho_a R_a^{1/2})\}^{1/2} - \beta R_a}{\rho_a + \rho R_a^2}$$

where: h = upper layer depth

ρ = " " density

H_d = floor-to-layer interface distance

ρ_a = ambient density

ρ_d = lower layer density

β = $(\dot{m}_{door} - \dot{m}_{py})/(C_i A_i)$

R_a = $(C_v A_v)/(C_i A_i)$

Cv,Ci = flow coefs. for ceiling vents, doors/windows

A_v, A_i = area of ceiling vents, doors/windows

$\dot{m}_{door}$ = hot gas mass flow rate out doors/windows

$\dot{m}_{py}$ = fuel flow or pyrolysis rate

This equation replaces Eq. 31 of Ref. 17 which was discovered to have an algebraic error. Equation 3.3-2(B) is the result of rederiving the vent gas velocity of the

scenario in question.

3.3-3 Large Fires

The model for large fires is also divided into two parts depending on the proximity of the ceiling vent to the fire plume axis. The distinction here is based on the ceiling impingement stagnation zone: $r/H < 0.2$. If any portion of the vent is within this zone, it will be considered to be centered over the fire plume axis; otherwise the vent is "far" from the fire plume axis. This is, admittedly, a gross simplification but in view of the scarcity of pertinent data it shall be assumed to be appropriate.

3.3-3(A) Vent Near Plume Axis

For ceiling vents centered above or near the fire axis, the CVMFR is calculated with Eq. 3.2(J) where V is defined by Eq. 3.2(H).

3.3-3(B) Vent Far From Plume Axis

For ceiling vents "far" from the fire, two situations occur: either part or all of the ceiling jet rises through the vent. If the ceiling jet partially rises through the vent, as shown in Fig. 3.2(C), the CVMFR is given by Eq. 3.2(O).

If the ceiling jet rises entirely through the ceiling vent the CVMFR is given by Eq. 3.2(R).

3.4 Required Programming

In order to incorporate the CVMFR model proposed by Mitler into CFC/WPI, a total of ten subroutines and four function routines are required. They are similar in function to subroutine HFLOW which is currently used by CFC/WPI. Figure 3.4(A) presents a flowchart of the alternate CVMFR model. Figure 3.4(B) is a decision flowchart which directs the calculation so that the "correct" CVMFR may be calculated, depending on the conditions encountered by the ceiling vent. A description of each of these subroutines is now provided.

3.4-1 CVMF01

This subroutine is the controlling routine for the alternate CVMFR model. Several "set up" calculations are performed; the plume source-to-ceiling-distance of object one is determined once for the entire run (and is subject to the limitations discussed in the Note of Sect 2.4-1), and the vent areas (provided by subroutine VENTA), total pyrolysis rate of all objects, total gas flow rate out through the doors/windows, two constants (R_a and β defined in Eq. 3.3-2(B) required in subsequent calculations, and

Figure 3.4(A)

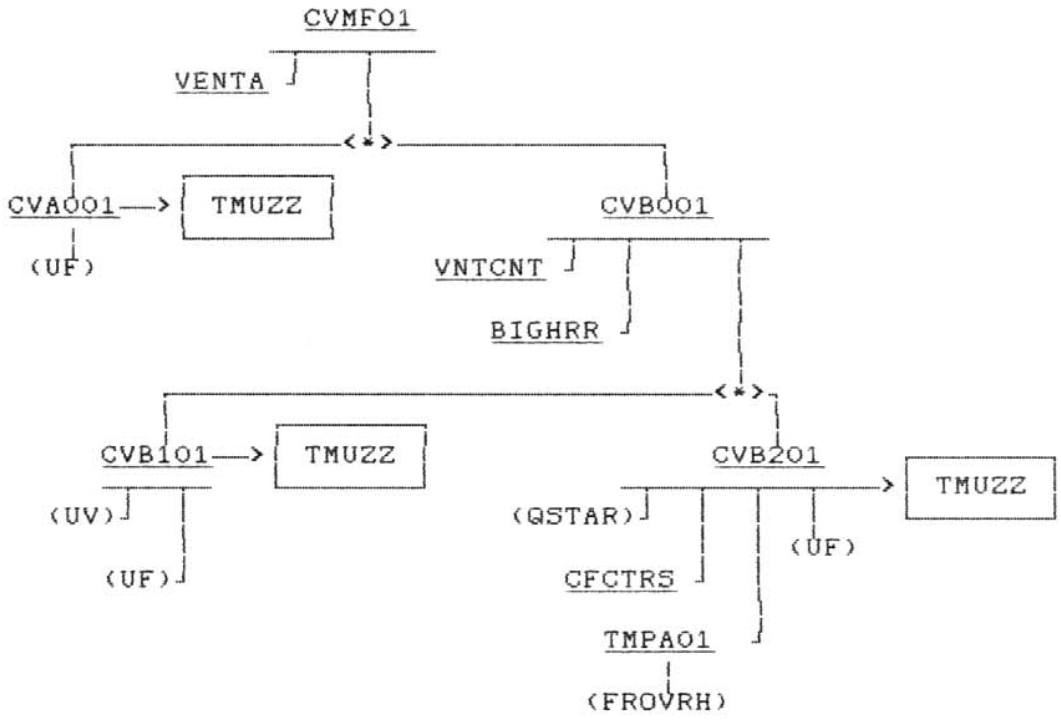

Underlined parameters are subroutine names and those in parentheses are function names as described in Section 3.4. All subroutines/functions shown were developed for the alternate CVMFR model. No existing CFC subroutines/functions were required.

Parameters in boxes are output variables: TMUZZ = ceiling vent mass flow rate. "<*>" indicates a decision: see Fig. 3.4(B) for additional information.

Alternate CVMFR Model Flowchart

Figure 3.4(B)

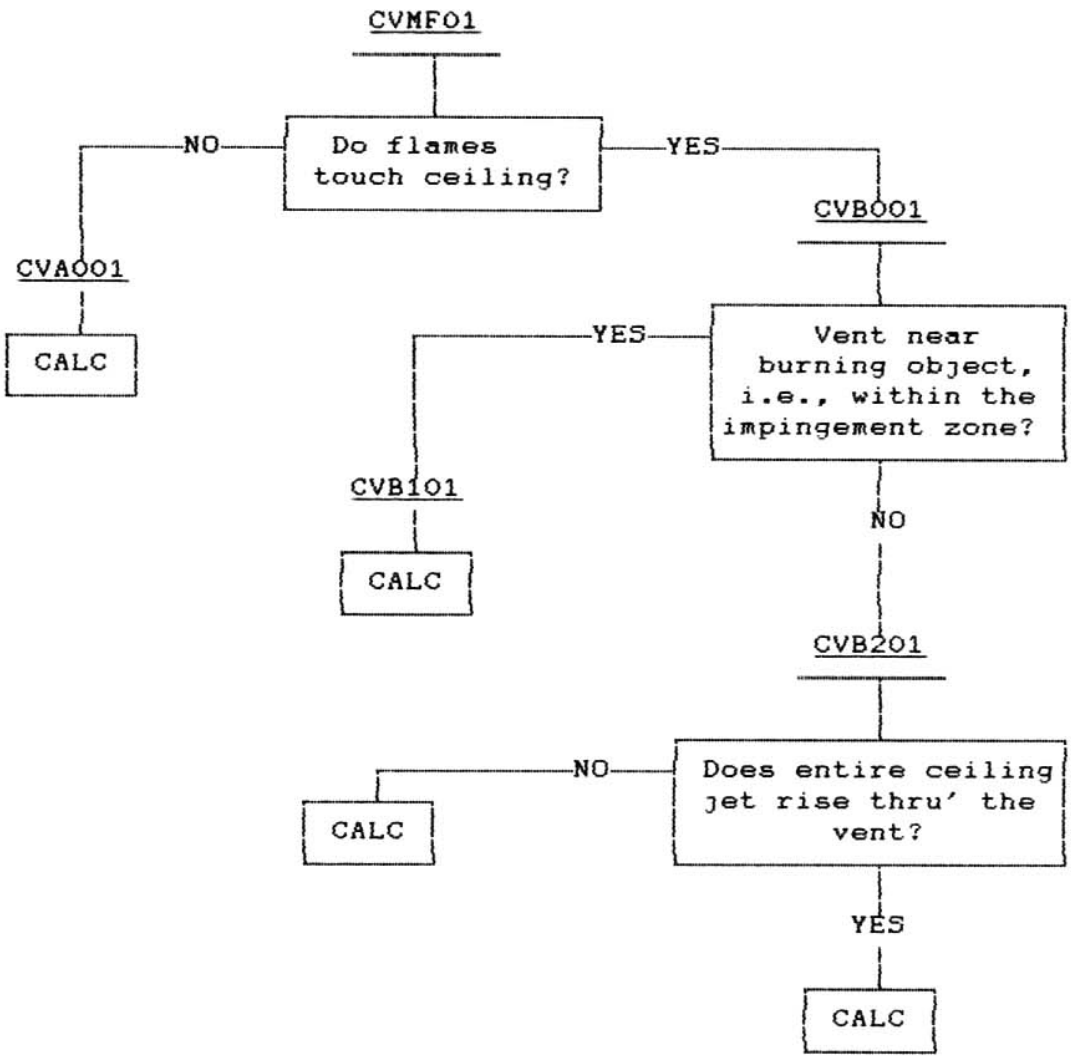

Boxes represent logic blocks and CALC indicates that the ceiling vent flow is calculated at that point. Subroutines making the decisions are underlined.

Alternate CVMFR Model Decision Flowchart

flame heights, Eq. 3.3-2(A), are determined for each iteration. Based on this flame height and the input height of the burning object, on-off switches are then set: a given object's flames either touch the ceiling or not and a given room either has a burning object whose flames touch the ceiling or not. Depending on the values of these switches, this routine calls either CVA001 or CVB001, refer to Fig. 3.4(B).

3.4-2 VENTA

This subroutine calculates vent areas and is described in Sect. 2.4-8.

3.4-3 CVA001

This routine calculates the CVMFR for ceiling vents of enclosures containing fires whose flames do not touch the ceiling. These fires are defined by Mitler to be "small" and as such the associated plume momentum does not play a role in CVMFR. This routine first calculates the vented gas velocity, Eq. 3.3-2(B), and then uses Eq. 3.2(J) to find the CVMFR of the vent in question.

3.4-4 CVB001

This is the controlling subroutine for ceiling vents of

enclosures containing fires whose flames touch the ceiling. This is defined by Mitler to be a "large" fire. The implication of a "large" fire being that the momentum of the fire plume/ceiling jet is large enough that it should be considered for CVMFR calculations. This routine first locates the center of the ceiling vent relative to the plume axis by calling VNTCNT. Next BIGHRR is called to determine the object with the highest heat release rate. A decision is made as to whether or not the ceiling vent is near the impingement zone. The routine then calls either CVB101 or CVB201, depending on the vent's proximity to the plume axis, refer to Fig. 3.4(B).

3.4-5 VNTCNT

This subroutine calculates the equivalent ceiling vent radii of all ceiling vents and the distances from the fire plume axis to the center of the vent. The impingement zone radius is calculated for the initially burning object which, in turn, determines whether or not the vent is near the plume axis. This is yet another programming simplification which is arbitrary and requires additional theoretical/experimental verification.

3.4-6 BIGHRR

This routine finds the object with the highest heat release rate by employing a simple sort algorithm. See assumption three of Sect. 2.3-1 for the reasoning behind this subroutine. Furthermore, the Note of Sect. 2.4-1 applies to this subroutine as well.

3.4-7 CVB101

This routine calculates the CVMFR for vents that are near the plume axis of a large fire whose flames touch the ceiling. This calculation differs from that of CVA001 by attempting to incorporate the momentum associated with the fire plume into the CVMFR calculation. It calls both function UV and function UF in order to determine the effective vent velocity of Eq. 3.2(H). This velocity is then used in Eq. 3.2(J) to provide the CVMFR.

3.4-8 CVB201

This subroutine calculates the CVMFR of a vent that is far from the plume axis of a large fire whose flames touch the ceiling. In this case, the momentum of the ceiling jet is assumed to add a dynamic pressure component to the pressure differential driving the CVMFR. A different expression is used to calculate CVMFR depending on whether

or not the ceiling jet rises partially or entirely through the ceiling vent, see Fig. 3-2(C). This routine calculates the thickness (as per assumption one Sect. 3.3-1), temperature, and density of the ceiling jet. This is accomplished by first finding the radial distance from the plume axis to the vent center and then calling QSTAR, CFCTRS, and TMPA01 to determine the local ceiling jet temperature at the vent center. The ideal gas law is then applied to find the local density. A pressure difference across the vent (D, Eq. 3.2(K)), gas acceleration (a, Eq. 3.2(L)), vent velocity (u_c, Eq. 3.2(N)), and the distance the ceiling jet rises through the vent (δ, Eq. 3.2(M)) are calculated. With these parameters calculated, the ceiling jet thickness and the distance it rises in the vent are compared in order to direct the calculation flow, again. The final step is to calculate the CVMFR, depending on the distance the ceiling jet rises.

3.4-9 QSTAR

This function calculates a dimensionless heat release rate and is described in Sect. 2.4-5.

3.4-10 CFCTRS

This routine calculates the correction factors when upper layer effects are significant and is fully described

in Sect. 2.4-6.

3.4-11 TMPA01

This subroutine calculates the local, near-surface gas temperature of the ceiling jet and is described in Sect. 2.4-7.

3.4-12 FOVRH

This function evaluates Eq. 2.3-2(B)2 and is described in Sect. 2.4-8.

3.4-13 UF

This function calculates the velocity component of the vented gas velocity attributable to the flames of a fire beneath a ceiling vent. This is defined in Eq. 3.2(I) as u_f.

3.4-14 UV

This function calculates the vented gas velocity for ceiling vents of enclosures with small fires and for ceiling vents near the plume axis of large fires. This is defined in Eq. 3.3-2(B). The two constants, R_a and β, calculated in CVMF01 are used here.

3.5 Model Verification

It should be noted that the alternate CVMFR routines have very limited experimental verification and as such are more valuable as a theoretical tool than as a predictive model: any results generated by these routines are necessarily suspect.

As stated previously, there is a lack of experimental data with which to verify this model. The results of Ref. 19 were considered as a possibility. However, the differences between the scenario of Ref. 18 and an enclosure fire, as described in Sect. 3.2, result in this possibility being unacceptable. Therefore, the default case of CFC will be used as a comparison vehicle. This comparison is described in Sect. 4.2.

4.0 Comparison of Results for the Standard CFC Case

This chapter is divided into three sections: one each for the alternate ECCHTX and CVMFR models alone and one for both of them together. The alternate models are used with the default case of CFC.

4.1 ECCHTX

The purpose of this case is to determine how the standard case changes when the alternate ECCHTX model is used. Therefore, other than using the alternate ECCHTX model, the only other change from the default data is that the room contains only one object. No target objects were used in order to reduce computation time by allowing CFC to work a little less. A standard case with one object and the original ECCHTX model was run to provide the comparison data. Also, a standard case using the alternate ECCHTX model and two objects was run for the sake of completeness after all of the bugs had been worked out.

The standard case using the current ECCHTX model with one object (CHTX) did not provide any surprises: it ended at 500 seconds with little problem. However, when using the alternate ECCHTX model with the default data, the program did not converge after 360 seconds. Upon further investigation it was discovered that Cooper's formulation

for ECCHTX was being used outside (implied) boundaries and as a result the first law of thermodynamics was being violated. This problem was overcome by adding logic to switch to CNVW when the ceiling jet temperatures rise above 1300K. Therefore, another default case was run with this switching logic and the alternate ECCHTX model (CHTX0K). As expected this switching does result in a discontinuity. The consequences of this switch are discussed below.

The standard case using the alternate ECCHTX model and two objects was not significantly different from the standard case with one object. Therefore, only the results of the "one object" case will be discussed.

The primary difference between these two ECCHTX models concerns the convection heat flow lost by the layer and the method by which it is assumed to be removed. Since the alternate model considers a ceiling jet as the driving force behind the convection, it should convect more energy due to the higher temperatures of the ceiling jet. This is shown in Figures 4.1(A) through 4.1(C) which present a graphical comparison of upper gas temperatures, extended ceiling surface temperature, time rate of change of convective heat flow from the upper layer to the extended ceiling, and convective heat flux from the hot layer to the extended ceiling.

Figure 4.1(A)

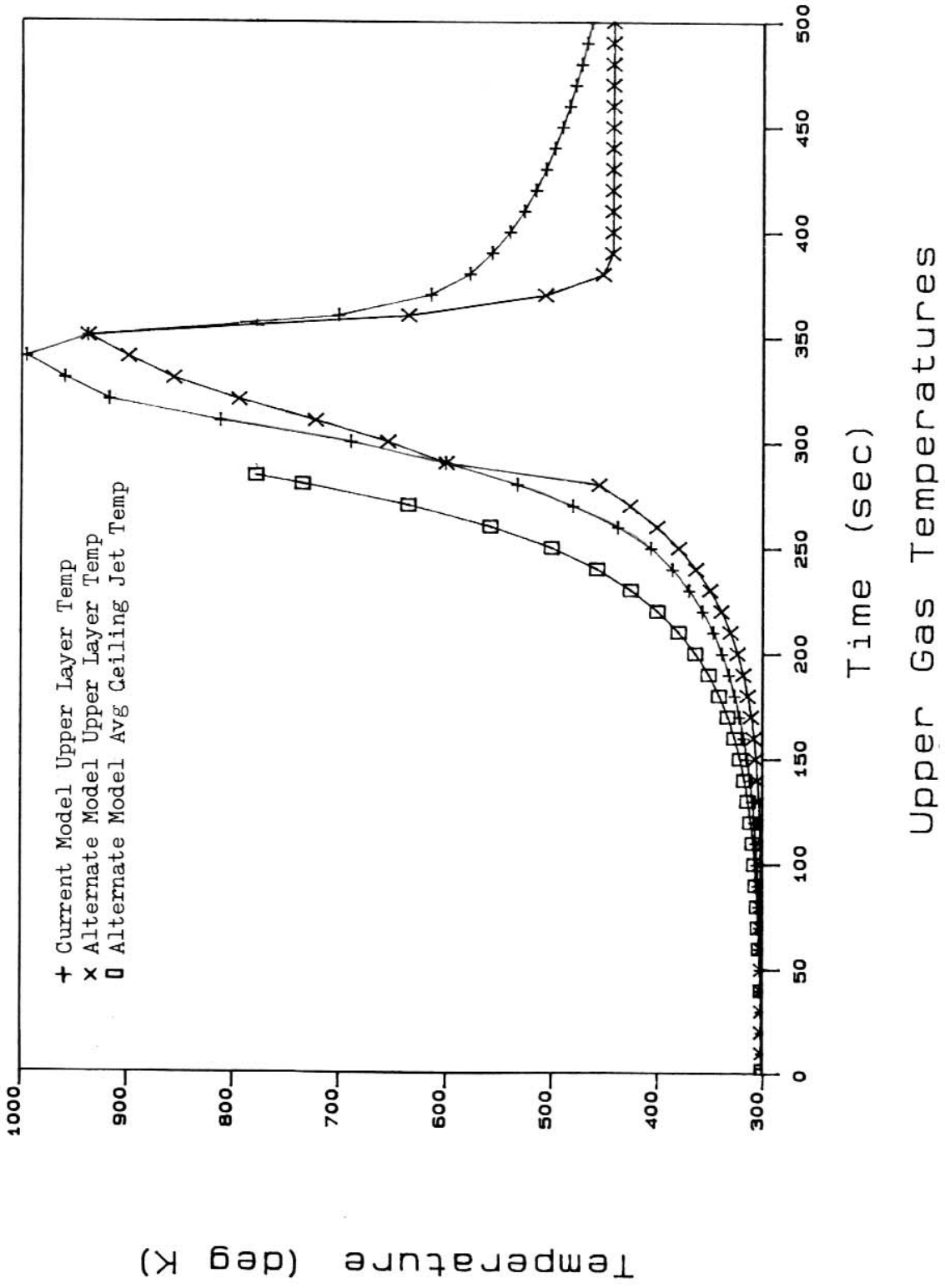
Upper Gas Temperatures
Temperature (deg K)
Time (sec)
+ Current Model Upper Layer Temp
× Alternate Model Upper Layer Temp
□ Alternate Model Avg Ceiling Jet Temp
1000
900
800
700
600
500
400
300
0
50
100
150
200
250
300
350
400
450
500

Figure 4.1(B)

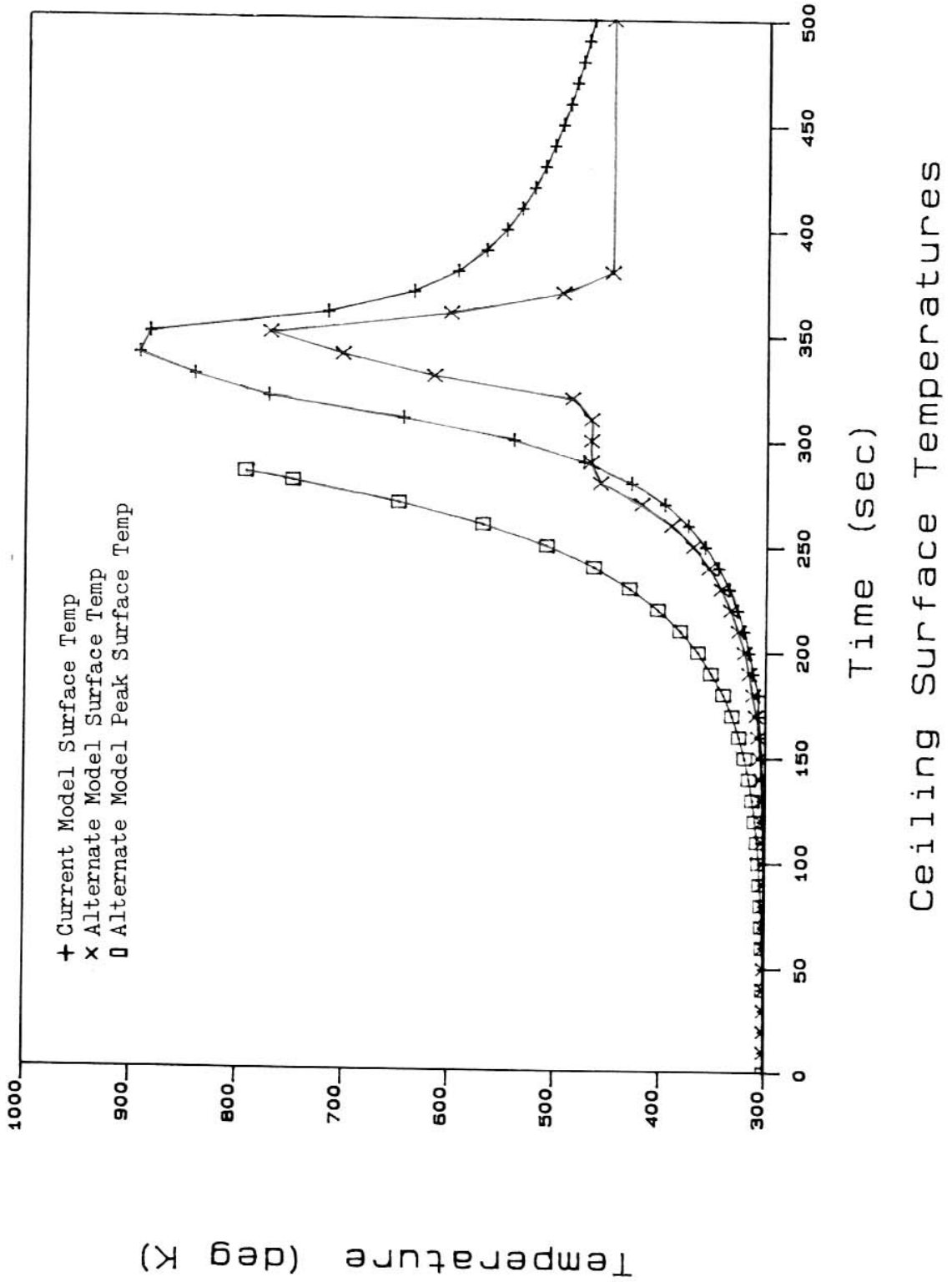
Ceiling Surface Temperatures
Time (sec)
Temperature (deg K)
+ Current Model Surface Temp
× Alternate Model Surface Temp
□ Alternate Model Peak Surface Temp
1000
900
800
700
600
500
400
300
0
50
100
150
200
250
300
350
400
450
500

Figure 4.1(C)

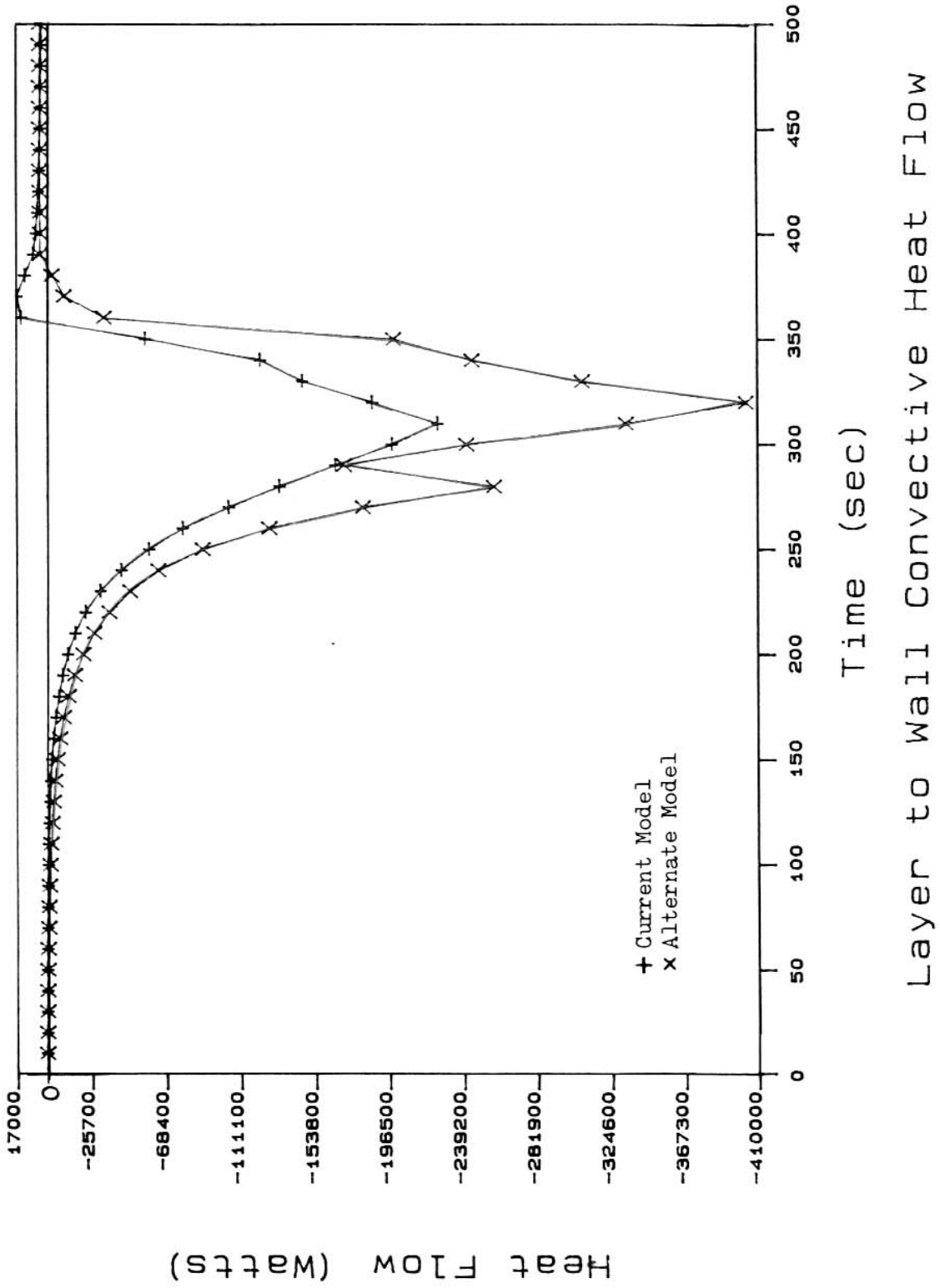
Layer to Wall Convective Heat Flow
Heat Flow (Watts)
Time (sec)
+ Current Model
× Alternate Model
17000
0
-25700
-68400
-111100
-153800
-196500
-239200
-281900
-324600
-367300
-410000
0
50
100
150
200
250
300
350
400
450
500

Figure 4.1(C) indicates the difference in heat flux between a ceiling jet driven ECCHTX model and one driven by the upper layer, i.e., up to the point where the alternate model switches to the current model, at about 280 seconds. As expected, the alternate ECCHTX (ceiling jet driven) model predicts higher convective heat flows. The discontinuity at 280 seconds can be attributed to the program switching from the alternate model to the current ECCHTX model due to elevated ceiling jet temperatures (> 1300K). When this switch is made, the peak surface and average ceiling jet temperatures are no longer calculated. Thus, their values remain constant at the last calculated values, as shown in Fig. 4.1(A) and 4.1(B).

The result of this increased convective heat flow, early in the fire, is that the upper layer temperature is lower and the extended ceiling surface temperature is higher than if they had been predicted by a bulk (i.e., current) model only. This can be seen in Fig. 4.1(A) and 4.1(B) between 0 and 280 seconds. When the switch is made to the current ECCHTX model at 280 seconds, a smaller heat flow is experienced by the extended ceiling and its surface temperature levels off for about 30 seconds, see Fig. 4.1(B). Since the surface temperature of the extended ceiling is determined after the various heat fluxes and rates, an approximately constant surface temperature is calculated between 280 and 310 seconds.

The lower convective heat flow causes the alternate ECCHTX model's prediction of the extended ceiling surface temperature to lag behind that of the current ECCHTX model. No discontinuity is observed because both models do not use the same temperature arrays to store the wall temperature profiles. On the other hand, the same memory locations are used to store the convective heat flows of the two models because it is, in essence, the same variable. (The "cure" for this condition would be to add the appropriate memory locations to store the area weighted average convective heat flux and flow as calculated by the alternate ECCHTX model. However, this may only eliminate the discontinuity as shown graphically in Fig. 4.1(C). A discontinuity might still be calculated when the program switches from the alternate to the current ECCHTX model.) Therefore, a discontinuity results when the method used to determine those convective heat flows is changed. From Fig. 4.1(A), the upper layer temperature, effectively, takes a step increase at the time of the switch. This, in turn, results in the second spike shown in Fig. 4.1(C). The temperature difference between the (bulk) upper layer temperature and the ceiling surface is greater between 280 and 325 seconds than at earlier times in the fire. Therefore, the convective heat flow increases during this period of time, also. Since the object burns out at approximately 380 seconds, its mass loss or burning rate begins to decrease prior to that, at about 350 seconds. The loss of the heat source results in the temperature and

heat flow decreases shown in Fig. 4.1(A) to 4.1(C) after 380 seconds.

Table 4.1(A) presents some computer-oriented results. Initially, some concern was expressed that, since the alternate model performs more local (convection) calculations per time step, more CPU time would be required. This is apparent from Table 4.1(A). The alternate ECCHTX model requires fewer time steps and this somewhat offsets the additional iterations. However, approximately two times more CPU time is required by the alternate ECCHTX model than for the current ECCHTX model. Therefore, the alternate ECCHTX model requires more time per time step to accommodate the increased number of local condition calculations. It should be noted that when modeling a larger room than the default case, more local points will be used by the alternate ECCHTX model. Therefore, the CPU time is expected to be larger than indicated by Table 4.1(A). However, as shown in Table 2.5(C), the enclosure surface materials and fire size relative to enclosure size also play a part in determining the total number of time steps and iterations and therefore, the CPU time required for a particular problem. From the CPU viewpoint, the worst case would be one modeling a small enclosure constructed of highly insulating material which contains a large fire, i.e., too large for the enclosure to contain without failure as implied by the attainment of the maximum possible ceiling

Table 4.1(A)

Calculation Information: ECCHTX Standard Cases

Case*	Total # of Time Steps	Total # of Iterations	CPU Time (min:sec)
CHTX	274	8557	2:47.67
CHTXOK	266	8902	5:23.47
STDRUN	276	9091	4:47.39
CHTXOL	271	9726	7:01.39

* CHTX = Standard run w/ 1 obj., current EXXHTC model

CHTXOK = Standard run w/ 1 obj., alternate EXXHTC model

STDRUN = Standard run w/ 2 obj., current EXXHTC model

CHTXOL = Standard run w/ 2 obj., alternate EXXHTC model

surface temperature rise.

The results of these preliminary cases indicate the ECCHTX may be more significant for confined enclosures early in the fire than as originally modeled with a uniform upper layer temperature. Also, please note that correctly implementing the alternate ceiling jet driven ECCHTX model described above could require a major revision of CFC. This will be discussed in a later section.

4.2 CVMFR

The purpose of this case is to determine the difference in ceiling vent mass flow when a static only model (the current CFC/WPI CVMFR model) is used and when a static plus dynamic model (the alternate CVMFR model) is used. The data obtained are more indicative of ceiling vent mass flow trends rather than absolute values of mass flow through the ceiling vent.

Several scenarios were considered, all based upon the default data, and a total of six cases were run. Two of these cases used the original CVMFR model, while the other four used the alternate CVMFR model. Of the two cases using the current CVMFR model, the case designated HSX uses a small (0.05m X 0.05m) ceiling vent in addition to the default door vent. This ceiling vent opens at ten seconds

into the fire so it essentially models leakage at the top of the enclosure. Case HLX uses a larger (0.25m X 0.25m) ceiling vent, plus the default door. This ceiling vent opens at 200 seconds, as if opened by a fire detection device (e.g., a fusible link). This vent size is typical of a ventilation system inlet/outlet.

Four cases are required for the alternate CVMFR model because, as previously stated, the radial distance between the fire plume axis and the vent plays a role in this model. Therefore, two cases were run with the small vent described above and two more with the larger vent. The two cases for a given vent size place the ceiling vent either near or far from the fire plume axis. In this case, if the geometrical center of the ceiling vent is within the impingement zone it is considered to be near the axis, otherwise it is far from the axis. The designations of these four cases are: CSN - small vent near, CSF - small vent far, CLN - large vent near, and CLF - large vent far.

At this point the distinction between near and far is entirely ad hoc and its only defense is its convenience; it is intuitively understood that "distance from source" will affect ceiling vents when considering gas flows. This distinction essentially categorizes the gas dynamics that the ceiling vent "sees" as either pre- or post-impingement (i.e., near or far): when the plume hits the ceiling and

turns 90°, it loses energy. Thus, the resultant ceiling jet will be less energetic than the plume is before the plume hits the ceiling. Quite simply, the further from the impingement zone, the slower the ceiling jet flow.

Figure 4.2(A) presents the ceiling vent mass flows from all three small vent cases. In this figure, the current model predicts a continuous and fairly smooth function for the ceiling vent mass flow. The alternate model does not fair as well, however. Between 0 and approximately 270 seconds the fire is "small" according to Mitler's definition and the calculation using the Heskestad flame height correlation (Ref. 13). For this condition the radial distance from the plume axis to the vent is not a factor, i.e., according to the formulation and assumptions. Therefore, both of the alternate small vent cases predict the same ceiling vent flow. However, between 270 and 350 seconds the fire is "large" and two different subroutines are used: one for the near vent (CVB101) and one for the far vent (CVB201). Of these two, the near vent scenario seems to provide a better qualitative prediction. With the plume near the vent, the plume momentum increases the vent flow and this is shown in Fig. 4.2(A). However, it was also expected that the ceiling vent flow through the far vent would also be increased due to the ceiling jet momentum. From Fig. 4.2(A) this does not appear to be so. Therefore, these results are inconclusive and indicate that a more

Figure 4.2(A)

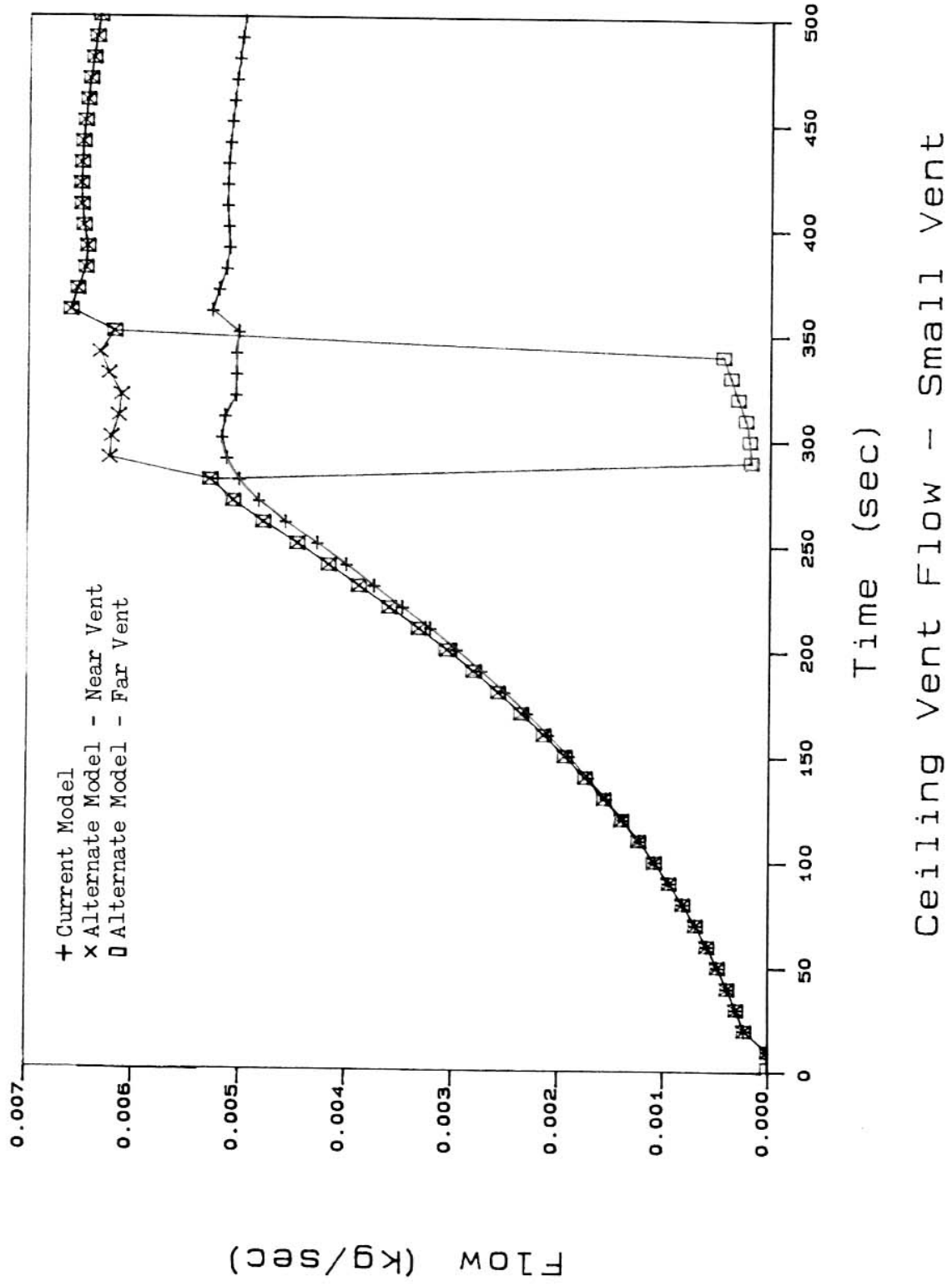
Ceiling Vent Flow - Small Vent
Time (sec)
Flow (kg/sec)
+ Current Model
× Alternate Model - Near Vent
□ Alternate Model - Far Vent
0.000
0.001
0.002
0.003
0.004
0.005
0.006
0.007
0
50
100
150
200
250
300
350
400
450
500

detailed analysis is required.

At approximately 350 seconds, the fire begins to die out and a "large" fire is no longer present. Therefore, the "small" fire alternate CVMFR model subroutine (CVA101) is used. Just as in the beginning of the fire, the location of the vent relative to the plume is no longer a consideration and the near/far distinction is no longer used. Thus, these two scenarios result in the same vent flow after 350 seconds.

The difference between the current and alternate models (excluding the far vent case) can be attributed to the differences in their formulations as described in Sect. 3.1 and 3.2: specifically, the difference in formulation between Eq. 3.2(B) and 3.2(G). Upon inspection it can be seen that these two formulations share the same variables. When these shared terms are eliminated, the pressure at the floor, p_f, is left from Eq. 3.2(B) and a more complicated term from Eq. 3.2(G). It has been presumed that p_f is accounted for in Mitler's derivation of Eq. 3.2(G). Therefore, the leftover, more complex term of Eq. 3.2(G) is assumed to account for p_f. Whether or not this is the case has yet to be determined since this problem was discovered too late to be fully addressed. In other words, the difference in the results of these two formulations appears to be in accounting for the pressure at the floor and at this point

in time, it is not apparent why this is so. However, the data of Fig. 4.2(A) is consistent with the hand calculation performed prior to implementing the alternate CVMFR model: higher ceiling vent mass flow than with the current CVMFR model for the "near" vent scenario.

Figures 4.2(B) - 4.2(D) are included to show that, as expected, this small ceiling vent has very little effect on the pressure at the floor and flows through the door. These figures are readily explained. The fire is oxygen starved between, roughly, 310 and 350 seconds. Prior to this time the fire grows, which in turn negatively increases both the pressure at the floor, Fig. 4.2(B), and mass flow rate of air into the enclosure, Fig. 4.2(D). Just before 350 seconds the fire ceases to be oxygen starved and the fire's oxygen requirement increases; this is shown by the spike at 350 seconds of Fig. 4.2(D). Also, since the object burns out at 380 seconds, its oxygen requirement begins to decrease prior to that, at about 350 seconds (Fig. 4.2(D) between 350 and 500 seconds). The upper door flow of Fig. 4.2(C) is essentially a mirror image of the lower door flow and is explained in a similar manner.

When comparing the alternate model small and large vent ceiling vent flows, Fig. 4.2(A) and 4.2(E), there is little qualitative difference between 200 and 380 seconds. After 380 seconds, the results from both the current and alternate

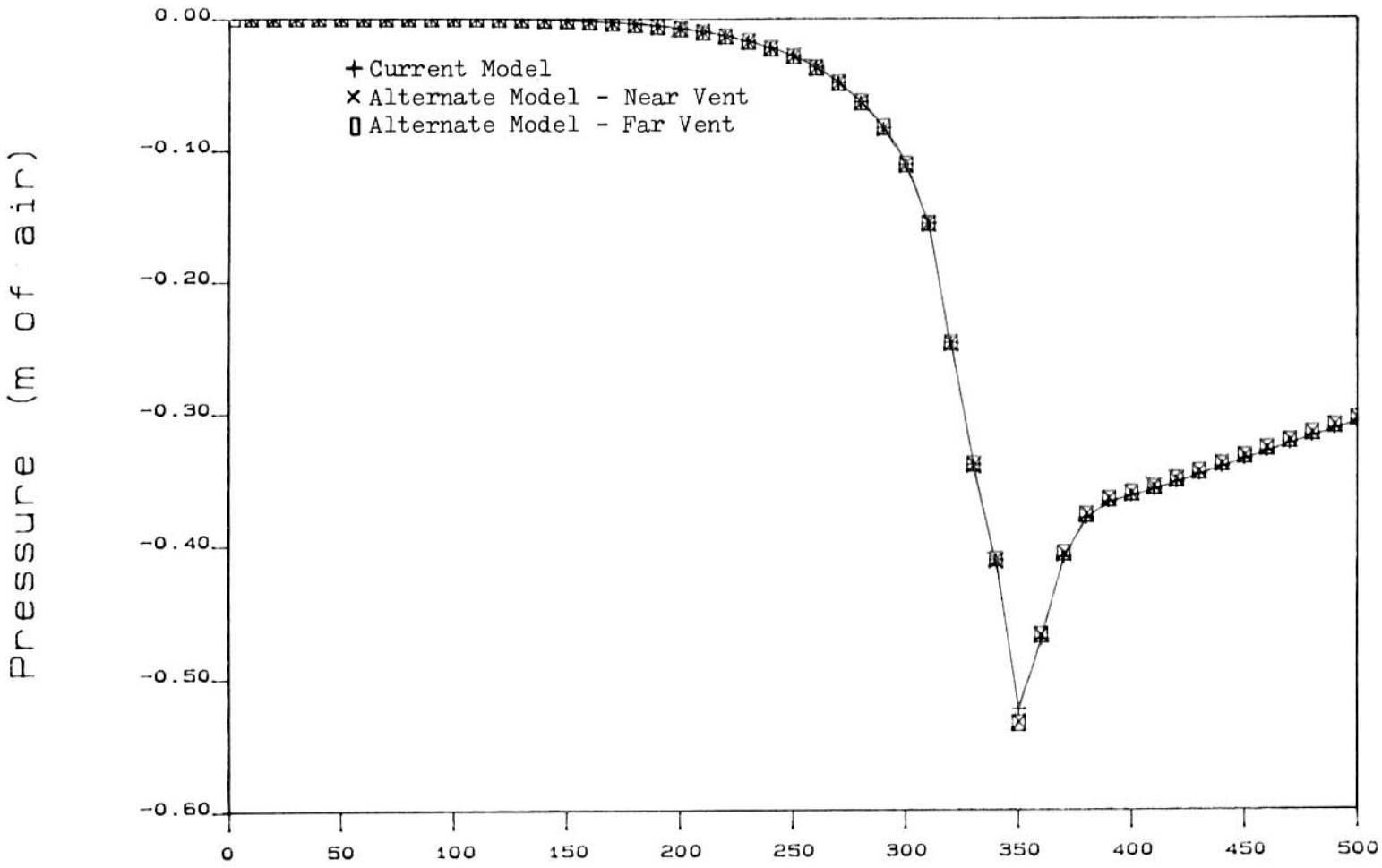
0.00
-0.10
-0.20
-0.30
-0.40
-0.50
-0.60
+ Current Model
× Alternate Model - Near Vent
▯ Alternate Model - Far Vent
0
50
100
150
200
250
300
350
400
450
500
Pressure (m of air)
Time (sec)
Pressure at Floor - Small Vent

Figure 4.2(B)

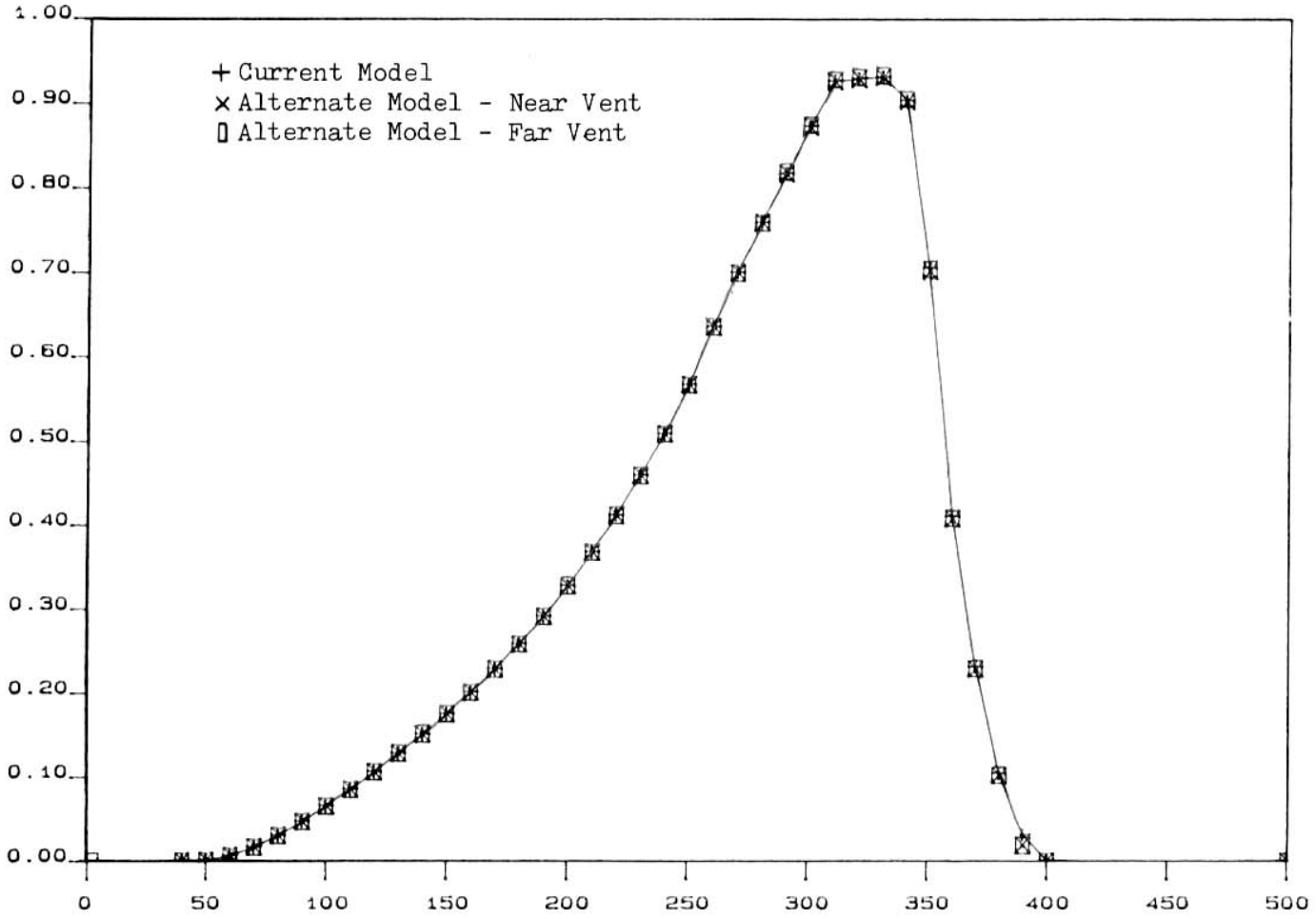
+ Current Model
× Alternate Model - Near Vent
▯ Alternate Model - Far Vent
1.00
0.90
0.80
0.70
0.60
0.50
0.40
0.30
0.20
0.10
0.00
0
50
100
150
200
250
300
350
400
450
500
Flow (kg/s)
Time (sec)
Upper Door Flow - Small Vent

Figure 4.2(c)

Figure 4.2(D)

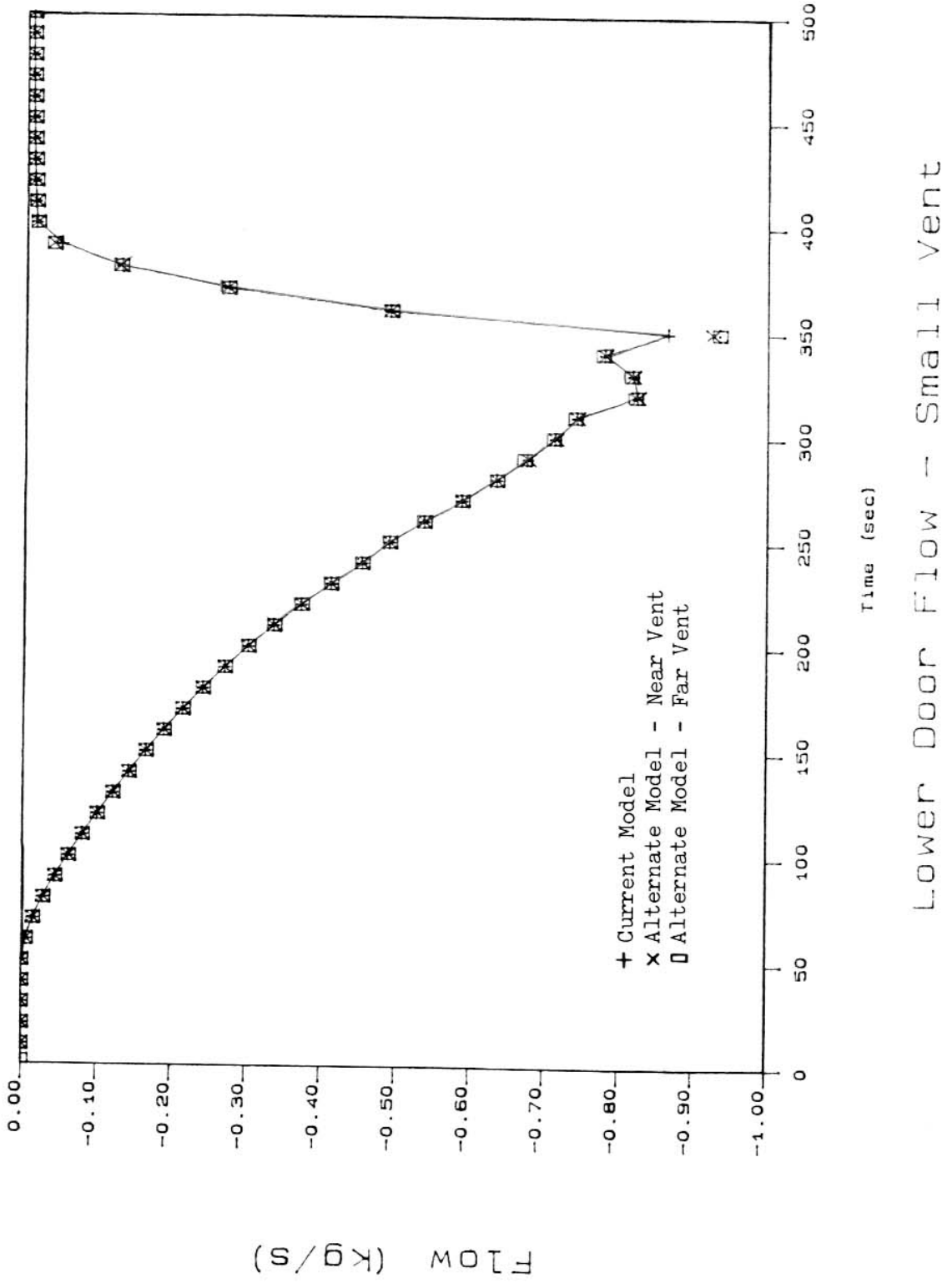
Lower Door Flow - Small Vent
Flow (kg/s)
Time (sec)
0.00
-0.10
-0.20
-0.30
-0.40
-0.50
-0.60
-0.70
-0.80
-0.90
-1.00
0
50
100
150
200
250
300
350
400
450
500
+ Current Model
× Alternate Model - Near Vent
□ Alternate Model - Far Vent

models become confusing, as shown in Fig. 4.2(E), 4.2(F), 4.2(H), and 4.2(I). The anomalous behavior at 400 seconds is somewhat perplexing until Fig. 4.2(J) is considered. This figure indicates that the large ceiling vent discharges enough mass to make the upper layer almost non-existent, i.e., the upper layer has very little mass. The small vent discharges so little that it has no significant effects on the conditions within the enclosure. The final layer depth for all the small vent cases is on the order of 10^{-1} while that of the large vent cases is 10^{-3}. The result of this condition is that the ceiling vent tries to convect more heat out of the upper layer than it contains. That is to say that, the change in energy of the upper layer due to convection out the ceiling vent is greater than the energy content of the layer. This appears to be one possible explanation for the behavior observed in the aforementioned figures. As shown by Fig. 4.2(I), the small upper layer mass may seriously affect the upper layer temperature calculation. From Ref. 16, CFC calculates the upper layer temperature as:

Eq. 4.2(A)

$$T_u = E/(M*C_p)$$

where: E = upper layer energy

M = upper layer mass

C_p = specific heat

This calculation indicates that for an equivalent

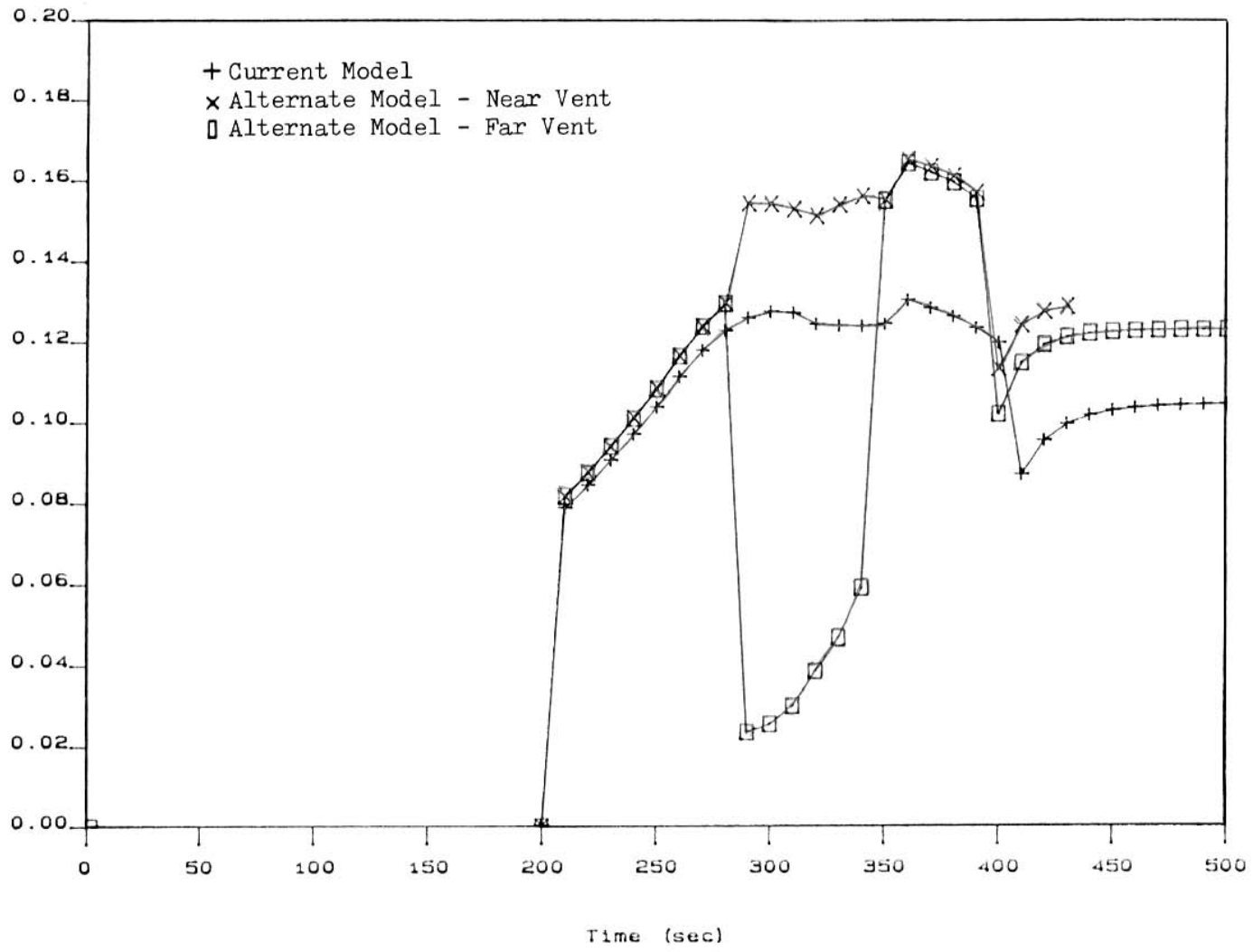
+ Current Model
x Alternate Model - Near Vent
□ Alternate Model - Far Vent
0.20
0.18
0.16
0.14
0.12
0.10
0.08
0.06
0.04
0.02
0.00
0
50
100
150
200
250
300
350
400
450
500
Time (sec)
Flow (kg/s)
Ceiling Vent Flow - Large Vent

Figure 4.2(E)

Figure 4.2(F)

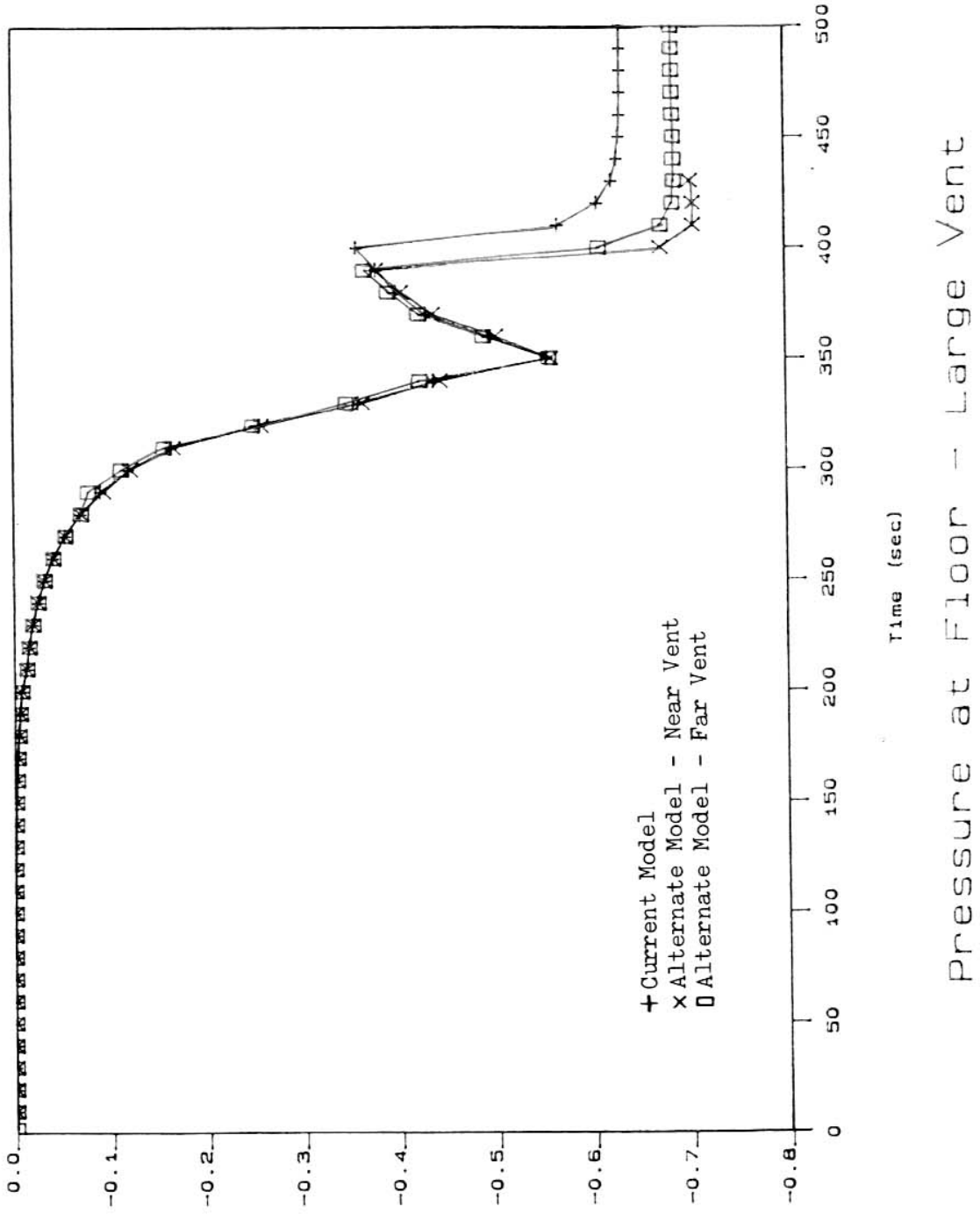
Pressure at Floor - Large Vent
Time (sec)
Pressure (m of air)
+ Current Model
× Alternate Model - Near Vent
□ Alternate Model - Far Vent
0.0
-0.1
-0.2
-0.3
-0.4
-0.5
-0.6
-0.7
-0.8
0
50
100
150
200
250
300
350
400
450
500

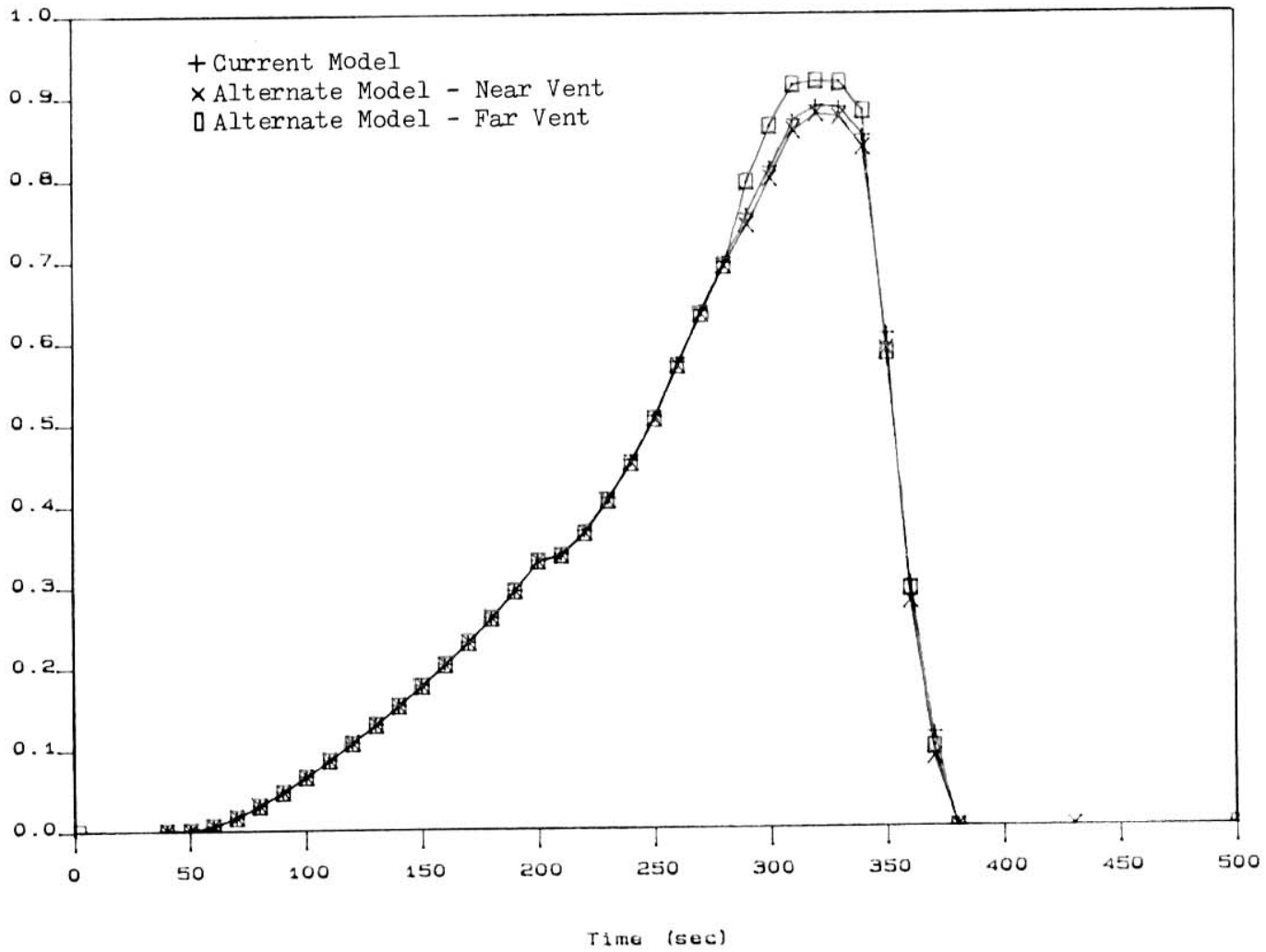
+ Current Model
× Alternate Model - Near Vent
▯ Alternate Model - Far Vent
1.0
0.9
0.8
0.7
0.6
0.5
0.4
0.3
0.2
0.1
0.0
0
50
100
150
200
250
300
350
400
450
500
Flow (kg/s)
Time (sec)
Upper Door Flow - Large Vent

Figure 4.2(G)

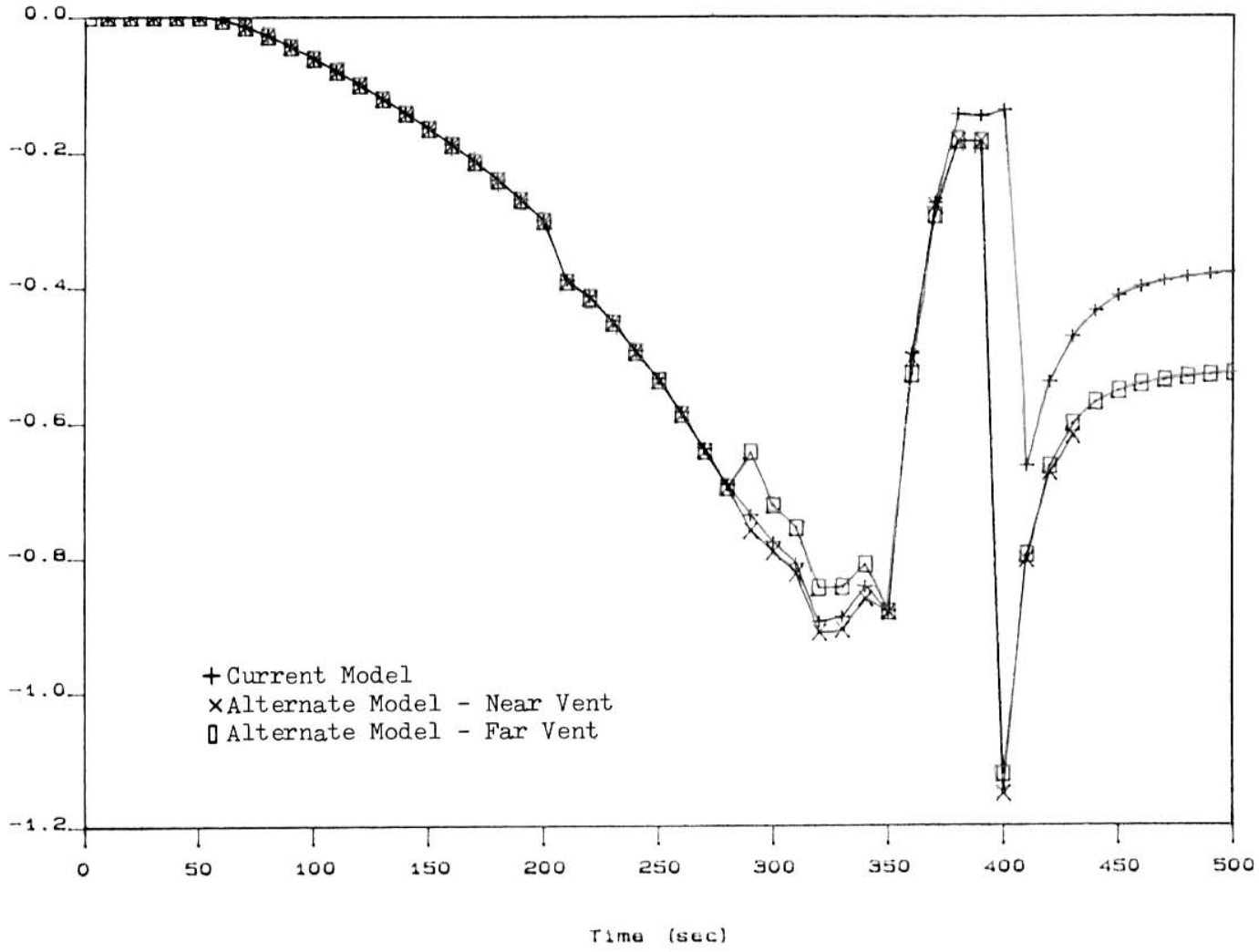
0.0
-0.2
-0.4
-0.6
-0.8
-1.0
-1.2
0
50
100
150
200
250
300
350
400
450
500
Flow (kg/s)
Time (sec)
+Current Model
×Alternate Model - Near Vent
□Alternate Model - Far Vent
Lower Door Flow - Large Vent

Figure 4.2(H)

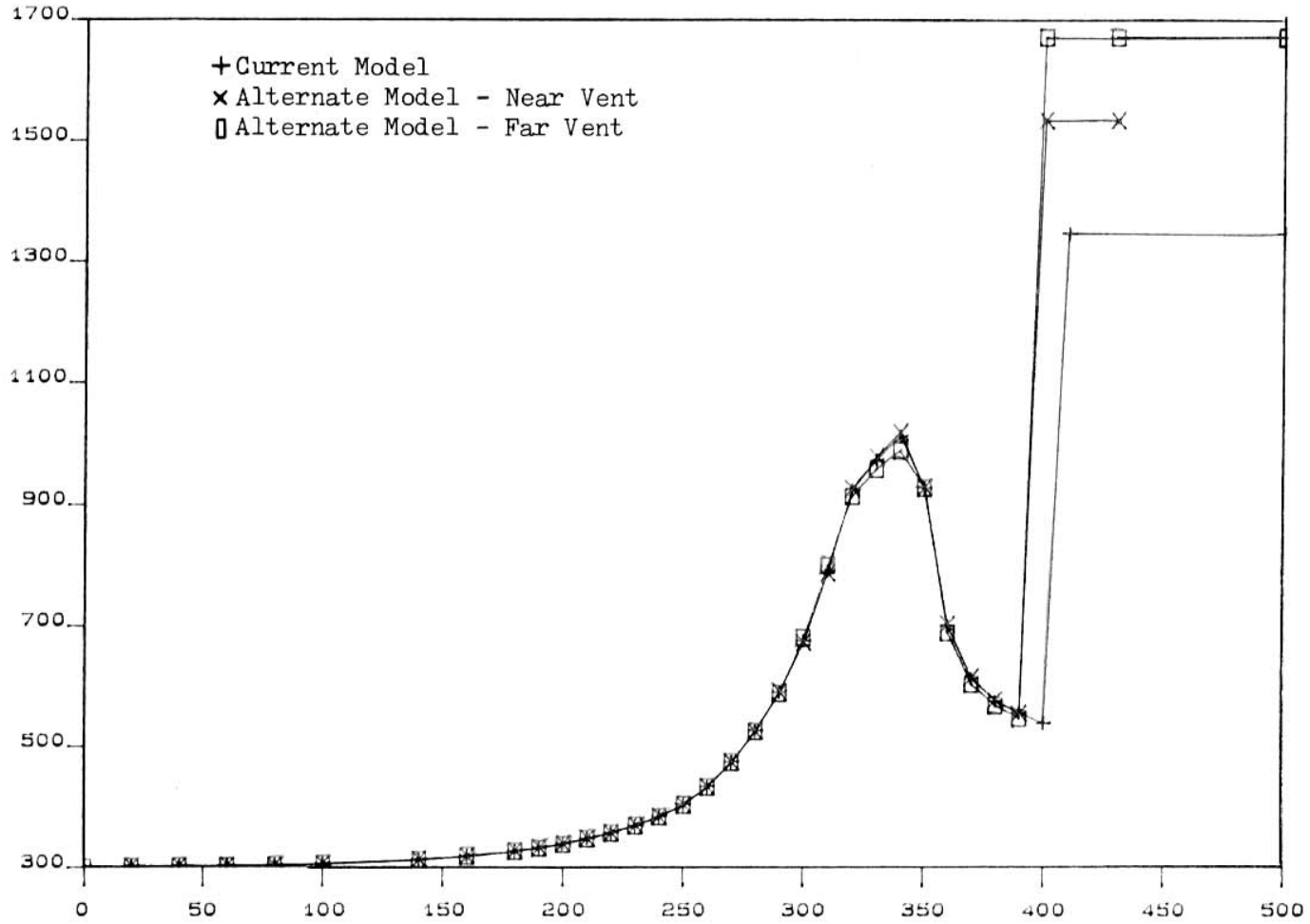

Upper Layer Temperature - Large Vent

Figure 4.2(I)

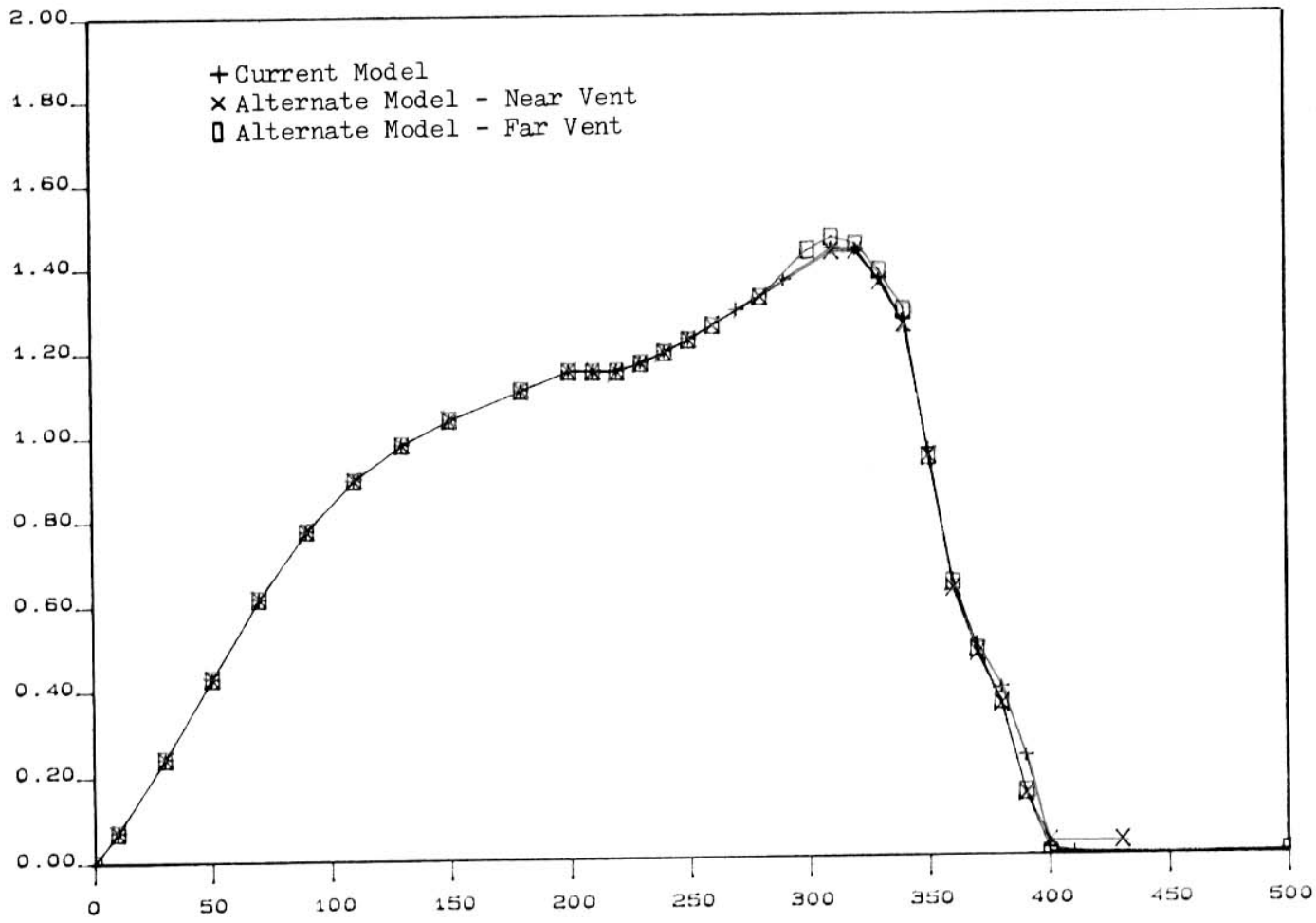

Upper Layer Depth - Large Vent

Figure 4.2(J)

amount of energy, a smaller upper layer mass will increase the upper layer, bulk temperature. However, it is difficult to say what is cause and what is effect: ignoring the thermodynamics or convecting more heat than is available. This simply indicates that, because a ceiling vent was not included in the original formulation of CFC, it is difficult to install any ceiling vent model without further research. Also, the exact cause for the large, near vent case, CLN, convergence problem is not known; presumably a result of the small layer depth or the model trying to convect more heat than is available.

Table 4.2(A) presents a comparison of the "computer oriented results" for these cases. From this table it can be seen that the alternate CVMFR model requires fewer time steps and iterations than the current model for a similar case. This is one advantage the alternate CVMFR model has over the current model. CPU times are not available for these cases.

4.3 ECCHTX and CVMFR Together

The purpose of this case is to determine how and if the alternate models may interact. For these runs the default data with one object and the large ceiling vent described in Sect. 4.2 are used.

Overall the results from the cases using both alternate

Table 4.2(A)

Calculation Information: CVMFR Standard Cases

Case[*1]	Total # of Time Steps	Total # of Iterations
HSX	291	9164
CSN	274	8554
CSF	274	8589
HLX	302	9127
CLN	267	8955[*2]
CLF	285	8830

*2 Problem end time = 430 seconds

CPU times not available for these cases.

*1 HSX = Current CFC/WPI model, small vent

CSN = Alternate CVMFR model, small near vent

CSF = Alternate CVMFR model, small far vent

HLX = Current CFC/WPI model, large vent

CLN = Alternate CVMFR model, large near vent

CLF = Alternate CVMFR model, large far vent

models is similar to the output from the cases using one or the other alternate. For example, the ceiling vent flow of Fig. 4.3(A) is very similar to that of Fig. 4.2(E). The most obvious difference between the two figures is that when using both alternate models for the far vent case, the program fails to converge at the point where the "large" fire becomes "small"; at roughly 350 seconds. Once again the results are inconclusive and further definition of "near/far" vents and "small/large" fires with regard to ceiling venting is required.

The only other significant difference is that the near vent case with both alternate models predicts a slightly different ceiling vent flow than the alternate CVMFR model by itself. This difference is also apparent when the pressure at the floor and the door flows of the two different cases are considered. Since these parameters are all (indirectly, at least) dependent on the upper layer temperature, one would expect that changing the method by which it is calculated would also affect the results of the ceiling vent flow model. This, indeed, is the effect of using the alternate ECCHTX model with the alternate CVMFR model. As discussed in Sect. 4.1, when the program switches from the alternate ECCHTX model to the current model, the upper layer essentially undergoes a step increase in temperature, at about 280 seconds, Fig. 4.3(E). This in turn affects the upper layer density, pressure at the floor,

Figure 4.3(A)

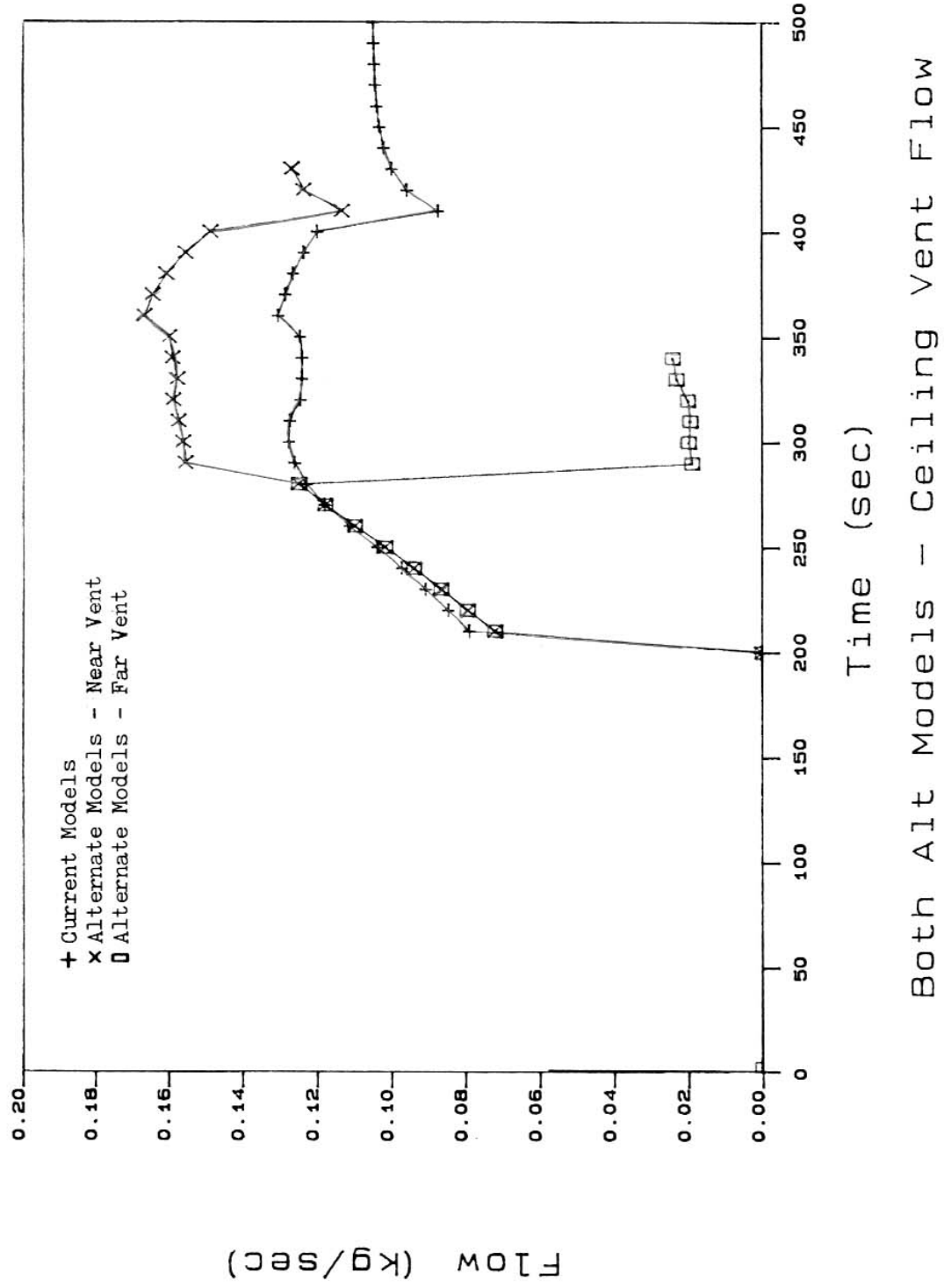
Both Alt Models - Ceiling Vent Flow
Time (sec)
Flow (kg/sec)
+ Current Models
× Alternate Models - Near Vent
□ Alternate Models - Far Vent
0.20
0.18
0.16
0.14
0.12
0.10
0.08
0.06
0.04
0.02
0.00
0
50
100
150
200
250
300
350
400
450
500

Fig. 4.3(B), and flows through the door, Fig. 4.3(C) and Fig. 4.3(D).

When considering the upper layer and ceiling surface temperatures, Fig. 4.3(E) and 4.3(F), the most obvious difference between using the alternate ECCHTX model alone and in conjunction with the alternate CVMFR model is that at 400 seconds the anomaly discussed in Sect 4.2 is present when both alternate models are used. From Fig. 4.3(H) it can be seen that the upper layer depth for the near vent case using both alternate models is greater than for the case using the current models. This tends to indicate that the numerical instability observed in Fig. 4.3(E) (and discussed in Sect. 4.2) is attributable to the ceiling vent attempting to convect more energy/heat from the upper layer than the layer contains. Once again, additional understanding of ceiling vent behavior, with regard to the conditions within the fire enclosure, is required.

With the exception of the anomaly discussed above, the heat transfer from the upper layer to the extended ceiling for the cases using both alternate models, Fig. 4.3(G), is qualitatively similar to the case using only the alternate ECCHTX model. See Sect. 4.1 for the discussion regarding the use of the alternate ECCHTX model by itself.

Table 4.3(A) presents the calculation information for

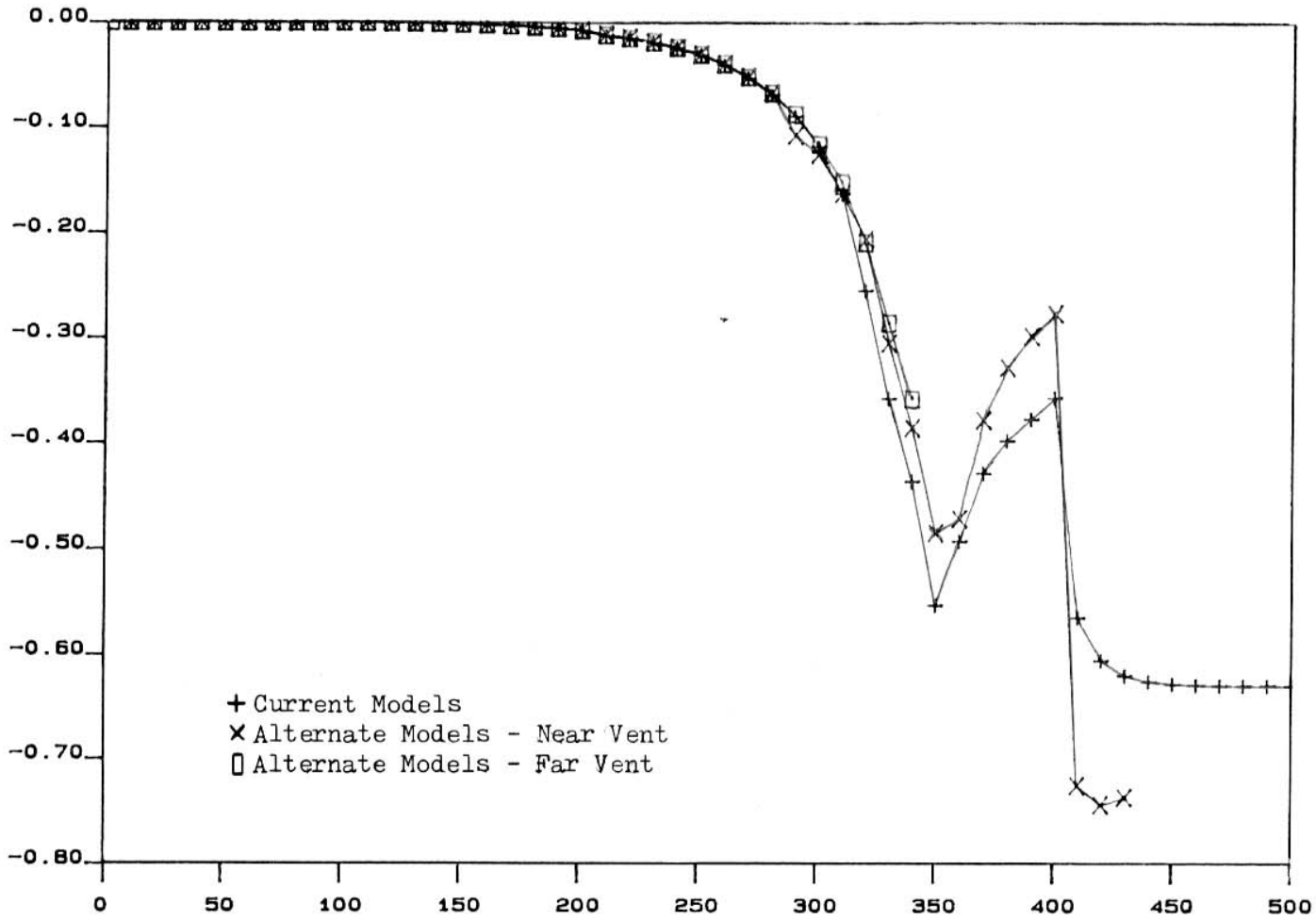
0.00
-0.10
-0.20
-0.30
-0.40
-0.50
-0.60
-0.70
-0.80
0
50
100
150
200
250
300
350
400
450
500
Pressure (m of air)
Time (sec)
+ Current Models
× Alternate Models - Near Vent
□ Alternate Models - Far Vent
Both Alt Models - Pressure at Floor

Figure 4.3(B)

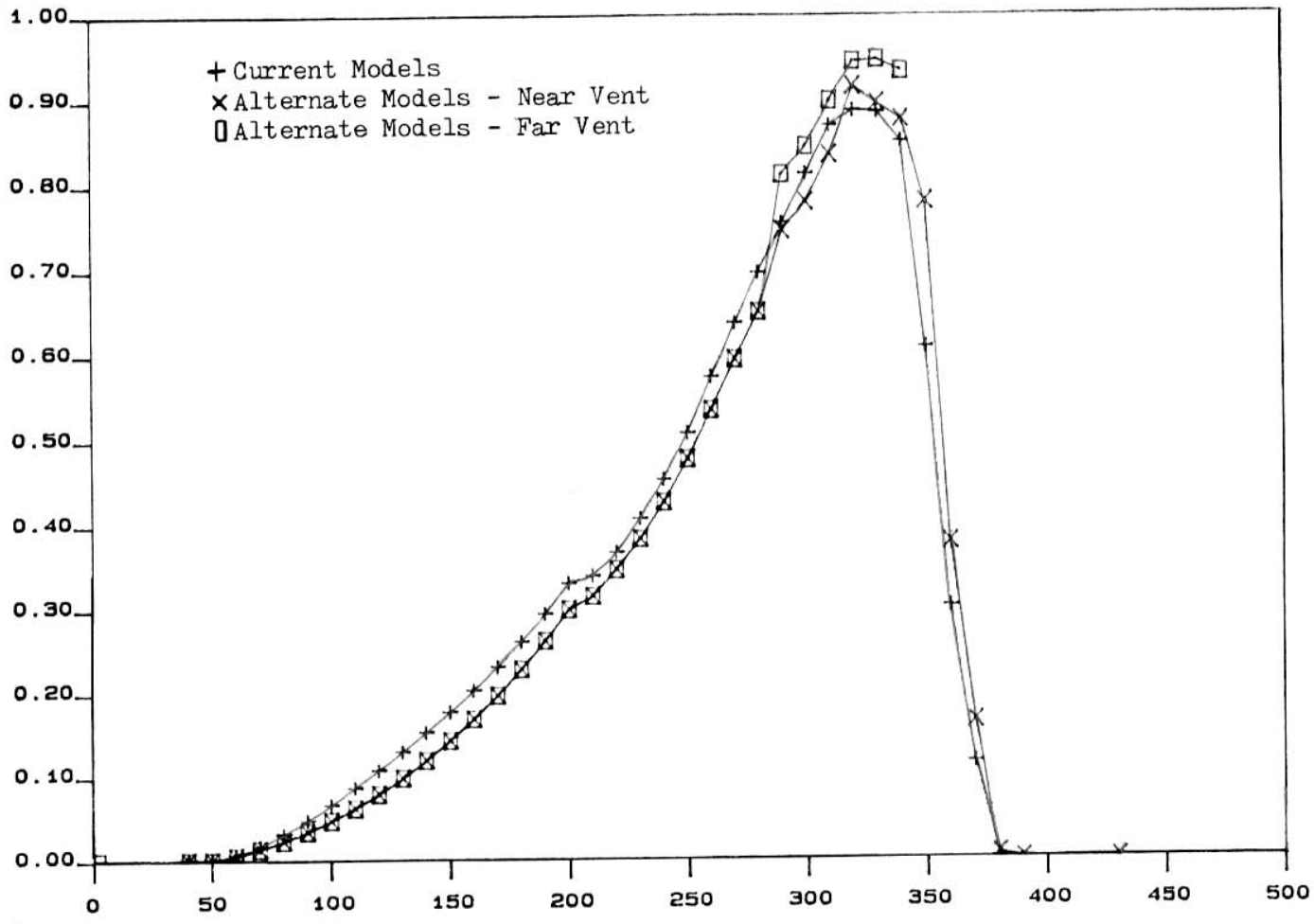
+ Current Models
× Alternate Models - Near Vent
□ Alternate Models - Far Vent
1.00
0.90
0.80
0.70
0.60
0.50
0.40
0.30
0.20
0.10
0.00
0
50
100
150
200
250
300
350
400
450
500
Flow (kg/sec)
Time (sec)
Both Alt Models - Upper Door Flow

Figure 4.3(C)

Figure 4.3(D)

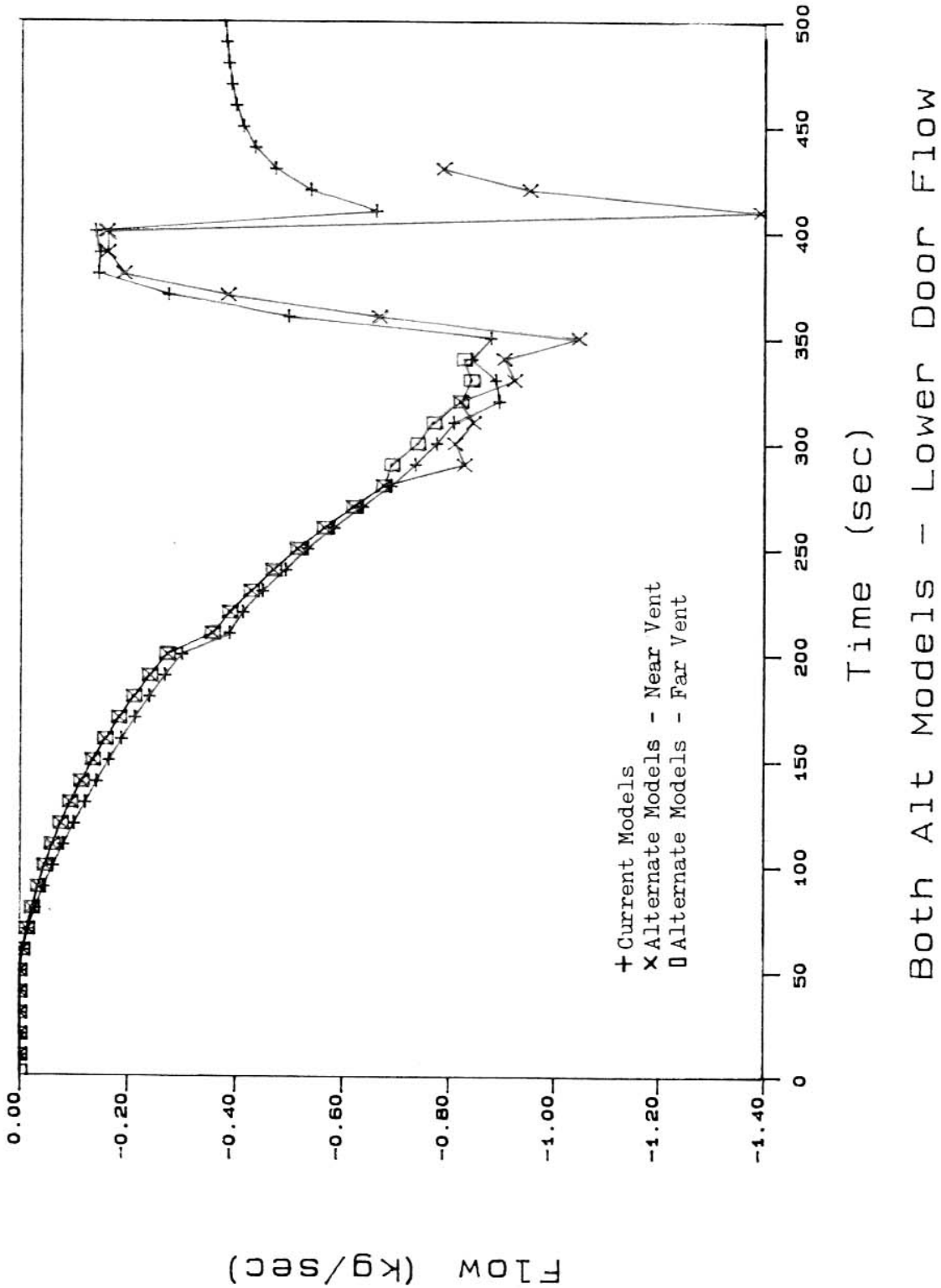
Both Alt Models - Lower Door Flow
Time (sec)
Flow (kg/sec)
0.00
-0.20
-0.40
-0.60
-0.80
-1.00
-1.20
-1.40
0
50
100
150
200
250
300
350
400
450
500
+ Current Models
× Alternate Models - Near Vent
□ Alternate Models - Far Vent

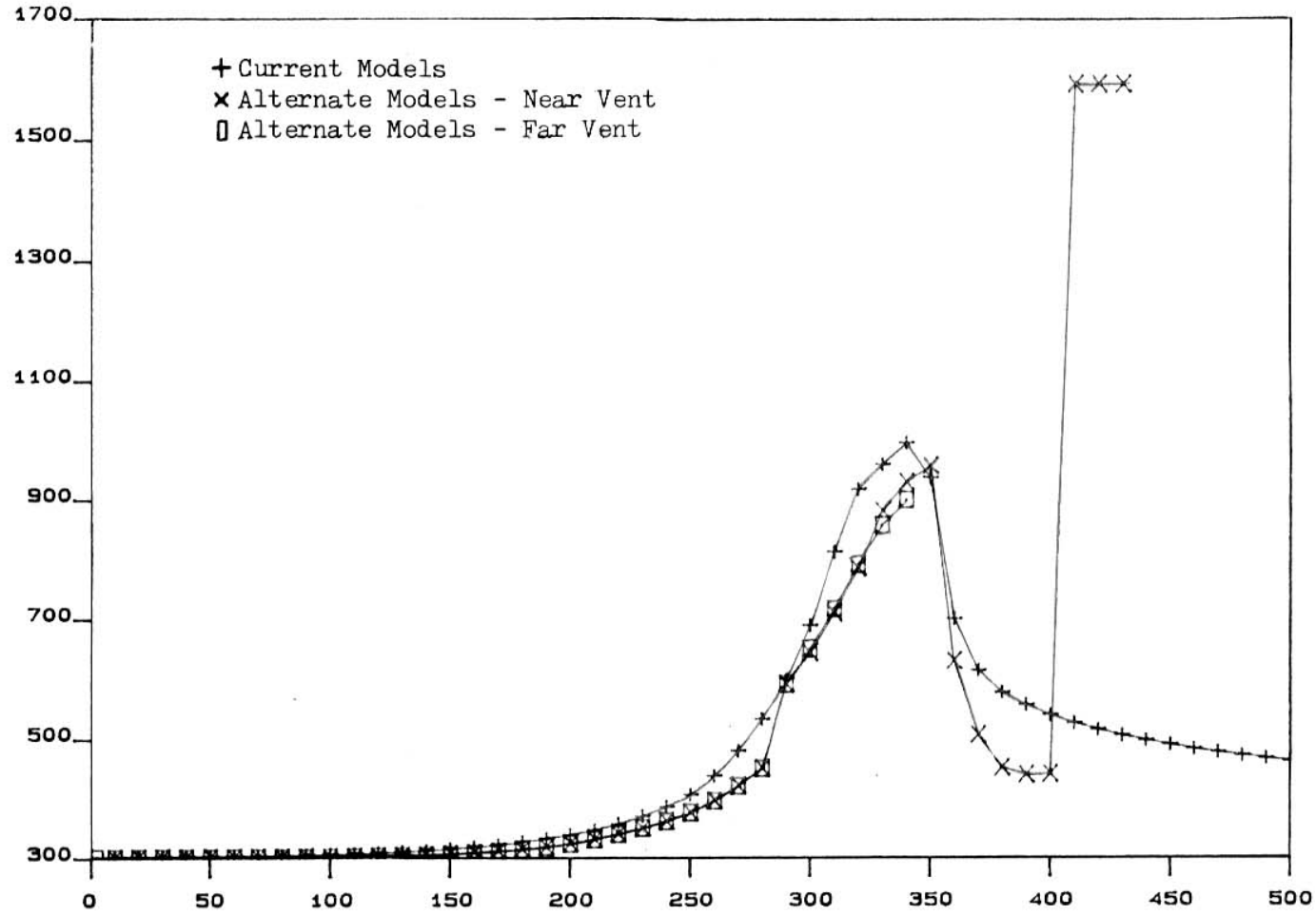
+ Current Models
× Alternate Models - Near Vent
□ Alternate Models - Far Vent
1700
1500
1300
1100
900
700
500
300
0
50
100
150
200
250
300
350
400
450
500
Temperature (deg K)
Time (sec)
Both Alt Models - Upper Layer Temp

Figure 4.3(E)

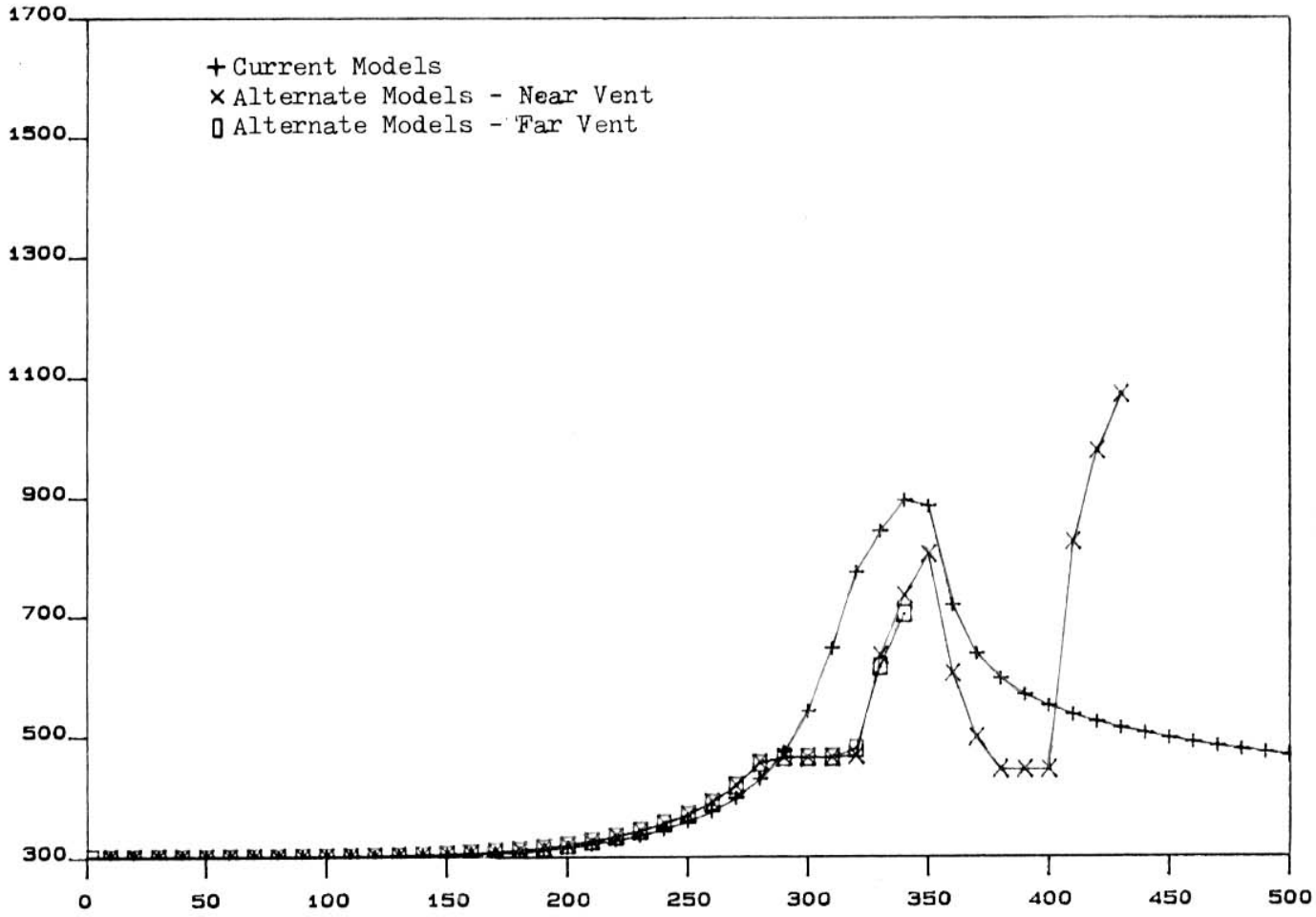
+ Current Models
× Alternate Models - Near Vent
□ Alternate Models - Far Vent
1700
1500
1300
1100
900
700
500
300
0
50
100
150
200
250
300
350
400
450
500
Temperature (deg K)
Time (sec)
Both Alt Models - Ceiling Surf Temp

Figure 4.3(F)

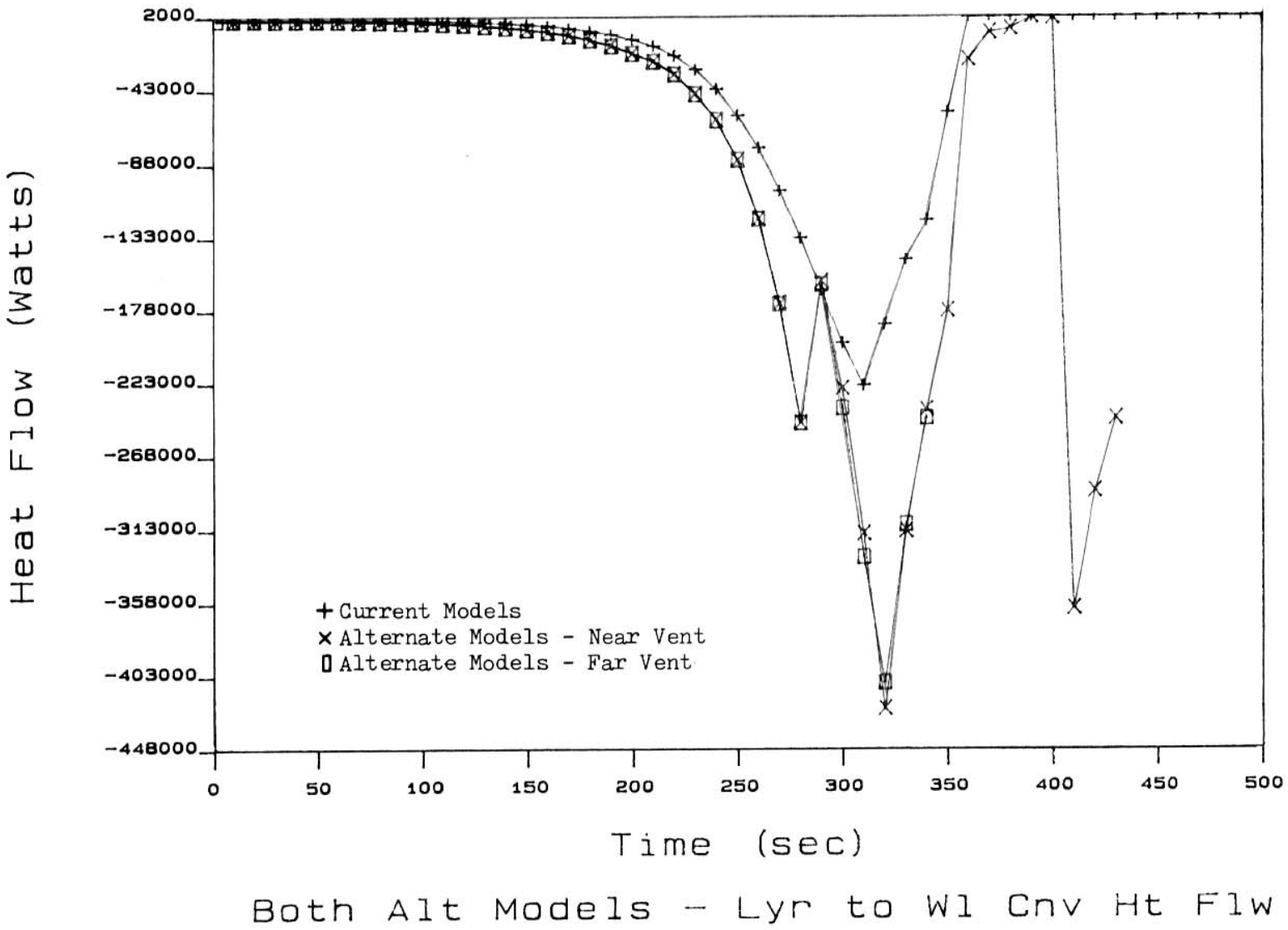
Heat Flow (Watts)
2000
-43000
-88000
-133000
-178000
-223000
-268000
-313000
-358000
-403000
-448000
0
50
100
150
200
250
300
350
400
450
500
Time (sec)
+ Current Models
× Alternate Models - Near Vent
□ Alternate Models - Far Vent
Both Alt Models - Lyr to Wl Cnv Ht Flw

Figure 4.3(G)

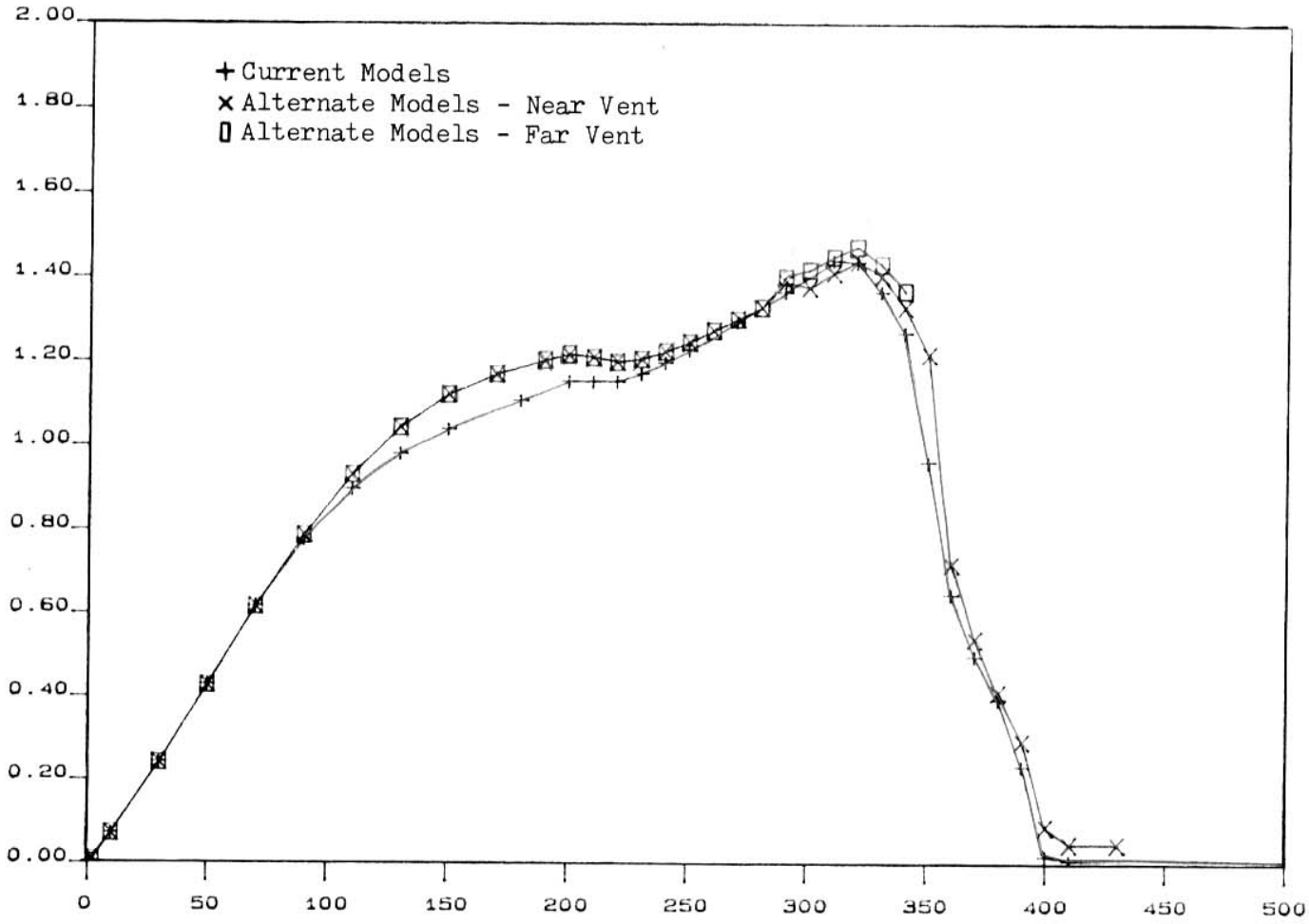
+ Current Models
× Alternate Models - Near Vent
□ Alternate Models - Far Vent
2.00
1.80
1.60
1.40
1.20
1.00
0.80
0.60
0.40
0.20
0.00
0
50
100
150
200
250
300
350
400
450
500
Depth (m)
Time (sec)
Both Alt Models - Upper Layer Depth

Figure 4.3(H)

these cases. This information is somewhat inconclusive since both of these cases had convergence problems. However, when comparing these values to those in Table 4.1(A) and 4.2(A), it appears that, if the convergence problems can be overcome, using both alternate models could decrease the time steps and iterations required for a given case. Once again, this is an advantage the alternate models have over the current models.

Table 4.3(A)

Calculation Information: "Both" Standard Cases

Case*3H	Total # of Time Steps	Total # of Iterations
HLX	302	9127
1	245	8416*1
2	181	6076*2

*1 Problem end time = 430 seconds

*2 Problem end time = 340 seconds

CPU times not available for these cases

*3 HLX = Current CFC/WPI model, large vent

1 = Both alternate models, large vent

2 = Both alternate models, large vent

5.0 Summary and Discussion of Results

This section attempts to present an overall picture of these alternate models: both in terms of the physics involved and some computational aspects.

5.1 ECCHTX

Generally speaking, the alternate ECCHTX model convects more energy to the ceiling than the current model. The reason for this is that higher gas temperatures are involved because the ceiling jet is the driving force of the convection heat transfer, instead of the upper layer. Therefore, ceiling surface temperatures are also higher and the conditions required for ceiling failure will occur sooner than in the current model. As a result, the upper layer temperature tends to be lower when the alternate ECCHTX model is used. These differences imply that current modeling practice may be suspect with respect to its physical formulation. In other words, the original assumption of one temperature difference being sufficient to realistically model ECCHTX is inadequate.

Specifically, Fig. 4.1(A) indicates a modeling inconsistency with regard to using a uniform upper layer temperature to characterize ECCHTX. If the uniform upper layer temperature is modeled as a function of the ceiling

jet temperature (i.e., as experimentally observed), then the uniform upper layer temperature would be higher than the current model's prediction and more in keeping with using a ceiling jet driven model, like the alternate ECCHTX model. Instead, the current model calculates the upper layer temperature from Eq. 4.2(A), the energy of the upper layer divided by the product of upper layer mass and a specific heat. This formulation ignores the physics of a ceiling jet/upper layer connection. In other words, information is lost to the model as a whole when the fire plume is assumed to be cut off at the interface between the upper and lower layers. In the current model the plume enters the upper layer and effectively disappears. However, it is now possible to connect the upper layer to the fire plume by way of the ceiling jet of the alternate ECCHTX model. Using this model, the upper layer conditions become more a function of the fluid and thermodynamics of the ceiling jet, i.e., a better, more realistic prediction would result. This scheme will be discussed further in Sect. 6.0.

5.2 CVMFR

Figures 4.2(A) and 4.2(E) indicate that the alternate CVMFR model predicts higher ceiling vent flows using the same data and theoretical basis as the current model. Specifically, both the alternate CVMFR model's "small" fire subroutine (CVA001) and the current model are essentially

static models; dynamic effects associated with ceiling jet momentum are not considered. Therefore, this subroutine truly provides an alternative methodology to the one currently employed.

However, the alternate CVMFR model may be incorrect and one possible refinement concerns the physical conditions at the vent location. Because a radial temperature distribution can be shown to exist for the gas temperatures near the ceiling surface under conditions where a static model is most valid, the ceiling jet model used in the alternate ECCHTX model can be used to predict the required radial temperature distribution and, more specifically, at the vent location itself. Thus, the alternate CVMFR model could be reformulated to always consider the conditions of the gases actually being vented, not those conditions represented by the bulk upper layer.

Figures 4.2(A) and 4.2(E) also indicate that the vents used in the scenarios of Sect. 4.2 may all be "near", i.e., the "near/far" distinction detailed in Sect. 3.3-3 is inappropriate and inadequate. From a qualitative viewpoint, the large fire, near vent subroutine, CVB101, provides the expected result: increased ceiling vent flow due to the close proximity of a strong plume/ceiling jet. The decreased CVMFR between 270 and 350 seconds was somewhat expected. Preliminary hand calculations indicated that this

alternate formulation would behave as indicated in Fig. 4.2(A) and 4.2(E). Unfortunately, at the time the hand calculations were performed, the significance of the differences between the various results was not recognized due to a lack of knowledge of the overall range of the ceiling vent mass flow that these models might predict. In other words, the calculations appear to be implemented correctly as given but there is some question as to whether or not they are the appropriate calculations. Section 6.2 presents recommendations intended to gather enough data to tune up this alternate CVMFR model.

5.3 Computational Considerations

As shown in Sect. 2.5 and 4.0, the alternate ECCHTX model can use a considerable amount of CPU time, as compared to the current model, while the alternate CVMFR model requires slightly less CPU time than the current model. The additional cost associated with the alternate ECCHTX model would be "worth the price" in scenarios where ceiling integrity is a primary concern. The alternate ECCHTX model can provide the detail necessary to reasonably predict when ceiling failure may occur. It must also be realized that total number of iterations is only a relative measure, not necessarily reflecting the actual CPU time, and is not entirely applicable to those cases which did not converge. Because CFC is still a developmental tool, less

emphasis should be placed on CPU expense than the physical models and logic required to effectively implement them.

6.0 Recommendations

Unfortunately, time constraints did not allow these alternate models to be fully exercised and investigated. This section details further work that may provide useful information regarding the use of these models. Two sections are used to discuss the recommendations: one each for the alternate ECCHTX and CVMFR models. Note that parts of the following discussion presume the reader is familiar with CFC and its use.

6.1 ECCHTX

For the alternate ECCHTX model, there are several recommendations: one for further model verification and the balance for other modeling aspects.

6.1-1 Further Model Verification

Although it appears that the alternate ECCHTX model is qualitatively reliable, there is a means that could make it quantitatively reliable as well. This would simply involve rerunning the 24 cases described in Sect. 2.5 with one major difference. Instead of modeling enclosures as such, i.e., rooms with relatively small aspect ratios, model the enclosure from a "large expansive ceiling" viewpoint. For example, instead of the small room being 2.4m X 3.6m X 2.4m

high, model it as a "room", say, 10m X 10m X 2.4m high. In this way a minimal upper layer will indeed be formed and the results are expected to come very close to those predicted in Ref. 6. This should also eliminate the "maximum vent size" problem discussed in Sect 2.5. However, it remains to be seen if this is a viable approach.

6.1-2 Future Modeling Considerations

One possible change to the alternate ECCHTX model concerns switching from the alternate to the current model. It is possible that instead of the switch being based on any one ceiling jet temperature, an average ceiling jet temperature could be used. At this point, however, determining the appropriate average ceiling jet temperature is more of a question than an answer.

The problem of switching from one ECCHTX model to another might be eliminated as unnecessary if CFC were revamped to incorporate all the data provided by the alternate ECCHTX model, instead of just some of its area weighted averages. In other words, CFC was "bent" a little in order to facilitate the alternate ECCHTX model. When the alternate model is in effect, the area weighted averages reduce the information available to the user and this also reduces the efficacy the user has to interpret the results. CFC could be revised to directly address the "new"

information provided by the alternate ECCHTX model. To this end, the following three points should be considered:

(1) The surface temperature at all of the points described in Sect. 2.3-4(A) should be included with the remainder of the system variables, instead of the current single value of extended ceiling surface temperature. In other words, the (maximum of) 14 surface temperatures should be placed in common block VAR (and those similar to it) such that they become part of the system of variables contained in JCOR (i.e., the variables involved in a given problem). With the proper coding, these surface temperatures, and the associated ceiling jet temperatures, and heat fluxes/flows if desired, could then be output for interpretation by the user.

(2) Enhance the data structure of CFC by providing a more complete connection between the lower plume (i.e., the portion below the layer interface) and the upper layer. This can be accomplished by considering the enthalpy transport of the plume as it passes through the upper layer and when it turns into a ceiling jet after it impinges on the ceiling. Since the radial temperature distribution is provided by point (1) above, it seems reasonable to consider the upper layer temperature to be a function of the ceiling jet conditions after the ceiling jet descends the wall as shown in Fig. 2.3-3(B) or Fig. 1.1(B). That is to say that

the upper layer is a direct result of the ceiling jet impinging on the wall and creating a downward wall jet. It is this wall jet energy or temperature that eventually determines the upper layer temperature/conditions. However, the crux of the problem is how to formulate the upper layer conditions as a function of the ceiling or wall jet conditions. At this point, it is not readily apparent but it should not be a major problem: one more of what averaging scheme is moat appropriate than anything else. (Currently CFC assumes that the lower plume is connected only to the upper layer and not to the upper plume or a ceiling jet.)

(3) The alternate ECCHTX model tends to indicate that the heat transfer to the extended ceiling is driven more by the ceiling jet conditions than the uniform upper layer conditions. Therefore, in addition to the convection to the extended ceiling being determined at a number of local points, the local radiation at those points should also be considered. The alternate ECCHTX model assumes that the radiation from the upper layer to the extended ceiling is driven by the uniform upper layer temperature, not by the local ceiling jet temperature, as Cooper does in Ref. 6.

By implementing the first two recommendations, the alternate ECCHTX model could be used to its fullest capacity instead of the "piggyback" mode used in this endeavor. Piggyback in this case refers to the fact that the alternate

ECCHTX model is significantly different from the original CFC formulation and as such is not a full part of the CFC methodology. To CFC, the alternate ECCHTX model "looks" like the current model, but the alternate model's potential is not fully realized. A major code modification would be required to incorporate these changes into CFC. As with other modeling techniques, the goal is to depict reality as accurately and practically as possible. Such modeling modifications would serve to increase the level of reality CFC is capable of reproducing.

As mentioned in Sect 2.3-4, an alternate method of placing the four points used to calculate the local conditions of the heated wall may be considered. Instead of the scheme employed by the alternate ECCHTX model described in Sect. 2.3-4, the four quarter circle equivalent radii also described in that section could also be used.

The temperature passed to function RE should be changed to use the local ceiling jet conditions. Currently the upper layer temperature is used and results in underpredicting the heat transfer coefficient of Eq. 2.3-2(A)1.

One final recommendation would be to incorporate more error checking into CFC. In other words, if CFC is to become a more useful theoretical tool, it would be helpful

if CFC checked the calculated temperatures to ensure that the first law of thermodynamics is not violated and to ensure that no more heat is transferred than is produced. While a remedy for these conditions way not be possible, certainly their existence can at least be detected by the program as an aid to the user.

6.2 CVMFR

Since very little is known of the alternate CVMFR model's capabilities, the recommendations for this alternate model are concerned with model refinements. It is thought that these refinements can ultimately result in a more complete understanding of the alternate CVMFR model and the process it details. Because no new variables have been introduced to the system of variables, this model does not have "piggyback" problems: the alternate CVMFR model is an optional method to computing a parameter already present in the system of variables, ceiling vent flow. (The alternate ECCHTX model, on the other hand, actually introduces a greater number of parameters, even though they are not fully utilized).

As discussed in Sect. 4.2, and shown in Fig. 4.2(A) and 4.2(E), using the alternate CVMFR model results in discontinuities when the fire size changes from "small" to

"large" or vice versa. Therefore, the scenarios to which each of the submodels (i.e., subroutines CVA001, CVB101, and CVB201) apply must be fully investigated and the "small/large" distinction recast. In other words, the Heskestad flame height correlation of Eq. 3.3-2(A) is an inappropriate measure of "small" and "large" when using the alternate CVMFR model as currently programmed.

In order to rectify this, each submodel should be used by itself, i.e., without switching to a different subroutine when the enclosure conditions change. This should provide some insight into when the momentum of the ceiling jet is significant (i.e., for large fires) and when it is not.

In conjunction with redefining "small/large" fires with regard to CVMFR, the "near/far" vent distinction should also be redefined. For example, for each of the three submodels mentioned above, two different room sizes could be considered. Within each room, several vent locations could also be used. Thus, all other things being equal, if three vent locations are used for each room, then 18 cases (three submodels, two rooms with three vent locations each) would be required. It is possible that the test rooms would be larger than a typical office or residential room in order to arrive at an acceptable definition of "far". In other words, subroutine CVB201 for "far" vents and "large" fires might be applicable only to rooms where the radial distance

between the plume axis and ceiling vent location is greater than a "typical" enclosure. The above procedure might also indicate that for the values of r/H of interest to CFC users, i.e., rooms with small aspect ratios, all vents may be "near" the fire plume such that subroutine CVB201 would be used only in extreme cases. This is suggested by the severe drop in ceiling vent flow shown in Fig. 4.2(A) and 4.2(E). It is expected that if the submodels of the alternate CVMFR model can be used individually, a sufficient amount of data can be gathered to reformulate the alternate CVMFR model subroutines into a more coherent and useful model.

One final recommendation would be to consider using a ceiling jet velocity that is a function of radial distance as opposed to one that considers only the fire strength, as per Eq. 3.2(N). This might be accomplished by using a ceiling jet model similar to that of the alternate ECCHTX model.

Because the alternate CVMFR model requires more development and experimental validation, it should not be used for critical CVMFR calculations. However, the above recommendations could provide the theoretical data against which experimental data could be compared. At the very least it seems that this theoretical data would provide some basis for intuition, and a starting place, when considering

CVMFR experiments.

7.0 User's Guide

This section is intended to educate the user in the practical aspects of using these alternate models. Specifically, this includes what differences the user encounters during the interactive input processing and those seen when interpreting the output data. Appropriately enough, two sections will be devoted to this endeavor: one each for the input and output. A third section details the program messages which may appear on the terminal screen when using the alternate models. It is assumed that the reader has some familiarity with using CFC.

7.1 Input

These alternate models were designed to conform to the input processing of CFC, version V. To this and, they are also user friendly. Only two new questions have been added to the "choices" for physical subroutines. Thus, instead of four choices, six are now provided: the fifth referring to the ECCHTX models and the sixth to the CVMFR models. Figure 7.1(A) shows an example of CFC's interactive input processing and how to access the alternate models previously discussed. The sequence of this figure begins with the output file name question at the top and then skips ahead to "changing the physics subroutines". At this point the user simply answers the questions depending on his wishes.

Figure 7.1(A)

```
WHAT IS THE OUTPUT FILE NAME (UP TO SIX CHARACTERS)
        :
        :
        V
CHANGE FROM STANDARD SET OF PHYSICS SUBROUTINES? (Y/N):
Y
WHICH VERSION OF TMPO DO YOU WANT (01 OR 02)
DEFAULT IS TMPO02:

WHICH VERSION OF ABSRB DO YOU WANT:
01 - Absorption coefficient grows exponentially with time
02 - Absorption coefficient proportional to soot fraction
03 - Broad-band approximation + soot (Modak)
DEFAULT IS ABSRB2:

Which plume entrainment law do you wish:
01 - Emmons-Mitler displaced virtual source
02 - McCaffrey (empirical data fit)
03 - Zukoski, Cetegen, Kubota (empirical data fit)
DEFAULT VERSION IS 01

WHICH VERSION OF THE BURNER FIRE DO YOU WANT:
01 - WITHOUT OXYGEN STARVATION
02 - WITH OXYGEN STARVATION
DEFAULT IS 02 - WITH

WHICH VERSION OF CNVW DO YOU WANT:
01 - MITLER: UNIFORM LAYER TEMP
02 - COOPER: CEILING JET
DEFAULT IS VERSION 01
2
WHICH VERSION OF CEILING VENT FLOW DO YOU WANT:
01 - STATIC ONLY
02 - STATIC PLUS DYNAMIC
DEFAULT IS VERSION 1
2

CHANGE FROM STANDARD GEOMETRIC AND PHYSICAL PARAMETERS
(DEFAULT USES DATA FOR HARVARD-FM BEDROOM TEST SERIES)? (Y/N)
        :
        :
        V
```

Input Processing Example

Answering "Y" to changing from the standard set and then "2" the final two questions, as shown in Fig. 7.1(A), will access the alternate models. As shown by this figure, the default versions for these models are the current versions in CFC/WPI: CNVW, et al., for the ECCHTX model and subroutine HFLOW for the CVMFR model. In other words, if these choices are not stored in an input file, then the alternate models described herein must be explicitly requested. This figure ends with the next question asked during the input processing.

7.2 Output

The most obvious change in CFC's output is the final line labeled "Ceiling:", as shown by "***" in Fig. 7.2(A). The first variable, ZKJZS is the area weighted average ceiling jet temperature, based on the locations determined by subroutine CNVW02. The second variable, ZKEZP is the peak extended ceiling surface temperature. This is the temperature at the impingement point of the plume on the ceiling: r/H = 0. When the alternate ECCHTX model is not being used, these variables are set equal to zero or their last calculated value.

The other significant change to the output is less apparent. When using the alternate ECCHTX model, the user must keep in mind that the convective flux and the extended

Figure 7.2(A)

T= 50.000	DT= 2.000	NT= 25	NIT= 566	IT= 36 G.S.
ROOM= 1:	TELZR= 6.3575E+01	TELZD=-3.3246E+02	ZMLZZ= 4.4629E+00	
	TMLZZ= 1.0047E-01	ZELZZ= 1.3511E+06	TELZZ= 3.0486E+04	
	ZHLZZ= 4.2732E-01	ZKLZZ= 3.0153E+02	ZYLOZ= 2.3136E-01	
	ZYLDZ= 7.5278E-04	ZYLMZ= 2.2346E-06	ZYLSZ= 6.2294E-05	
	ZYLWZ= 1.1988E-04	ZPRZZ= 5.4659E-09	ZKDZZ= 3.0000E+02	
	ZYCO = 2.3180E-01	ZYCD = 5.0051E-04	ZYCM = 0.0000E+00	
	ZYCS = 0.0000E+00	ZYCW = 0.0000E+00	TMIXM= 0.0000E+00	
OBJ= 1:	FQLOR= 1.7426E+00	FQWOR= 1.4341E+02	FQPOR= 9.7801E+03	
(ID= 1)	ZKOZZ= 7.2700E+02	ZMOZZ= 6.8508E+00	TMOZZ=-4.4848E-05	
	TEOZZ=-8.2786E+02			
	ZHPZZ= 1.4011E+00	TMPZZ= 1.0086E-01	TEPZZ= 3.0872E+04	
	TEPZR= 3.4794E+02			
	ZRFZZ= 6.1030E-02			
OBJ= 2:	FQLOR= 1.9899E+00	FQWOR= 4.5761E+02	FQPOR= 0.0000E+00	
(ID= 2)	ZKOZZ= 3.0001E+02	ZMOZZ= 1.0963E+00	TMOZZ= 0.0000E+00	
	TEOZZ= 0.0000E+00			
VENT= 1:	TEUZZ= 1.1715E+02	TMUZZ= 3.8696E-04	TMDZZ= 4.0145E-04	
WALL= 1,1:	FQLWR= 5.0801E+00	FQPWR= 0.0000E+00	FQLWD= 3.1068E+01	
	ZKWZZ= 3.0025E+02			
WALL= 1,2:	FQLWR= 0.0000E+00	FQPWR= 0.0000E+00	FQLWD=-6.2802E-12	
	ZKWZZ= 3.0000E+02			
WALL= 2,1:	FQLWR= 0.0000E+00	FQPWR= 0.0000E+00	FQLWD= 0.0000E+00	
	ZKWZZ= 3.0000E+02			
WALL= 2,2:	FQLWR= 0.0000E+00	FQPWR= 0.0000E+00	FQLWD= 0.0000E+00	
	ZKWZZ= 3.0000E+02			
*** CEILING:	ZKJZS= 3.0221E+02	ZKEZP= 3.0169E+02		

Tabular Output Example

ceiling surface temperature on the exposed side of the wall, FQLWD(1,1) and ZKWZZ(1,1), and the time rate of change of convective heat flow of the upper layer, TELZD(1), are based on the conditions represented by the ceiling jet, until the program switches to the current ECCHTX model. As explained in Sect. 4.1, these variables undergo a discontinuity when this switch is made. Also, as explained in Sect. 4.1, the hot upper layer temperature, ZKLZZ(1), experiences a discontinuity that appears less drastic, as shown in Fig. 4.1(A).

7.3 Program Messages

When using the alternate ECCHTX model, two different messages may appear both on the terminal screen and in the output disk file. The most likely message is printed when switching from the alternate to the current ECCHTX model. The message states:

*** CONVECTIVE HEAT TRANSFER MODEL CHANGED TO CNVW

*** CEILING JET TEMP > 1300K AT "time"

Note that instead of "time", the program prints the time, in seconds, at which the switch to the current model is made. This message is printed whenever a ceiling jet gas temperature greater than 1300K is calculated and when the number of iterations is greater than five. Requiring the

number of iterations to be greater than five tends to ensure that, indeed, the 1300K value is a valid prediction. In other words, the gas temperature may be calculated to be above 1300K at the beginning of the time step due to the extrapolation procedure used by CFC. This is not the value that should be used to trip this message. Five iterations are usually enough to bring the values of these parameters to within a small percentage of their values at the end of the time step. This 1300K restriction can easily be changed should experimental data warrant such a modification.

The second message may or may not be printed; it depends on several factors, including the enclosure and fire sizes. This message states:

```
*** CEILING SURFACE TEMP EXCEEDS 1300K     ***
*** SUBSEQUENT RESULTS MAY BE QUESTIONABLE  ***
```

This message is printed whenever any point on the extended ceiling surface rises above 1300K and when the number of iterations is greater than five. In addition to printing this message, the program imposes a maximum of 1300K for any calculated ceiling surface temperature.

Also of note is that whenever this message was printed during the model verification described in Sec. 2.5, the

program failed to converge and changed the time step. When the output was analyzed, the wall surface temperature prediction appeared to be reasonable. Therefore, the message is attributed to the time step size being too large and thus it can be ignored. No surface temperatures were observed to be above 1300K at the time when the message was printed. However, if the message is printed at the time when the extended ceiling surface temperature exceeds 1300K, then the subsequent results are more likely to be suspect since this temperature exceeds the (approximate) adiabatic flame temperature. Therefore, care must be taken when analyzing output if the alternate ECCHTX model is used. Due to the program's ability to switch algorithms and the higher calculated temperatures, the output may be misleading at first glance. Also, since this message is printed only once, there is potential for confusion. If the message is printed early in the fire due to a convergence related problem (and therefore of little concern), it will not be printed a second time, if the surface temperature actually rises above 1300K. In this case the constant 1300K temperature will indicate that the upper temperature limit had been met and that the ceiling has, essentially, failed or ignited.

No messages are printed when the alternate CVMFR model is used. However, if the alternate CVMFR model, as described herein, remains intact, then "switching" messages

should be included for the "small" to "large" fire switch, as described in Sect. 3.3-2.

8.0 Conclusion

Of these two alternate models, the alternate ECCHTX model has more practical application, i.e., it can be used with more confidence, than the alternate CVMFR model. To this end, the alternate ECCHTX model can be used to predict ceiling surface temperature distributions, and specifically the impingement point ceiling surface temperature. The alternate ECCHTX model is applicable at early times in the fire and up to the point where the ceiling jet temperature rises above the time averaged flame temperature, as described in Sect. 2.5. In this way, ceiling failure due to increased temperatures may be predicted. (With additional modeling the alternate ECCHTX model could also be used to predict the gas temperatures experienced by fire detection devices such as the fusible links of automatic sprinklers.

As indicated in Sect. 3.3, this alternate CVMFR model was implemented to perform a series of numerical experiments since it was not evident what the correlations would predict over the course of a fire simulation. These experiments indicate that the alternate CVMFR model requires further investigation and modification. In its present form, the alternate CVMFR model appears to be applicable to only "near" vents. This is, however, an improvement over the current model since momentum of the flames/fire plume in the "near" scenario can be included as part of the driving force

for flow through the ceiling vent. However, a more appropriate definition of "near/far" is required before this alternate CVMFR model can be used with confidence.

The current work is intended to provide a basis or starting point for future work in modeling some of these convection phenomena associated with enclosure fires. It is admittedly limited and fraught with (at least two) shortcomings: a serious lack of experimental verification on the part of CVMFR and it is, essentially, limited to only the initially burning object due to the lack of data describing the interaction of multiple fire plumes/ceiling jets. This tends to point out that experimental research is severely needed in the areas of ceiling vents and their behavior under specific conditions, in a given enclosure. Research concerning pre-flashover enclosure fires in which more than one object is burning should also be undertaken but this area is not as critical as that concerning ceiling venting.

In conclusion then, from the view point of using CFC as a theoretical tool, both of the alternate models for fire convection phenomena can provide useful and meaningful results. If the recommendations described in Sect. 6.1-2 and 6.2 are implemented, these alternate models can further understanding regarding the modeling of fire convection phenomena.

References

1) Alpert, R.L. (1972) "Calculation of Response Time of Ceiling Mounted Fire Detectors", Fire Technology, Vol. 8.

2) Byeler, C.L. (1986) "Fire Plumes and Ceiling Jets", Fire Safety Journal, Vol. 11.

3) Conte, S. D. and de Boor, C. (1980) Elementary Numerical Analysis, 3rd ed., McGraw-Hill, New York.

4) Cooper, L. Y. (1982) "Heat Transfer from a Bouyant Plume to an Unconfined Ceiling", Journal of Heat Transfer, Transactions ASME, Vol. 104, No. 3, AUG82.

5) Cooper, L. Y. (1982) "Convective Heat Transfer to Ceilings Above Enclosure Fires", Nineteenth Symposium (International) on Combustion, The Combustion Institute, Pittsburgh, PA.

6) Cooper, L. Y. (1984) Thermal Response of Unconfined Ceilings Above Growing Fires and the Importance of Convection Heat Transfer, NBSIR 84-2856, National Bureau of Standards, Washington, D.C.

7) Cooper, L.Y. and Woodhouse, A. (1985) The Buoyant Plume-Driven Temperature Revisited, NBSIR 85-3134, National Bureau of Standards, Washington, D.C.

8) Cooper, L.Y. (1986) Ceiling Jet Properties and Wall Heat Transfer in Compartment Fires Near Regions of Ceiling Jet-Wall Impingement, NBSIR 86-3307, National Bureau of Standards, Washington, D.C.

9) Evans, D. D. (1984) "Calculating Fire Plume Characteristics in a Two-Layer Environment", Fire Technology, Vol. 20, No. 3.

10) Fang, J. B. (1980) Static Pressure Produced by Room Fires, NBSIR 80-1984, National Bureau of Standards, Washington, D.C.

11) Heskestad, G. and Delichatsios, M. A. (1979) "The Initial Convective Flow in Fire", Seventeenth Symposium (International) on Combustion, The Combustion Institute, Pittsburgh, PA.

12) Heskestad, G. (1980) Pressure Profiles Generated by Fire Plumes Impacting on Horizontal Ceilings, Norwood, MA.: Technical Report FMRC J.I. OFOE1.RV, Factory Mutual Research.

13) Heskestad, G. (1983) "Luminous Heights of Turbulent Diffusion Flames", Fire Safety Journal, Vol. 5.

14) James, M. L., Smith, G. M., and Wolford, J. C. (1985) Applied Numerical Methods for Digital Computation, Harper & Row, New York.

15) Kennedy, L. A. and Cooper, L. Y. (1987) "Before the Smoke Clears", Mechanical Engineering, Vol. 109, No. 4, APR87.

16) Mitler, H.E. and Emmons, H.W. (1981) Documentation for CFC V, The Fifth Harvard Computer Fire Code, NBS-GCR 81-344, National Bureau of Standards, Washington, D.C.

17) Mitler, H. E. (1983) "Some Effects of Opening a Vent in a Burning Room".

18) Thomas, P. H., Hinkley, P. L., Theobald, C. R., and Simms, D. L. (1963) Investigations Into the Flow of Hot Gases in Roof Venting, Herts, England: Fire Research Technical Paper No. 7, U.K. Fire Research Station, Boreham Wood.

19) You, H-Z, and Faeth, G. M. (1979) "Ceiling Heat Transfer During Fire Plume and Fire Impingement", Fire and Materials, Vol. 3, No. 3.

APPENDIX A: CURRENT CFC/WPI CEILING VENT MODEL

The ceiling vent model currently used by CFC/WPI treats the fluid in an enclosure containing a fire as if it were at rest "far" from the fire. That is to say, that because the fire plume is cut off at the interface between the hot, upper layer and the cold, lower layer, the fluid is not accelerated in either the horizontal or vertical directions. Therefore, the enclosure can be considered from a hydrostatic viewpoint. The fluid is stratified into essentially two layers due to temperature/density differences induced by the fire. These two layers are assumed to be in static equilibrium. In this scenario pressure will decrease with increasing elevation above the floor because the weight per unit cross-sectional area of the layers of fluid lying between the vertically spaced points whose pressure difference is being measured decreases with increasing height above the reference plane of the floor. With these conditions in mind, an expression can be derived for ceiling vent mass flow rate, by starting with

Eq. A1

$$\dot{m} = \rho A u C_D$$

where: ρ = vented gas density

A = cross-sectional vent area

u = vented gas velocity

C_D = discharge coefficient

and by applying Bernoulli's theorem to find the vent velocity, U.

From Bernoulli's theorem it can be shown that

Eq. A2a

$$\frac{\rho u^2}{2} = \Delta P_{Pa}$$

where: $\Delta P_{Pa} =$ pressure difference in Pascals

Solving for u results in:

Eq. A2b

$$u = \left(\frac{2\Delta P_{Pa}}{\rho} \right)^{1/2}$$

which, when plugged into Eq. A1, results in

Eq. A3

$$\dot{m} = A C_D (2\rho \Delta P_{Pa})^{1/2}$$

As stated above, the ΔP pressure difference for this scenario is a function of gas density and height above the enclosure floor. In order to relate ΔP_{Pa} to this height, equate ΔP_{Pa} and the elevation head:

Eq. A4

$$\Delta P_{Pa} = \rho_a g h$$
$$= \rho_a g \Delta P_m$$

where: ρ_a = ambient density

ΔP_m = pressure difference in meters of air

Therefore, Eq. A3 now becomes

Eq. A5

$$\dot{m} = AC_D(2\rho(\rho_a g \Delta P_m))^{1/2}$$
$$= (\rho_a g)^{1/2} AC_D(2\rho\Delta P_m)^{1/2}$$

The pressure difference ΔP_m is simply the pressure at the floor, P_f (measured in meters of air) plus the pressure change associated with some height, h, above the floor. Strictly speaking, the pressure difference is:

Eq. A6a

$$\Delta P_m = P_f + \int_o^h \frac{\rho_a - \rho}{\rho_a} dz$$

where: ρ = density at height

Solving the integral for both the upper layer (between the layer interface and the ceiling) and the lower layer (between the floor and the layer interface) yields the following expression for the pressure difference driving the mass flow of a ceiling vent, assuming the pressure on the discharge side of the vent is at ambient:

Eq. A6b

$$\Delta P = P_f + (h_R - h_L)\frac{\rho_a - \rho_L}{\rho_a} + h_L \frac{\rho_a - \rho_u}{\rho_a}$$

where: h_R = room height

h_L = upper layer thickness

ρ_u = " " density

ρ_L = lower " "

The final expression for the ceiling vent mass flow rate used by CFC/WPI is:

Eq. A7

$$\dot{m} = (\rho_a g)^{1/2} A C_D (2\rho \mid \Delta P \mid)^{1/2} \operatorname{sgn}(\Delta P)$$

where: sgn(ΔP) = sign (+ or -) of Δp

Subroutine HFLOW performs the above calculations for CFC/WPI.

Appendix B: Listings of Required Subroutines

This appendix is divided into two sections. The first deals with the alternate ECCHTX model and the second with the alternate CVMFR model. The subroutines in each section are listed alphabetically: see Sec. 2.4 and 3.4, also.

Alternate ECCHTX Model Subroutines

```
C ********************************************************************************
C
      SUBROUTINE BIGHRR(OERR,NOBJ)
C
C ********************************************************************************
C
C CALLED BY CNVW02 AND CVB001
C
C CODED, ETC., BY D. BELLER JAN87
C
C THIS ROUTINE FINDS THE OBJECT WITH THE HIGHEST RELEASE RATE
C
C   LINDX IS AN ARRAY CONTAINING THE OBJECT NUMBERS
C   TMPERR IS AN ARRAY CONTAINING THE-VALUES OF OBJECT HT REL RATE
C   THESE TWO ARRAYS ARE FIRST SORTED INTO ASCENDING ORDER (IF 0 OF
C   OBJECTS IS GREATER THAN 1) SO THAT LRGST = LINDX(NOBJ). LRGST IS
C   STORED IN ECCHTX.CMN
C
      IMPLICIT REAL*8 (A-H,O-Z)
      INCLUDE 'BD:ECCHTX.CMN'
C
      DIMENSION TMPERR(5),LINDX(5),OERR(5)
C
      KOBJ = NOBJ
C
C ASSIGN TEMPORARY VALUES OF HEAT RELEASE RATE AND OBJECT NUMBERS
      DO 11 1 = 1, KORJ
            TMPERR(I+0) = DABS(OERR(I+O))
            LINDX(I) = I
11    CONTINUE
C EMPLOY SORT ALGORITHM
      KOM = KOBJ - 1
      DO 13 I = 1, KOM
            IP1 = I + I
            DO 12 J = IP1, KOBJ
                  IF (TMPERR(I) .LE. TMPERR(J)) GO TO 12
```

```
                  T1= TMPERR(I)
                  L1 = LINDX(I)
                  TMPERR(I) = TMPERR(J)
                  LINDX(I) = LINDX(J)
                  TMPERR(J) = T1
                  LINDX(J) = L1
12          CONTINUE
13    CONTINUE
C
      LRGST = LINDX(KOBJ)
C
      RETURN
      END
```

```
C ******************************************************************************
C
      SUBROUTINE CFCTRS(TA,TU,QS,Z,HI,D,HHTLYR,QHTLYR,THTLYR)

C
C ******************************************************************************
C
C CALLED BY CNVW02 AND CVB201
C
C EQUATIONS BY L.Y. COOPER
C
C CODING BY D. BELLER FALL86
C
C THIS ROUTINE DETERMINES THE CORRECTION FACTORS TO USE WHEN HOT LAYER
C EFFECTS SHOULD BE CONSIDERED.
C
C INPUT IS:
C     TA = AMBIENT TEMP
C     TU = UPPER LAYER TEMP
C     QS = DIMENSIONLESS HEAT RELEASE RATE
C     Z  = PLUME SOURCE-TO-LAYER INTERFACE DISTANCE
C     HI =   "     "     " CEILING DISTANCE
C     D  = UPPER LAYER DEPTH
C
C OUTPUT IS:
C     HHTLYR = PLUME SOURCE-TO-CEILING CORRECTION FACTOR
C     QHTLYR = HEAT RELEASE RATE CORRECTION FACTOR
C     THTLYR = TEMPERATURE CORRECTION FACTOR
C
      IMPLICIT REAL*8 (A-H,O-Z)
C
      EXP1 = 2. / 3.
      EXP2 = 1. / 5.
      EXP3 = 3. / 5.
C
      THTLYR = TU / TA
C
```

```
      QHTLYR = (0.210 * (1. - THTLYR) / QS**EXP1) + 1.
      IF (QHTLR .LT. 0.) QHTLYR = DABS(QHTLYR)
C
      HHTLYR = (D / HI) + ((1. - D/HI) * (THTLYR**EXP3)
      1                      / (QHTLYR**EXP2))
C
      RETURN
      END
```

```
C ******************************************************************************
C
      SUBROUTINE CNVL02(TELZD1)
C
C ******************************************************************************
C
C CALLED BY CALS, CALS1
C
C EQUATIONS BY H. EMMONS
C CODED BY L. TREFETHEN, C. GRAMLICH, AUGUST 1977
C RECODED BY M. GILSON, B. LONDON, AUGUST 1978
C PIRATED AND REFITTED TO HANDLE THE MORE DETAILED ECCHTX CALCULATION
C BY D. BELLER, JAN87
C
C CALCULATES THE RATE OF LOSS OF ENERGY OF THE HOT LAYER OF ROOM KR,
C DUE TO CONVECTION (I.E. TO THE AUGMENTED CEILING).
C
C THIS ROUTINE TREATS THE CONV HEAT TRANSFER TO THE EXTENDED CEILING AS
C IF IT IS COMPOSED OF TWO COMPONENTS: ONE FOR THE CEILING PROPER AND
C THE OTHER FOR THE HEATED PORTION OF THE WALLS. THE AREAS OF EACH WALL
C AND THE CEILING ARE USED AS WELL AS THE LOCAL CONV HEAT FLUXES STORED
C IN ECCHTX.CMN (I.E., WALL AREAS MINUS VENT AREAS).
C
C OUTPUT: TELZD1 = TIME RATE OF CHANGE IN HOT LAYER CONVECTIVE ENERGY
C
C THE FOLLOWING VARIABLES ARE REQUIRED, IF FROM A COMMON BLOCK,
C THE BLOCK NAME IS IN PARENTHESES AFTER THE DESCRIPTION:
C
C     ZELZZ       = ENERGY OF THE HOT LAYER (VAR)
C     TELZZ       = TIME CHANGE IN ENERGY OF THE HOT LAYER (VAR)
C     FQWLOC      = LOCAL CONVECTIVE HEAT FLUXES (ECCHTX)
C     TELD        = LOCAL TELZD
C     FQW,FQW0    = LOCAL SUMS OF INSIDE/OUTSIDE HEATED WALL HEAT FLUXES
C     AQW,AQW0    = "TIME INTEGRATED" FQW'S
C     AQWTOT      = SUM OF AQW'S
C     NOPNTS      = NUMBER OF POINTS USED IN ECCHTX CALCS
```

```
C     RP          = RADII USED IN ANNULAR CEILING AREA CALCS (ECCHTX)
C     DATOVC      = RADIAL DISTANCE, PLM AXIS TO VENT CENTER
C
      IMPLICIT REAL*8 (A-H,O-Z)
C
      INCLUDE 'BD:VAR.CMN'
      INCLUDE 'BD:OLDVAR.CMN'
      INCLUDE 'BD:CONTRL.CMN'
      INCLUDE 'BD:POINTR.CMN'
      INCLUDE 'BD:ROOM.CMN'
      INCLUDE 'BD:CVENT.CMN'
      INCLUDE 'BD:HVNTEB.CMN'       !ADDED  260CT86  DKB
C ADDED NEXT 3 LINES FOR ECCHTX  12FEB87  DKB
      INCLUDE 'BD:ECCHTX.CMN'
      INCLUDE 'BD:CVMFR.CMN'
      INCLUDE 'BD:CONST.CMN'
C
      DIMENSION AQW(4), FQW(4), AQW0(4), FQW0(4),
      1     TELD(14)
C
      DATA AQW, FQW / 4*0.D0,4* 0.D0 /
C
C THIS ROUTINE IS GOOD FOR ONE ROOM ONLY!!!
C
      KR = 1
      KW = 1
      NP = NOPNTS
      NPP4 = NP + 4
C
      IF (INEWT .NE. 1) GO TO 5
C
      DO 10 I = 1, 4
            AQW0(I) = AQW(I)
            FQW0(I) = FQW(I)
10    CONTINUE
C
```

```
      RETURN
C
5     IF (INEWT .EQ. 2) GO TO 700
C
      DO 20 J = 1, 4
            FQW(J) = FQWLOC(J) + FQLWD(KW,2)
            AQW(J) = AQW0(J) + (FQW(J) + FQW0(J)) * DT / 2.
20    CONTINUE
C
C CALC LOCAL CONVECTIVE HEAT TRANSFER NPP4 TIMES AND TOTAL TELZD
C
      TELZDT = 0.0
      DO 70 K = 1, NPP4
            TELD(K) = ACNVHT(K) * FQWLOC(K)
            TELZDT = TELZDT + TELD(K)
70    CONTINUE
      TELZD1 = -TELZDT
C
C CHECK IF LAYER IS INCREASING IN ENERGY (I.E., INCREASING IN HEIGHT)
C AND, IF SO, SUBTRACT OUT THE ENERGY DEPOSITED IN THE 'COOL' WALL
C (T.R. 34, PG. 50-51)
C
      IF (TELZZ(KR) * ZELZZ(KR) .LE. 0.) GO TO 700
C
      AQWTOT = 0.0
      DO 80 L = 1, 4
            AQWTOT = AQWTOT + AQW(L)
80    CONTINUE
C
C ADJUST ACCORDINGLY
C
C
      TELZD1 = TELZD1 - 0.5 * THTXAW * AQWTOT * TELZZ(KR) / ZELZZ(KR)
C
C CHECK MAGNITUDE OF OUTPUT VARIABLE
C
```

```
700   CONTINUE
      BNDS = 2.E6 * ZLRZY(KR) * ZLRZX(KR)
      IF (DABS(TELZD1) .GT. BNDS) TELZD1 = TELZDP(KR)
C
      RETURN
      END
```

```
C ***********************************************************************************
C
      SUBROUTINE CNVW02(RLX,RLY,HR,HLH,NNO,ERRO,RERRO,MXV,
      1                 INWT,ZKA,ZKL,DELT,ZTZ,QLWR,QPWR,QLWDP,FOLWDl)
C
C ***********************************************************************************
C
C CALLED BY CALS
C
C CODING BY D.BELLER SEP86
C
C THIS IS THE CONTROLLING ROUTINE FOR THE CONVECTION HEAT TRANSFER
C TO THE EXTENDED CEILING, INSIDE AN ENCLOSURE WITH A FIRE; I.E.,
C KW = 1, JSIDE   1.
C SUBR CNVW01 IS STILL USED FOR KW = 1, JSIDE = 2
C
C CALCULATIONS ARE MADE WITH RESPECT TO THE OBJECT HAVING THE HIGHEST
C HEAT RELEASE RATE
C
C NOTE: THE GEOMETRY OF THE PROBLEM IS BASED SOLELY ON OBJECT ONE
C SINCE IT IS INITIALLY BURNING AND MOST LIKELY "LRGST"
C
C OUTPUT IS: FQLWD1
C     NOTE: FQLWD1 IS AN AREA WEIGHTED AVERAGE OF UP TO
C           14 POINTS
C
C INPUT IS:   LOCAL     CFC   DESCRIPTION
C     RLX   = ZLRZX  = ROOM X DIMENSION         !1R:ONE ROOM ONLY
C     RLY   = ZLRZY  =  "   Y     "             !1R:ONE ROOM ONLY
C     HR    = ZHRZZ  =  "   HEIGHT              !1R:ONE ROOM ONLY
C     HLH   = ZHLZZ  = HOT LAYR DEPTH           !1R:ONE ROOM ONLY
C     NNO   = NO     = NUMBER OF OBJECTS
C     ERRO  = TEOZZ  = ENRG RELEASE RATE OF OBJECTS
C     RERR0 = TEPZR  = RAD POWR LOSS FROM FLAMES
C     INWT  = INWET  = CALC INDEX
C     MXV   = NUMBER OF VENTS
```

```
C     ZKA   = ZKAZZ  = (INITIAL) AMBIENT TEMP   !1R:ONE ROOM ONLY
C     ZKL   = ZKLZZ  = UPPER LAYER TEMP         !1R:ONE ROOM ONLY
C     DELT  = DT     = TIME STEP SIZE
C     ZTZ   = ZTZZZ  = TIME
C     QLWR  = FQLWR  = LAYR TO WALL RADIENT HEAT FLUX
C     QPWR  = FQPWR  = PLUME TO WALL RADIENT HEAT FLUX
C     QLWDP = FQLWDP = CONV HEAT FLUX FROM PREVIOUS TIME STEP
C
C PARAMETERS FROM COMMON
C     ZXOZZ = OBJ X COOR
C     ZYOZZ =  "  Y  "
C     ZHOZZ =  "  HEIGHT
C     ISTAT = STATE OF OBJECTS
C     VMWZZ = WALL DENSITY
C     ZCWZZ =  "   SP. HEAT
C     ZJWZZ =  "   CONDUCTIVITY
C     PI    = 3.14159...
C     LRGST = # OF OBJ WITH HIGHEST HEAT REL RATE (IN ECCHTX.CMN)
C     VAHTX = VENT AREAS USED FOR HEAT TRANSFER CALCS (CVMFR.CMN)
C     VAREA =  "     "   CALC'D IN VENTA (CVMFR.CMN)
C     AVWT  = TOTAL WALL VENT AREAS COVERED BY HOT LAYER
C     THTXAW = TOTAL HEAT TRANSFER AREA OF THE HEATED WALL
C     THTXAC =   "     "      "     "    "  "  CEILING
C     ACNVHT = ARRAY CONTAINING ECCHTX AREAS (ECCHTX.CMN)
C     AHTXT  = TOTAL SUM OF ACNVHT'S (ECCHTX.CMN)
C     NOPNTS = # OF PNTS USED TO CHARACTERIZE THE CEILING (ECCHTX)
C     BVWT   = TOTAL WALL VENT WIDTH
C     HV     = HL - ZHTZZ
C     ZHVZZ  = VENT HEIGHTS (CVENT)
C     ZBVZZ  =  "   WIDTHS     "
C
C LOCAL PARAMETERS ARE:
C     H     = PLUME SOURCE-TO-CEILING DISTANCE OF OBJ 1 (ECCHTX)
C     HZ    = PLUME SOURCE-TO-LAYER INTERFACE DISTANCE
C     RH    = R / H
C     LFLG  = LAYR DEPTH FLAG = 0, ZHL .LT. 0.24 * HR
```

```
C                       = 1, ZHL .GT. 0.24 * HR
C     QSTR   = DIMENSIONLESS HEAT RELEASE RATE
C     RHOCTG = (RHO * SP HT * TEMP FOR AMB AIR) * G**0.5
C     RHOCG  = (RHO * SP HT FOR AMB AIR) * G**0.5
C            = (1.177 * 1004 * 9.8**0.5)
C     INITC5 = INITIALIZATION FLAG
C     TAD    = LOCAL NEAR SURFACE GAS TEMP
C     TSRF   = LOCAL CEILING SURFACE TEMP
C     HTC    = LOCAL HTX COEF FOR CEILING
C     FQWLOC = LOCAL CONV HEAT FLUXES FOR EXTENDED CEILING
C     QAVGC  = AVG     "    "   FLUX FOR CEILING
C     QAVGW  = AVG     "    "   FLUX FOR HEATED WALL
C     ISWCH  = CALC SWITCH: 0 = CEILING CALC
C                           1 = HEATED WALL CALC
C     RMAX   = RADIUS OF EQUIVALENT CEILING AREA
C     RHMAX  = MAX VALUE OF R/H (SHOULD BE < 2.2)
C     R      = RADII WHERE THE LOCAL CONVECTIVE HTX CONDITIONS
C              ARE CALC'D (STORED IN ECCHTX.CMN)
C     RP     = RADII USED IN CEILING AREA CALCS
C              (STORED IN ECCHTX.CMN)
C     PREDRH = ARRAY CONTAINING PREDETERMINED VALUES OF R/H: # OF
C              POINTS USED DEPENDS ON RHMAX:10 MAX FOR THE CEILING
C     PREDRP = ARRAY CONTAINING PREDETERMINED VALUES OF R/H ASSOC
C              W/ PREDRH VALUES: THESE VALUES OF R/H "BECOME" THE
C              RADII USED IN THE CEILING AREA CALCS
C     QRTCRD = ARRAY CONTAINING THE RADII OF THE 1/4 CIRCLE EQUIV
C              HEAT TRANSFER AREAS
C
      IMPLICIT REAL*8 (A-H,O-Z)
C
      INCLUDE 'BD:CONST.CMN'
      INCLUDE 'BD:ECCHTX.CMN'
      INCLUDE 'BD:OBJECT.CMN'
      INCLUDE 'BD:IO.CMN'
      INCLUDE 'BD:CVENT.CMN'
      INCLUDE 'BD:CVMFR.CMN'
```

```
      INCLUDE 'BD:HVNTEB.CMN'
      INCLUDE 'BD:CONTRL.CMN'
C
      DIMENSION ERRO(5),RERRO(5)
      DIMENSION PREDRH(10), PREDRP(10)
      DIMENSION QTRCRD(4)
C
      DATA INITC5,LFLG /2 * 0/
      DATA RHOCG / 0.369933E+4 /
      DATA PREDRH / 0.0,0.2,0.33,0.59,0.8,1.1,1.5,1.9,2.2,50.0 /
      DATA PREDRP / 0.05,0.265,0.4,0.65,0.95,1.3,1.7,2.05,2.2,2.35 /
      DATA ACNVHT / 14 * 0. /
C
      KO = NNO
      MAXV = MXV
      IF (INWT .EQ. 1) GO TO 1
      IF (INWT .EQ. 2) GO TO 700
      GO TO 35
C
C CALC H AND R FOR OBJ #1, BUT ONLY ONCE:
C POINTS 1 THRU 4 ARE FOR THE HEATED WALL CALCS
C POINTS 5 THRU 14 ARE FOR THE CEILING CALC
C RMAX IS THE RADIUS OF THE EQUIVALENT CIRCULAR CEILING AREA.
C THUS OBJECT ONE IS CONSIDERED TO BE CENTERED UNDER A
C CIRCULAR CEILING.
C
1     CONTINUE
C
C CALC VENT AREAS AND (ONLY ONCE) THEIR LOCATION REL TO PLM AXIS
C
      CALL VENTA(MAXV)
      IF (INITC5 .EQ. 0) CALL VNTCNT(MAXV,KO)
C
      IF (INITC5 .NE. 0) GO TO 200
      INITC5 = INITC5 + 1
```

```
      H = HR - ZHOZZ(1),
C
      R(1) = ZYOZZ(1)
      R(2) = RLX - ZXOZZ(1)
      R(3) = RLY - ZYOZZ(1)
      R(4) = ZXOZZ(1)
C
C CALC 4 EQUIV 1/4 CIRCLE RADII, 1 FOR EA QUAD W/ OBJ 0 ORIGIN;
C FIND RMAX, (R/H)MAX
C
C CALC EQUIV 1/4 CIRCLES AND FIND RMAX
      QTRCRD(1) = DSQRT(4. * R(1) * R(2) / PI)
      RMAX = QTRCRD(1)
      QTRCRD(2) = DSQRT(4. * R(3) * R(2) / PI)
      IF (RMAX .LT. QTRCRD(2)) RMAX = QTRCRD(2)
      QTRCRD(3) = DSQRT(4. * R(3) * R(4) / PI)
      IF (RMAX .LT. QTRCRD(3)) RMAX = QTRCRD(3)
      QTRCRD(4) = DSQRT(4. * R(4) * R(1) / PI)
      IF (RMAX .LT. QTRCRD(4)) RMAX = QTRCRD(4)
C CALC (R/H)MAX
      RHMAX = RMAX / H
      IF(RHMAX .GT. 2.2) THEN
            WRITE(IWTTY, 1000)
            WRITE(IWDSK, 1000)
1000  FORMAT(/,' *** CAUTION: (R/H)MAX IS TOO LARGE, OUTPUT ',
      1     'IS QUESTIONABLE ***',/)
            NOPNTS = 10
            GO TO 20
      END IF
C
C "PLACE" (R/H)MAX TO FIX NOPNTS
      DO 10 J = 1, 9
            IF((RHMAX .GT. PREDRH(J)).AND.(RHMAX .LE. PREDRH(J+1))) THEN
                  NOPNTS = J+1
                  GO TO 20
            END IF
```

```
10    CONTINUE
C
C SET VALUES OF R AND RP
20    CONTINUE
      NPM1P4 = (NOPNTS - 1) + 4
      DO 30 K = 5, NPM1P4
            R(K) = PREDRH(K-4) * H
            RP(K-4) = PREDRP(K-4) * H
30    CONTINUE
      R(NOPNTS+4) = RMAX
C DETERMINE EITHER THE 2 LARGEST HTX AREA RADII OR ONLY THE LARGEST
      IF (NOPNTS .LE. 9) THEN
            RP(NOPNTS-1) = (((RHMAX - PREDRH(NOPNTS-1)) / 2.) +
     1                     PREDRH(NOPNTS-1)) * H
            RP(NOPNTS) = RMAX
      ELSE
            RP(NOPNTS) = RMAX
      END IF
C
C CALC ANNULAR CEILING AREAS
C
      NPP4 = NOPNTS + 4
C
      ACNVHT(5) = RP(1) * RP(1) * PI
C
      NPP4M1 = NPP4 - 1
C
      DO 120 IQ = 1, 4
            DO 110 JP = 5, NPP4M1
                  IF (RP(JP-3) .LE. QTRCRD(IQ)) THEN
                        ACNVHT(JP+1) = (0.25 * ((RP(JP-3) * RP(JP-3)) -
     1                        (RP(JP-4) * RP(JP-4))) * PI) +
     2                        ACNVHT(JP+1)
                        GO TO 110
                  ELSE
```

```
                        TEMPA = (0.25 * ((QTRCRD(IQ) * OTRCRD(IQ)) -
     1                                  (RP(JP-4) * RP(JP-4))) * PI)
                        IF (TEMPA .LT. 0.)GO TO 110
                        ACNVHT(JP+1) = TEMPA + ACNVHT(JP+1)
                        GO TO 110
                    END IF
110         CONTINUE
120   CONTINUE
C
200   CONTINUE
C
C FIND OBJECT WITH HIGHEST HEAT RELEASE RATE
C
      IF (KO .GT. 1) THEN
            CALL BIGHRR(ERRO,KO)
      ELSE
            LRGST = I
      END IF
C CHECK AT BEGINNING OF FIRE FOR LRGST (SHOULDN'T BE) > 1
      IF (ZTZ .LE. 2.0) LRGST = 1
C
      RETURN
C
C CALC QSTAR FOR EACH OBJECT: FOR ONE ROOM ONLY!!!!
C
35    CONTINUE
C
      DO 40 I = 1, K0
            IF (ISTAT(I+0) .NE. 5) GO TO 40
            QSTR(I) = OSTAR(RERRO(I), ERRO(I), H)
40    CONTINUE
C
C DETERMINE IF HOT LAYR EFFECTS ARE SIGNIF AND CALC CORRECTION FACTORS
C IF NEEDED. ONLY GOOD FOR ONE ROOM 'CAUSE HLH AND HR ARE NOT ARRAYS!
C
      LFLG = 0
```

```
      IF (HLH .GE. (0.24 * HR)) LFLG = 1
      IF(LFLG .EQ. 1) THEN
            HZ = H - HLH
            IF(HZ .LT. 0.) HZ = DABS(HZ)  !TO AVOID NUMERICAL PROBLEMS
            QSTRZ = QSTAR(RERRO(LRGST),ERRO(LRGST),HZ)
            CALL CFCTRS(ZKA,ZKL,QSTRZ,HZ,H,HLH,
      1           HCRCTR,QCRCTR,TCRCTR)
      ELSE
            HCRCTR = 1.
            QCRCTR = 1.
            TCRCTR = 1.
      END IF
C
C CALC A MAX OF 10 VALUES OF CEILING HTX COEF AND
C NEAR SURF GAS TEMP AND 4 VALUES OF SAME FOR "HEATED WALLS"
C
C NOTE: THESE ARE CALC'D FOR ONE ROOM ONLY
C
      DO 50 IP = 1, NPP4
            ISWCH = 1
            IF (IP .GE. 5) ISWCH = 0
            CALL HTXC01(IP+O,ZKL,ZKA,RHOCG,ISWCH,ROVRH(IP),ZOLZJ(IP))
            HTC = ZOLZJ(IP)
            RH = ROVRH(IP)
            CALL TMPA01(RH,ZKA,ZKJZZ(IP))
C
C CHECK LIMIT ON CEILING JET TEMP IF > 1300K...
C SWITCH IVRSN(5) TO 1
C
      IF(ZKJZZ(IP) .GT. 1300. .AND. IT .GT. 5) THEN
            IVRSN(5) = 1
            WRITE(IWTTY,2000) ZTZZZ
            WRITE(IWDSK,2000) ZTZZZ
2000  FORMAT(/,' *** CONVECTIVE HEAT TRANSFER MODEL CHANGED TO CNVW',
      1      /,' *** CEILING JET TEMP > 1300K AT ',F7.3,/)
      CALL CNVW(FQLWD1,1,1)
```

```
            GO TO 700
      END IF
      TAD = ZKJZZ(IP)
C
C
      TSRF = ZKWZP(1,IP)
C
C CALC LOCAL CEILING CONV HT FLUXES
C
      FQWLOC(IP) = HTC * (TAD - TSRF)
50    CONTINUE
C
C CALC VENT AREAS COVERED BY THE HOT LAYER
C
      AVWT = 0.0
      DO 60 IV = 1, MAXV
            IF (ICLVNT(IV+0) .EQ. 0) THEN
            HV = HLH - ZHTZZ(IV+O)
            BVO = 0.0
            IF((HV .GE. 0.).AND.(HV .LE. ZHVZZ(IV+O)))
      1           BVO   = ZBVZZ(IV+O)
              IF (HV .LT. 0.0) HV = 0.0
              IF (HV .GT. ZHVZZ(IV+O)) HV = ZHVZZ(IV+O)
              VAHTX(IV) = HV * ZBVZZ(IV+O)
              AVWT = VAHTX(IV+O) + AVWT
            ELSE
              VAHTX(IV) = VAREA(IV)
            END IF
60    CONTINUE
C
C CALC AREA OF WALLS COVERED BY HOT LAYER
C WALL VENT AREA SUBTRACT FROM WALL 1 AREA (I.E., WALL W/ DOOR IN IT)
C
      ACNVHT(1) = RLX * HLH - AVWT
      ACNVHT(2) = RLY * HLH
      ACNVHT(3) = ACNVHT(1) + AVWT
```

```
      ACNVHT(4) = ACNVHT(2)
C
C SUBTRACT CEILING VENT AREAS FROM APPROPRIATE ANNULII: BASED ON
C RADIAL DISTANCE FROM THE PLUME AXIS TO THE VENT CENTER
      DO 80 IV = 1, MAXV
            IF (ICLVNT(IV+O) .EQ. 0) GO TO 80   !CAUSE VENT ISN'T CEILING
            IF (IPRINT(IV+O) .EQ. 0) GO TO 80   !CAUSE VENT ISN'T OPEN YET
C
C IF VENT OUTSIDE EQUIV. CIRC. AREA, TAKE VENT AREA OUT
C OF OUTSIDE ANNULUS
C
            LRG = LRGST
            IF (DATOVC(LRG,IV+O) .GT. RP(NP)) THEN
                  ACNVHT(NP) = ACNVHT(HP) - VAHTX(IV+O)
                  GO TO 80
            END IF
            DO 70 J = 1, NP
                  IF(DATOVC(LRG,IV+O) .LE. RP(J+O)) THEN
                        ACNVHT(J) = ACNVHT(J+O) - VAHTX(IV+O)
C
C ANNULUS SMALLER THAN VENT: TAKE EXCESS VENT AREA OUT OF
C NEXT LARGER ANNULUS
C
                        IF(ACNVHT(J) .LT. 0.0) THEN
                              ACNVHT(J+1) = ACNVHT(J+1) + ACNVHT(J)
                              ACNVHT(J) = 0.0
                        END IF
                  END IF
70          CONTINUE
80    CONTINUE
C
C CALC TOTAL ECCHTX AREA
C
      THTXAW = 0.0
      THTXAC = 0.0
```

```
      AHTXT = 0. 0
      DO 90 IA = 1, 4
            THTXAW = THTXAW + ACNVHT(IA)
90    CONTINUE
      IF (THTXAW .EQ. 0.) THTXAW = 1.
      DO 95 IA = 5, NPP4
            THTXAC = THTXAC + ACNVHT(IA)
95    CONTINUE
      IF (THTXAC .EQ. 0.) THTXAC = 1.
      AHTXT = THTXAW + THTXAC
      IF (AHTXT .EQ. 0.) AHTXT = 1.
C
C CALC AVG CONV HEAT FLUX ON EXTENDED CEILING
C
      QAVGW = 0.0
      QAVGC = 0.0
      DO 100 JP = 1, 4
            QAVGW = QAVGW + ((ACNVHT(JP) / THTXAW) * FQWLOC(JP+0))
100   CONTINUE
C
      DO 105 JP = 5, NPP4
            QAVGC = QAVGC + ((ACNVHT(JP) / THTXAC) * FQWLOC(JP+O))
105   CONTINUE
C
C CALC TOTAL CONV HT FLX TO XTNDED CEILING
C
      FQLWD1 = (THTXAW * QAVGW + THTXAC * QAVGC) / AHTXT
C
C CHECK MAGNITUDE OF OUTPUT VARIABLE
C
700   CONTINUE
C
      IF(DABS(FQLWD1) .GT. 2.E6) FQLWD1 = QLWDP
C
      RETURN
      END
```

```
C ***********************************************************************************
C
      FUNCTION FROVRH(RRHH)
C
C ***********************************************************************************
C
C CALLED BY TMPA01
C
C EQUATION BY L.Y. COOPER
C
C CODING BY D. BELLER FALL86
C
C THIS FUNCTION ACCEPTS A VALUE OF R OVER H AND USES IT TO CALC A
C VALUE OF F(R/H) DEFINED BY COOPER IN REF. 4, EQ.7.
C
      IMPLICIT REAL*8 (A-H,O-Z)
      INCLUDE 'BD:CONTRL.CMN' !@#
C
C CALC NUMERATOR
      XNMRTR = 1. - (1.1 * (RRHH**0.6)) + (0.808 * (RRHH**1.6))
C
C CALC DENOMENATOR
      DNMNTR = l.- (1.1 * (RRHH**0.8)) + (2.2 * (RRHH**1.6)) +
      1     (0.69 * (RRHH**2.4))
C
      FROVRH = XNMRTR / DNMNTR
      RETURN
      END
```

```
C ******************************************************************************
C
      SUBROUTINE HTXC01(NP,ZKL,ZKA,RCG,ISWTCH,ROVRH1,20LZJI)
C
C ******************************************************************************
C
C CALLED BY CNVW02
C
C EQUATIONS BY L.Y. COOPER
C
C CODING BY D.BELLER FALL66
C
C THIS ROUTINE CALCS THE LOCAL HT TX COEF,ZOLZJ1, AT A POINT FOR
C A GIVEN OBJECT. THE FACTORS HOVRH, QOVRQ, AND TOVRT ARE CORRECTION
C FACTORS TO ACCOUNT FOR HOT LAYER EFFECTS. THEY EQUAL 1.0 WHEN HOT
C LAYER EFFECTS ARE NOT SIGNIFICANT; OTHERWISE THEIR VALUES ARE CALC'D
C IN ROUTINE CFCTRS, WHICH IS CALLED BY CNVW02. TWO EXPRESSIONS FOR
C THE HT TX COEF ARE USED DEPENDING ON THE VALUE OF ROVRH (=RADD/HH).
C ROVRH IS PASSED AS AN OUTPUT TO AVOID CALC'ING IT ELSEWHERE ALSO.
C ISWTCH IS A CALC SWITCH: IF EQUAL TO ZERO, DO A CEILING CALC; IF
C EQUAL TO 1 DO A HEATED WALL CALC.
C
C THE MINIMUM HEAT TRANSFER COEFFICIENT WILL BE 5 W/M**2-DEG K
C
C INPUT IS:
C     NP    = INDEX OF POINT IN QUESTION
C     ZKL   = UPPER LAYER TEMP
C     ZKA   = AMBIENT TEMP
C     RCG   = CONSTANT DEFINED IN CNVW02
C     ISWTCH= CALC SWITCH
C
C PARAMETERS FROM COMMON
C     LRGST = INDEX OF OBJECT W/ LARGEST HEAT RELEASE RATE
C     R = RADIAL DISTANCE FROM PLUME AXIS
C     H = PLUME SOURCE-TO-CEILING DISTANCE
C     QSTR = DIMENSIONLESS HEAT RELEASE RATE
```

```
C     HCRCTR      = HH  CORRECTION FACTOR
C     QCRCTR      = QSTR     "       "
C     TCRCTR      = TEMP     "       "
C
C OUTPUT IS:
C     ROVRH1 = RADIAL DISTANCE FROM PLUME AXIS / HH
C     (FOR ROUTINES TMPP01 AND TMPA01)
C     ZOLZJ1 = HT TX COEF
C
C OTHER PARAMETERS:
C     PSCH = CORRECTED PLUME SOURCE-TO-CEILING HEIGHT
C     REH = LOCAL REYNOLDS NUMBER
C     HWGL = NORMALIZING HT TX COEF
C     HZ = OBJ SURFACE-TO-LAYER INTERFACE DISTANCE
C     CONV1 = CONVENIENCE PARAMETER
C
      IMPLICIT REAL*8 (A-H,O-Z)
C
      INCLUDE 'BD:ECCHTX.CMN'
      DATA INIT / 0 /
C
C CALC EXPONENTS AND CONV1 ONLY ONCE
C
      IF (INIT .NE. 0) GO TO 100
            EXP1 = 1. / 3.
            EXP2 = 2. / 3.
            CONV1 = 110.4 / ZKA
            INIT = INIT + 1
100   CONTINUE
C
C CALC LOCAL PLM SRC-TO-CEILING HEIGHT, REYNOLDS NUMBER AND "H WIGGLE"
C
      LARGE = LRGST
      PSCH = H * HCRCTR
C
      REH = (((HCRCTR**EXP2) * (QCRCTR**EXP1) * (TCRCTR + CONV1))
```

```
     1           / ((TCRCTR**2.5) * (1. + CONV1)))
     2           * RE(PSCH,QSTR(LARGE),ZKL)
C
      HWGL = ((QCRCTR**EXP1) / (HCRCTR**EXP1)) * (1. / TCRCTR) *
     1                 (RCG * DSORT(PSCH) * (QSTR(LARGE)**EXP1))
C
C CALC RADD OVER HH FOR THE OBJECT
C
      INDXP = NP
      RADDIS = R(INDXP)
      ROVRH1 = RADDIS / PSCH
C
C CHOOSE PROPER VALUE FOR PRANDTL NUMBER, PR
C
      IF (ISWTCH .EQ. 0) THEN
            PR = 0.7**-EXP2
      ELSE
            PR = 1. / 0.7
      END IF
C
C PERFORM DIFFERENT CALC DEPENDING ON VALUE OF ROVRH1
C
      IF (ROVRH1 .LT. 0.2) THEN
            ZOLZJ1 = HWGL * (8.82 * (REH**-0.5) * PR) *
     1           (1.0 - (5.0 - (0.28 * (REH**0.2)))  ROVRH1)
            GO TO 700
      ELSE
            IF (ISWTCH .EQ. 0) THEN
                  ZOLZJ1 = HWGL * 0.283 * (REH**-0.3) * PR *
     1                 (ROVRH1**-1.2) * (ROVRH1 - 0.0771)
     2                 (ROVRH1 + 0.279)
                  GO TO 700
            ELSE
                  ZOLZJ1 = HWGL * 0.89 * (REH **-0.42) * PR *
     1                 (ROVRH1**-1.02)
                  GO TO 700
```

```
            END IF
      END IF
C
C CHECK MAGNITUDE OF ZOLZJ AND ROVRH1
C
700   CONTINUE
      IF (ZOLZJ1 .LT. 5.0) ZOLZJ1 = 5.0
      IF (ROVRH1 .GT. 2.2) ROVRH1 = 2.2
C
      RETURN
      END
```

```
C ******************************************************************************
C
      FUNCTION QSTAR(QQR, 00, HH)
C
C ******************************************************************************
C
C CALLED BY CNVW02 AND CVB201
C
C EQUATIONS BY L.Y. COOPER
C
C CODING BY D. BELLER FALL86
C
C FOR EACH OBJECT, THIS FUNCTION CALCULATES A DIMENSIONLESS HEAT RELEASE
C REQUIRED BY THE ROUTINES CALCULATING ECCHTX HEAT TRANSFER COEFFICIENTS
C AND ADIABATIC NEAR-SURFACE GAS TEMPERATURES
C
C INPUT IS:
C     QQR   = RADIENT ENERGY LOSS OF THE FLAMES
C     QQ    = ENERGY RELEASE RATE OF FIRE
C     HH    = PLUME SOURCE-TO-CEILING DISTANCE
C
C LOCAL PARAMETERS ARE:
C     RLMDA = FRACTION OF 00 LOST BY RADIATION
C     RTCG  = (RHO*CP*TEMP OF AMBIENT AIR)*G**0.5
C           = (1.177 KG/M**3)*(1004 J/KG-DEG C)*
C                             (300 DEG K)*(9.8**0.5)
C
C NOTE: THE ABSOLUTE VALUE OF THE HEAT RELEASE RATE IS USED AND THE
C INVERSE OF LAMDA IS USED WHEN RLMDA IS CALC'D .GT. 1.0 (TYPICALLY
C OCCURS AT TIME = 0.0 SEC)
C
      IMPLICIT REAL*8 (A-H,O-Z)
C
      DATA RTCG / 0.11098E+7 /
C
      IF (QQ .NE. 0.0) THEN
```

```
      ABSQQ = DABS(QQ)
      RLMDA = QQR / ABSQQ
      IF(RLMDA .GT. 1.0) RLMDA = 1. / RLMDA
       QSTAR = (1. - RLMDA) * ABSQQ / (RTCG * (HH**2.5))
      RETURN
ELSE
      QSTAR = 0.0
      RETURN
END IF
END
```

```
C ***************************************************************************
C
      FUNCTION RE(HH, QSTR, ZKL)
C
C ***************************************************************************
C
C CALLED BY HTXC01
C
C EQUATIONS BY L.Y. COOPER
C
C CODING BY D. BELLER FALL86
C
C THIS FUNCTION CALCS THE REYNOLDS NUMBER OF THE PLUME/CEILING JET
C RESULTING FROM A BURNING OBJECT.
C
C INPUT IS:
C     HH = PLUME SOURCE-TO-CEILING DISTANCE
C     QSTR = DIMENSIONLESS HEAT RELEASE RATE
C     ZKL = UPPER LAYER TEMP
C     XNU = TEMP DEPENDENT UPPER LAYR KIN. VISC.
C
      IMPLICIT REAL*8 (A-H,O-Z)
C
C SQROTG = 9.8**0.5
      DATA SQROTG / 3.130495 /
C
C CALC KINEMATIC VISCOSITY
      XNU = VISC(ZKL)
C
      RE = (SQROTG * (HH**(3./2.)) * (QSTR**(l./3.))) / XNU
      IF (RE .EQ. 0.0) RE = 1.0
C
      RETURN
      END
```

```
C ******************************************************************************
C
      SUBROUTINE TMPA01(RRHH,TAMB,ZKJZZ1)
C
C ******************************************************************************
C
C CALLED BY CNVW02 AND CVB201
C
C EQUATIONS BY L.Y. COOPER
C
C CODING BY D.BELLER, FALL86
C
C THIS ROUTINE CALCS THE LOCAL, NEAR SURFACE GAS TEMP UNDER THE CEILING,
C ZKJZZ1, DUE TO THE CEILING JET OF A FIRE PLUME. THIS LOCAL TEMP IS A
C FUNCTION OF RADIAL DISTANCE / PLUME SOURCE-TO-CEILING DISTANCE, RRHH,
C DIMENSIONLESS HEAT RELEASE RATE, QSTR, AND AMBIENT TEMP, TAMB. HCRCTR
C AND QCRCTR ARE CORRECTION FACTORS = 1.0 IF HOT LAYER EFFECTS ARE NOT
C SIGNIFICANT OR TO A VALUE DETERMINED BY ROUTINE CFCTRS IF HOT LAYER
C EFFECTS ARE SIGNIFICANT. FROVRH IS A FUNCTION SUBROUTINE WHICH
C EVALUATES THE NEAR SURFACE GAS TEMPERATURE DISTRIBUTION DEVLOPED BY
C COOPER
C
C LOCAL PARAMETERS ARE:
C     DLTSTR = DELTA(T:SUB AD:STAR)
C           DIMENSIONLESS TEMP AS F(R/H) AS DEFINED BY COOPER,
C           WHICH REQUIRES TWO EQUATIONS FOR DEFINITION
C
C PARAMETERS FROM COMMON
C           TCRCTR, QCRCCTR, HCRCTR = CORRECTION FACTORS ACCOUNTING FOR
C                                     HOT LAYER EFFECTS
C           QSTAR = DIMENSIONLESS HEAT RELEASE RATE
C           LRGST = OBJECT HAVING HIGHEST HEAT RELEASE RATE
C
      IMPLICIT REAL*8 (A-H,O-Z)
C
      INCLUDE 'BD:ECCHTX.CMN'
```

```
      INCLUDE 'BD:CONTRL.CMN' !@#
      LOGICAL TSET
C
C DETERMINE WHICH EXPRESSION TO USE FOR DLTSTR
C
C     IF (IT .EQ. 1)WRITE(5,*)' RRHH= ',RRHH    !@#
      IF (RRHH .LE. 0.2) THEN
            DLTSTR = 10.22 - (14.9 * RRHH)
      ELSE
            FROH = FROVRH(RRHH)
C     IF(IT .EQ. 1)WRITE(5,*)' FROH= ',FROH     !@#
            DLTSTR = 8.39 * FROH
      END IF
C     IF(IT .EQ. 1)WRITE(5,*)' DLTSTR= ',DLTSTR !@#
C
C CALC ZKJZZ1
C
      ZKJZ21 = DLTSTR * (TAMB * TCRCTR) * ((QCRCTR * (HCRCTR**2.5) *
      1     QSTR(LRGST))**(2./3.)) + (TAMB * TCRCTR)
C     IF(IT.EQ.1)WRITE(5,*)' ZKJZZ1= ',ZKJZZ1   !@#
C
      RETURN
      END
```

```
C ******************************************************************************
C
      SUBROUTINE TMPW02(ZKWZZ1,ZKWZZ2,KW)
C
C ******************************************************************************
C
C MODIFIED VERSION OF TMPW0l TO HANDLE THE (MAXIMUM OF) 14 POINTS
C REQUIRED BY CNVW02. THIS ROUTINE PERTAINS ONLY TO THE EXTENDED
C CEILING; I.E., KW = 1, JSIDE = 1. MAJOR DIFFERENCE BETWEEN TMPWO1
C AND TMPW02 IS THAT ARRAYS ZKW(20,5) AND ZKWO(20,5) IN TMPWO1 HAVE
C BEEN REPLACED BY ZKWZP(20,14) AND ZKWZPP(20,14).
C
C CALLED BY CALS.
C
C EQUATIONS BY H. EMMONS
C CODED BY D. LAPP, N. BILLIKOPF, L. TREFETHEN, AUGUST 1977
C B. LONDON, JULY 1978
C M.SPIVAKOVSKY, AUGUST 1980
C
C MODIFIED AS STATED ABOVE BY D. BELLER DEC86
C
C CALCULATES THE TEMPERATURE PROFILE WITHIN WALL KW USING A DISCRETE
C GRID. THE WALL IS HEATED OR COOLED ON EACH SIDE BY CONVECTION
C AND RADIATION AND THE HEAT DIFFUSES THROUGH IT BY CONDUCTION.
C
C OUTPUT: ZKWZZ1,ZKWZZZ,ZKJZS,ZKEZP
C
      IMPLICIT REAL*8 (A-H,O-Z)
C
      INCLUDE 'BD:VAR.CMN'
      INCLUDE 'BD:OLDVAR.CMN'
      INCLUDE 'BD:CONTRL.CMN'
      INCLUDE 'BD:IO.CMN'
      INCLUDE 'BD:POINTR.CMN'
      INCLUDE 'BD:CONST.CMN'
      INCLUDE 'BD:ROOM.CMN'
```

```
      INCLUDE 'BD:WALL.CMN'
      INCLUDE 'BD:ECCHTX.CMN'
C
      DIMENSION FQWA2(14), FQW12(14)

C     DATA IONCE / 0    !@#
C
      NPP4 = NOPNTS + 4
      KR1 = KRW(KW,1)
      KR2 = KRW(KW,2)
      IF(KR2 .EQ. 0) KR2 = NR+l
C
C INITIAL CALCULATION:
      IF ((ZTZZZ .NE. 0.) .OR. (INEWT .NE. 1)) GO TO 15
C CALC MIN SPACE INCREMENT AND ACTUAL SPACE INCREMENT USED
            DXM = DSQRT(2. * ZGWZZ(KW) * DT)
            M = ZNWZZ(KW) / DXM + 1
            N(KW) = MINO(M,20)
            IF (N(KW) .LE. 1) N(KW) = 2
            WRITE (IWTTY,5) KW,N(KW)
5     FORMAT (' *** TMPW02: NO. OF GRID POINTS (WALL=',I2,') =',I3)
            DX = ZNWZZ(KW) / (N(KW) - 1)
C COMPUTATION PARAMETERS
            AW(KW) = 2. * ZGWZZ(KW) / (DX * DX)
            BW(KW) = DX / ZJWZZ(KW)
            IIII = N(KW)
C INITIALIZE TEMPS
            DO 10 I=1,IIII
                  DO 10 IP = 1, NPP4
                        ZKWZP(I,IP) = ZKAZZ
                        ZKWZPP(I,IP) = ZKAZZ
10          CONTINUE
            ZKEZP = ZKAZZ
            ZKJZS = ZKAZZ
            ZKEZPP = ZKAZZ
            ZKJZSP = ZKAZZ
```

```
      RETURN
15    CONTINUE
C
C CALCULATION AT TIME ZTZZZ:
      TEMP=1.-AW(KW)*DT
      NM1 = N(KW)-l
      IF (INEWT.NE.1) GO TO 25
      IIII = N(KW)
      DO 20 I=1,IIII
            DO 20 IP = 1, NPP4
                  ZKWZPP(I,IP) = ZKWZP(I,IP)
20    CONTINUE
      IF (N(KW).LE.2) RETURN
C CALC INTERNAL GRID POINT WALL TEMPS
      DO 30 I=2,NM1
            DO 30 IP = 1, NPP4
                  ZKWZP(I,IP) = ZKWZPP(I,IP)*TEMP+AW(KW)*(DT/2.)*
      1               (ZKWZPP(I-1,IP)+ZKWZPP(I+1,IP))
30    CONTINUE
      ZKEZPP = ZKEZP
      ZKJZSP = ZKJZS
      RETURN
C
25    IF (INEWT .EQ. 2) GO TO 700
C
      DO 50 IP = 1, NPP4
            FQWA2(IP) = FQWLOC(IP+O) + FQLWR(KW,1) + FQPWR(KW,1)
C
C NOW WE TAKE INTO ACCOUNT ENERGY
C LOSS BY RADIATION:
C
            FQW12(IP) = FQWA2(IP) - SIGMA * (ZKWZP(1,IP)**4)
C     IF(ZTZZZ.EQ.276. .AND. IP.EQ.1)WRITE(5,*)' FQW12(1)=
C     9 FQW12(IP),' BEFORE DUM'     !@#
            DUM = ZHLZZ(KR1)*ZULZZ(KR1)
            IF(DUM.LT.30.) THEN
```

```
            FQW12(IP) = FQWA2(IP) - (SIGMA * ZKW2P(1,IP)**4) +
     1           (DEXP(-ZHLZZ(KR1) * ZULZZ(KR1)) * SIGMA * ZKDZZ(KR1)**4)
      IF(FQW12(IP) .LT. 0.) FQW12(IP) = DABS(FQW12(IP))     !FUDGE
C     IF(ZTZZZ.EQ.276. .AND. IP.EQ.1)WRITE(5,*)' FQW12(1)= ‘,     !@#
C     9 FQW12(IP),' AFTER DUM'      !@#
            END IF
C
C AN ADDITIONAL FACTOR OF .5 WAS REMOVED FROM THE LAST TERM OF
C THE EXPRESSION FOR FQW1 ON 9/25/80 BY J. GAHM.
C
C THE OUTSIDE OF THE WALL IS HERE (INCORRECTLY) ASSUMED TO REMAIN
C COOL:
C
            FQW2 = FOLWD(KW,2) + FOLWR(KW,2) + FQPWR(KW,2)
C CALC INSIDE AND OUTSIDE SURFACE TEMPS
            ZKWZP(1,IP) = ZKWZPP(1,IP) * TEMP + AW(KW) * DT
     1                (ZKWZPP(2,IP) + BW(KW) * FQW12(IP))
C
C LIMIT THE INTERIOR SURFACE TEMP:  !@#
C
            IF(IT .GT. 5 .AND. ZKWZP(1,IP) .GE. 1300.) THEN
                  ZKWZP(1,IP) = 1300.
                  IF(IONCE .GT. 0) GO TO 100
                  IONCE = IONCE + 1
                  WRITE(IWTTY,1000)
                  WRITE(IWDSK,1000)
1000  FORMAT(/,' *** SURFACE TEMP EXCEEDS 1300K       ***’,/,
     1        ‘ *** SUBSEQUENT RESULTS MAY BE QUESTIONABLE ***’,/)
100               CONTINUE
            END IF
C
C     IF(IP.EQ.1.AND.ZTZZZ.EQ.12.)WRITE(5,*)' TEMP=   ',TEMP,
C     9' AW= ',AW(KW)   !@#
C     IF(IP.EQ.1,AND.ZTZZZ.EQ.12.)WRITE(5,*)' BW=     ',BW(KW),
C     9' FQW12= ',FQW12(IP)!@#
C     IF(IP.EQ.1.AND.ZTZZZ.EQ.12.)WRITE(5,*)' DT= ',DT,' ZKWZPP= ',!@#
```

```
C     9ZKWZPP(1,IP),' ZKWZPP2 = ',ZKWZPP(2,IP)!@#
C
            ZKWZP(N(KW),IP) = ZKWZPP(N(KW),IP) * TEMP +
      1           AW(KW) * DT * (ZKWZPP(NM1,IP) + BW(KW) * FQW2)
50    CONTINUE
C AVERAGE THE INSIDE LOCAL HEATED WALL SURFACE TEMPS, AS WELL AS THE
C CEILING JET TEMP
      TTEMP1 = 0.0
      TTEMP2 = 0.0
      TTEMP3 = 0.0
      DO 60 IP = 1, NPP4
            TTEMP1 = ((ACNVHT(IP) / AHTXT) * ZKWZP(1,IP)) + TTEMP1
C     IF (IP.EQ.5.AND.ZTZZZ EQ. 12.) THEN !@#
C     WRITE(5,*)' ACNVHT(',IP,')= ',ACNVHT(IP),' ZKWP= ',ZKWZP(1,IP)!@#
C     WRITE(5,*)' ZKJZZ(',IP,')= ',ZKJZZ(IP)          !@#
C     WRITE(5,*)' TMPW02: ACNVHT(',IP,')= ',ACNVHT(IP)            !@#
C     END IF !@#
            TTEMP2 = ((ACNVHT(IP) / AHTXT) * ZKWZP(N(KW),IP)) + TTEMP2
            TTEMP3 = ((ACNVHT(IP) / AHTXT) * ZKJZZ(IP)) + TTEMP3
60    CONTINUE
C     IF(IT EQ.   1)WRITE(5,*)' AHTXT(TMPW02)= ',AHTXT      !@#
C     IF(IT EQ. 1)WRITE(5,*)' ZKLZZ= ',ZKLZZ(1) !@#
      ZKWZZ1 = TTEMP1
      ZKWZZ2 = TTEMP2
      ZKJZS = TTEMP3
C
C SET PEAK CEILING TEMPS
C
      ZKEZP = ZKWZP(1,5)
C
C     IF(ZTZZZ.EQ.12.)WRITE(5,*)' ZKEZP= ',ZKEZP !@#
C
C CHECK MAGNITUDE OF OUTPUT VARIABLES
C
700   CONTINUE
```

```
      IF ((ZKWZZ1 .LT. ZKDZZ(KR1)) .OR. (ZKWZZ1 .GT. 2500.))
      1           ZKWZZ1 = ZKWZZP(KW,1)
C
      IF ((ZKWZZ2 .LT. ZKAZZ) .OR. (ZKWZZ2 .GT. 2500.))
      1           ZKWZZ2 = ZKWZZP(KW,2)
C
      IF ((ZKJZS .LT. ZKDZZ(KR1)) .OR. (ZKJZS .GT. 2500.))THEN
C     WRITE(5,*)' ZKJZS= ',ZKJZS    !@#
            ZKJZS = ZKJZSP
      END IF      !@#
C
      IF ((ZKEZP .LT. ZKDZZ(KR1)) .OR. (ZKEZP .GT. 5000.))THEN
C     WRITE(5,*)' ZKEZP= ',ZKEZP
            ZKEZP = ZKEZPP
      END IF      !@#
C
       RETURN
      END
```

```
C ***********************************************************************************
C
      SUBROUTINE VENTA(MXV)
C
C ***********************************************************************************
C
C CALLED BY CVMF01 AND AND CNVL02
C
C CODED, ETC. BY D.BELLER JAN87
C
C CALCS VENT AREAS AT TIME = 0. AND AFTER AN INITIALLY CLOSED VENT
C OPENS. ISWCH CONTROLS THE CALCS: IF = 0 NO CALC MADE, IF = I CALC
C VENT AREAS. INPUT IS MXV = MAX NUMBER OF VENTS
C ALSO CALCS TOTAL DOOR/WINDOW AREA, ASUBI, AND TOTAL CEILING VENT
C AREA, ASUBV
C
      IMPLICIT REAL*8 (A-H,O-Z)
C
      INCLUDE 'BD:CVMFR.CMN'
      INCLUDE 'BD:CVENT.CMN'
      INCLUDE 'BD:HVNTEB.CMN'
      INCLUDE 'BD:CONTRL.CMN' !@#
C
      DATA INITC1 / 0 /
C
C SET CORRECT VALUE OF ISWCH
C
      LV = MXV
      ISWCH = 0
      DO 20 MV = 1, LV
C     IF(IT.EQ.10)WRITE(5,*)' IPRINT(',MV,')= ',IPRINT(MV)  !@#
      IF ((INITC1 .EQ. 0) .OR. (IPRINT(MV) .EQ. 1)) ISWCH = 1
20    CONTINUE
      INITC1 = INITC1 + 1
C
```

```
      IF (ISWCH .EQ. 1) THEN
C
C CALC VENT AREAS: AT TIME = 0. AND AFTER AN INITIALLY CLOSED VENT OPENS
C
            ASUBI = 0.0
            ASUBV = 0.0
            DO 5 L = 1, LV
                  IF (IHVNT(L) .EQ. 0)THEN
                        VAREA(L) = ZBVZZ(L) * ZHVZZ(L)
                        ASUBI = ASUBI + VAREA(L)
                  ELSE
                        VAREA(L) = ZBVZH(L) * ZLVZH(L)
                        IF (ICLVNT(L) .EQ. 1) ASUBV = ASUBV + VAREA(L)
                  END IF
C     IF(IT.EQ.10)WRITE(5,*)' VAREA(',L,')= ',VAREA(L)      !@#
5           CONTINUE
            INITC1 = INITC1 + 1
      ELSE
            RETURN
      END IF
C
      RETURN
      END
```

```
C ******************************************************************************
C
      SUBROUTINE VNTCNT(MXV,MXO)
C
C ******************************************************************************
C
C CALLED BY CVB00l AND CNVW02
C
C CODED, ETC., BY D. BELLER   JAN87
C
C THIS ROUTINE CALCS THE DISTANCE FROM THE AXES OF THE PLUMES
C TO THE CENTERS OF THE CEILING VENTS AND WHETHER OR NOT THE
C VENT IS NEAR A PLUME AXIS
C
C INPUT IS: MXV = NUMBER OF VENTS
C           MXO =    "   "  OBJECTS
C
C PARAMETERS FROM COMMON:
C     H = PLUME SOURCE-TO-CEILING DISTANCE
C     LRGST = INDEX OF OBJECT WITH HIGHEST HEAT RELEASE RATE
C     ZBVZH,ZLVZH = CEILING VENT DIMENSIONS
C     ZXVZH,ZYVZH =    "      "  CENTER COORDINATES
C     ZXOZZ,ZYOZZ = OBJECT CENTER X, Y COORDINATES
C     NDXOBJ = OBJ INDEX:O = OBJ'S FLAMES DON'T TOUCH CEILING
C                        1 =  "       "   DO      "      "
C
C LOCAL PARAMETERS:
C     RIZ = IMPINGEMENT ZONE RADIUS
C     NEARAX = "VENT NEAR AXIS" FLAG: 0 = NO, 1 = YES
C     EQVNTR = EQUIVALENT VENT RADIUS
C     DATOVC = DISTANCE FROM AXIS TO VENT CENTER
C     ISWTCH = CALC CONTROL SWITCH: IF = 0 NO CALC
C                                   IF = 1 DO CALC CAUSE VENT OPEN
C
      IMPLICIT REAL*8 (A-H,O-Z)
```

```
      INCLUDE 'BD:HVNTEB.CMN'
      INCLUDE 'BD:CVMFR.CMN'
      INCLUDE 'BD:OBJECT.CMN'
      INCLUDE 'BD:CVENT.CMN'
      INCLUDE 'BD:ECCHTX.CMN'
      INCLUDE 'BD:CONTRL.CMN' !@#
C
      DATA INITC2 / 0 /
      DATA PI / 3.141592654 /
C
C DO CALCS AT TIME = 0. AND AFTER AN INITIALLY CLOSED VENT OPENS
C
      JV = MXV
      JO = MXO
C     WRITE(5,*)' JV= ',JV,' JO= ',JO     !@#
      ISWTCH = 0
      DO 20 MV = 1, JV
C     WRITE(5,*)' IPRINT(',MV,')= ',IPRINT(MV)  !@#
            IF ((INITC2 .EQ. 0) .OR. (IPRINT(MV) .EQ. 1)) ISWTCH  1
C     WRITE(5,*)' ISWTCH= ',ISWTCH  !@#
20    CONTINUE
      INITC2 = INITC2 + 1
C
      IF (ISWTCH .EQ. 1) THEN
C
C CALC EQUIVALENT RADIUS OF CEILING VENTS AND DISTANCE FROM AXIS TO
C VENT CENTER
            DO 10 J = 1, JO
C CALC RADIUS OF IMPNG ZONE
C REALLY ONLY GOOD FOR FIRST OBJECT BECAUSE H IS FOR OBJECT ONE
            RIZ = 0.2 * H
C     IF(IT.EQ.1)WRITE(5,*)' RIZ= ',RIZ,' H= ',H      !@#
            DO 10 1 = 1, JV
                  IF (ICLVNT(I) .EQ. 0) GO TO 10
                        EQVNTR(I+O) = DSORT((ZBVZH(I+O)*ZLVZH(I+O))/PI)
```

```
                        XDIST = ZXVZH(I) - ZXOZZ(J)
                        YDIST = ZYVZH(I)  - ZYOZZ(J)
C     IF(IT.EQ.1)WRITE(5,*)' XDIST= ',XDIST,' YDIST= ',YDIST      !@#
                        DATOVC(J,I) = DSORT((XDIST*XDIST)+(YDISTRYDIST))
C     IF(IT.EQ.1)WRITE(5,*)' DATOVC(',J,I,')= ',DATOVC(J,I) !@#
                        IF (DATOVC(J,I) .LE. (RIZ + EQVNTR(I)))
      1                       NEARAX(J,I) = 1
10    CONTINUE
C
      ELSE
            RETURN
      END IF
C
      RETURN
      END
```

Alternate CVMFR Model Subroutines

```
C ******************************************************************************
C
      SUBROUTINE CVA001(G,RHO,RHOA,RHOD,H,HD,CH,IV,CVF)
C
C ******************************************************************************
C
C CALLED BY CVMF01
C
C EQUATIONS BY H.E. MITLER
C
C CODED BY D. BELLER, FALL 86
C
C THIS ROUTINE CALC'S THE CEILING VENT MASS FLOW RATE, CVF, OF
C ENCLOSURES CONTAINING FIRES WHOSE FLAMES DO NOT TOUCH THE CEILING.
C THIS IS DEFINED BY MITLER TO BE A SMALL FIRE.
C
C INPUT IS:
C     G     = ACCELERATION OF GRAVITY
C     RHO   = UPPER LAYER DENSITY
C     RHOA  = AMBIENT        "
C     RHOD  = LOWER LAYER    "
C     H     = UPPER LAYER DEPTH
C     HD    = FLOOR-TO-LAYER INTERFACE DISTANCE
C     CH    = CEILING VENT FLOW COEFFICIENT
C     IV    = VENT IN QUESTION
C
C PARAMETERS FROM COMMON:
C     VAREA       = VENT AREA
C     RSUBA       = AS DEFINED IN CVMF01
C     VBETA       = AS DEFINED IN CVMF01
C LOCAL PARAMETERS ARE:
C     USUBV       = VENTED GAS VELOCITY
C
      IMPLICIT REAL*8 (A-H,O-Z)
C
      INCLUDE 'BD:CVMFR.CMN'
```

```
      INCLUDE 'BD:CONTRL.CMN' !@#
C
C CALC VENTED GAS VELOCITY
C
      USUBV = UV(G,H,HD,RHO,RHOA,RHOD,RSUBA,VBETA)
C
C CALC CVMFR
C
C     IF(IT.EQ.10)WRITE(5,*)' VAREA(',IV,')= ',VAREA(IV)
C     IF(IT.EQ.10)WRITE(5,*)' RHO= ',RHO,' USUBV= ',USUBV   !@#
      CVF = CH * VAREA(IV) * RHO * USUBV
C
      RETURN
      END
```

```
C ******************************************************************************
C
      SUBROUTINE CVB001(TEPR,TEO,G,RHO,RHOD,RHOA,ZHL,ZKL,ZHI,ZPR,ZHR,
     1                  ZKA,IV,PI,MAXO,MAXV,CVF)
C
C ******************************************************************************
C
C CALLED BY CVMF01
C
C EQUATIONS BY H.E. MITLER
C
C CODING BY D. BELLER
C
C THIS ROUTINE IS THE CONTROLLING ROUTINE FOR VENTS IN AN ENCLOSURE WITH
C A FIRE WHOSE FLAMES TOUCH THE CEILING. THIS IS DEFINED BY MITLER TO BE
C A LARGE FIRE. THIS ROUTINE DETERMINES VENT LOCATION RELATIVE TO THE
C PLUME AXIS BY FIRST CALC'NG AN EQUIVALENT CIRCULAR VENT AREA AND
C RADIUS AND THEN CALC'NG THE DISTANCE FROM THE PLUME AXIS TO THE VENT
C CENTER.
C
C OUTPUT IS:CVF = CVMFR
C
C INPUT IS
C     TEPR  = RADIANT ENERGY LOST BY FLAMES
C     TEO   = ENERGY RELEASE RATE OF OBJECTS
C     G     = ACCELERATION OF GRAVITY
C     RHO   = UPPER LAYER DENSITY
C     RHOA  = AMBIENT        "
C     RHOD  = LOWER LAYER    "
C     ZHL   = UPPER LAYER DEPTH
C     ZHI   = FLOOR-TO-LAYER INTERFACE DISTANCE
C     ZPR   = PRESSURE AT THE FLOOR
C     ZHR   = ROOM HEIGHT
C     ZKA   = AMBIENT TEMPERATURE
C     Pi    = 3.14159…
C     IV    = VENT IN QUESTION
```

```
C     MAXV  = NUMBER OF VENTS
C     MAXO  =   "    "  OBJECTS
C
C
      IMPLICIT REAL*8 (A-H,O-Z)
C
      INCLUDE 'BD:HVNTEB.CMN'
      INCLUDE 'BD:CVMFR.CMN'
      INCLUDE 'BD:ECCHTX.CMN'
      INCLUDE 'BD:CONTRL.CMN' !@#
C
      DIMENSION TEO(5),TEPR(5)
C
C DETERMINE VENT LOCATION WRT IMPINGEMENT ZONE (WHEN/IF THE OBJECT
C BURNS): ONLY ONCE
C
C     WRITE(5,*)'IN CVB001 MAXV= ',MAXV
      CALL VNTCNT(MAXV,MAXO)
C
C DETERMINE WHETHER OR NOT VENT IV IS ACTUALLY NEAR AN OBJECT WHOSE
C FLAMES TOUCH THE CEILING AND IS THEREFORE WITHIN AN IMPGMNT ZONE.
C THEN THE APPROPRIATE CVMFR ROUTINE IS CALLED
C
C CALL BIGHRR TO DETERMINE WHICH OBJECT HAS THE HIGHEST HEAT RELEASE
C RATE
      IF (MAXO .GT. 1) THEN
            CALL BIGHRR(TE0,MAX0)
      ELSE
            LRGST = 1
      END IF
C
      IF (NEARAX(LRGST,IV) .EQ. 1) THEN
            CALL CVB101(TEO(LRGST),G,RHO,RHOD,RHOA,ZHL,ZHI,CH,IV,
      1                 CVMFB1)
            CVF = CVMFB1
C     IF(IT.EQ.1)WRITE(5,*)' CVF(CVB101)= ',CVF       !@#
```

```
            RETURN
      ELSE
            CALL CVB201(G,ZPR,ZHR,RHOA,RHO,RHOD,ZHL,ZKL,
      9                 TEPR(LRGST),TEO(LRGST),IV,CVMFB2)
            CVF = CVMFB2
C     IF(IT.EQ.1)WRITE(5,*)' CVF(CVB201)= ',CVF !@#
            RETURN
      END IF
      WRITE(5,*)' *** NO CVMFR CALCD BY CVB001 *** '
      RETURN
      END
```

```
C ******************************************************************************
C
      SUBROUTINE CVB101(TEO,G,RHO,RHOD,RHOA,ZHL,ZHI,CH,IV,CVF1)
C
C ******************************************************************************
C
C CALLED BY CVB001
C
C EQUATIONS BY H.E. MITLER
C
C CODING BY D. BELLER, FALL86
C
C THIS ROUTINE CALC'S THE CVMFR OF VENT IV WHICH IS NEAR THE PLUME AXIS
C OF A (LARGE) FIRE WHOSE FLAMES TOUCH THE CEILING( I.E., NDXOBJ =1,
C AND NEARAX = 1)
C
C OUTPUT IS:CVF1 = CVMFR
C
C INPUT IS
C     TEO   = ENERGY RELEASE RATE OF OBJECT IN QUESTION
C     G     = ACCELERATION OF GRAVITY
C     RHO   = UPPER LAYER DENSITY
C     RHOA  = AMBIENT        "
C     RHOD  = LOWER LAYER    "
C     ZHL   = UPPER LAYER DEPTH
C     ZHI   = FLOOR-TO-LAYER INTERFACE DISTANCE
C     CH    = VENT FLOW COEF
C
C PARAMETERS FROM COMMON:
C     RSUBA = AS DEFINED IN CVMF01
C     VBETA = "      "    "   "
C     VAREA = VENT AREA
C
C LOCAL PARAMTERS ARE:
C     USUBV = VENTED GAS VELOCITY
C     USUBF = FLAME 'VELOCITY'
```

```
C     VSUBV = TOTAL GAS VELOCITY
C
      IMPLICIT REAL*8 (A-H,O-Z)
C
      INCLUDE 'BD:CVMFR.CMN'
      INCLUDE 'BD:CONTRL.CMN' !@#
C
C CALC TOTAL GAS VELOCITY AS A FUNCTION OF VENTED GAS VELOCITY AND
C FLAME 'VELOCITY'
C
C CALC USUBV
      USUBV = UV(G,ZHL,ZHI,RHO,RHOA,RHOD,RSUBA,VBETA)
C     IF(IT.EQ.1)WRITE(5,*)' USUBV= ',USUBV     !@#
C
C CALC USUBF
      USUBF = UF(TEO)
C     IF(IT.EQ.1)WRITE(5,*)'  USUBF= ',USUBF    !@#
C
      VSUBV = DSQRT((USUBV * USUBV) + (USUBF * USUBF))
C     IF(IT.EQ.1)WRITE(5,*)'  VSUBV= ',VSUBV    !@#
c     IF(IT.EQ.1)WRITE(5,*)'  VAREA(',IV,')= ',VAREA(IV)
C     IF(IT.EQ.1)WRITE(5,*)'  CH= ',CH,' RHO= ',RHO   !@#
C
C CALC CVMFR
C
      CVF1 = CH * VAREA(IV) * RHO * VSUBV
C
      RETURN
      END
```

```
C ******************************************************************************
C
      SUBROUTINE CVB201(G,ZPR,ZHR,RHOA,RHO,RHOD,ZHL,ZKL,TEPR,
     1                  TEO,IV,CVF2)
C
C ******************************************************************************
C
C CALLED BY CVB001
C
C EQUATIONS BY H.E. MITLER
C
C CODING BY D. BELLER, FALL 86
C
C THIS ROUTINE CALC'S THE CVMFR OF VENT IV WHICH IS IN AN ENCLOSURE WITH
C A FIRE WHOSE FLAMES TOUCH THE CEILING. THE VENT IS "FAR" FROM THE
C PLUME AXIS OF THE FIRE WHOSE FLAMES TOUCH THE CEILING. TWO EXPRESSIONS
C ARE USED TO EVALUATE THE CVMFR DEPENDING ON HOW MUCH OF THE CEILING
C JET RISES THRU' THE VENT: EITHER PARTIALLY OR ENTIRELY.
C
C GOOD FOR ONE ROOM ONLY!
C
C PRESSURE IN THIS ROUTINE IS NOT IN UNITS OF M OF AIR!!!
C PRESSURE UNITS ARE NEWTONS/M**2
C
C OUTPUT IS: CVF2 = CVMFR
C
C INPUT IS:
C     G     = ACCELERATION OF GRAVITY
c     ZPR   = ROOM PRESSURE (AT THE FLOOR)
C     ZHR   =  "   HEIGHT
C     RHO   = UPPER LAYER DENSITY
C     RHOA  = AMBIENT        "
C     RHOD  = LOWER LAYER    "
C     ZHL   = UPPER LAYER DEPTH
C     TEO   = ENERGY RELEASE RATE OF OBJECT LRGST
C     TEPR = RADIENT ENERGY LOST BY THE FLAME OF OBJECT LRGST
```

```
C     IV    = VENT IN QUESTION
C
C PARAMETERS FROM COMMON:
C     RSUBA = DEFINED IN CVMF01
C     DATOVC = DISTANCE FROM PLUME AXIS TO VENT CENTER
C     H     = PLUME SOURCE-TO-CEILING DISTANCE
C     ZKAZZ = AMBIENT TEMP
C     VMAZZ =    "    DENSITY
C     CH    = VENT FLOW COEF
C     ZBVZH,ZLVZH = HORZ VENT DIMENSIONS
C     LRGST = NUMBER OF OBJECT W/ HIGHEST HEAT RELEASE RATE
C
C LOCAL PARAMETERS:
C     QSTR  = NONDIMENSIONAL HEAT RELEASE RATE
C     HCRCTR,OCRCTR,TCRCTR = CORRECTION FACTORS FOR HT LAYR EFFECTS
C     ZHJZZ = CEILING JET THICKNESS
C     ZHJZU = DISTANCE CEILING JET RISES THRU THE VENT
C     XLTLA = ACCELERATION OF GASES THRU THE EILING VENT
C     BIGD = PRESSURE DIFFERENCE ACROSS THE CEILING VENT
C     INITC3 = INITIALIZATION SWITCH
C     VMJZZ = CEILING JET DENSITY
C     ROH = RADIAL DISTANCE TO VENT CENTER / H
C     USUBC,UCWGL = VENT VELOCITY
C     A,AA = CONVENIENCE PARAMETERS
C     XLSBVP = VENT LENGTH (ZBVZH) PRIME
C     XLTLR = RHO /RHOA
C     XLTLX = 1 + (XLTLR * RSUBA**2)
C     PCNVRN = PRESSURE CONVERSION FACTOR:M OF AIR TO N/M**2
C
            IMPLICIT REAL*8 (A-H,O-Z)
C
            INCLUDE 'BD:CVMFR.CMN'
            INCLUDE 'BD:ECCHTX.CMN'
            INCLUDE 'BD:ROOM.CMN'
            INCLUDE 'BD:HVNTEB.CMN'
            INCLUDE 'BD:CONTRL.CMN'       !@#
```

```
C
      DATA ZHJZUP, INITC3 / 10*0.0,0 /
      DATA PCNVRN / 11.5433 /
C
C CALC CEILING JET THICKNESS ONCE
C
      IF(INITC3 .NE. 0) GO TO 10
      ZHJZZ 0.124 * ZHR
      INITC3 = INITC3 + 1
10    CONTINUE
C
C CALC RAD DISTANCE/HEIGHT, CEILING JET TEMP AND THEN
C CEILING JET DENSITY
C
      IF(H .LE. 0.)WRITE(5,*)' H(CVB201)= ',H   !@#
      ROH = DATOVC(LRGST,IV) / H
C
C CALC QSTAR FOR OBJECT LRGST (I.E., OBJECT ONE)
      QSTR(LRGST) = QSTAR(TEPR, TEO, H)
C CALC HOT LAYER CORRECTION FACTORS
      IF(LFLG .EQ. 1) THEN
            HZ = H - ZHL
            CALL CFCTRS(ZKAZZ,ZKL,OSTR(LRGST),HZ,H,ZHL,
      1                 HCRCTR,OCRCTR,TCRCTR)
      ELSE
            HCRCTR = 1.
            QCRCTR = 1.
            TCRCTR = 1.
      END IF
      CALL TMPA01(ROH,ZKAZZ,ZKLZJ)
C LIMIT CEILING JET TEMP TO A MAX
      IF (ZKLZJ .GT. 1300.) ZKLZJ = 1300.
C     IF (ZTZZZ .EQ. 308.)WRITE(5,*)' CVB201 JET TEMP ',ZKLZJ     !@#
C
      VMJZZ = VMAZZ * ZKAZZ / ZKLZJ
C     IF(ZTZZZ .EQ. 308.)WRITE(5,*)' JET DENSITY = ',VMJZZ        !@#
```

```
C
C CALC PRESSURE DIFFERENCE ACROSS THE VENT
C
      BIGD = (ZPR * PCNVRN) + G * (RHOA - RHOD) * (ZHR + ZHJ2UP(IV))
      1       + (G * ZHL) * (RHOA - RHO) + (G * ZHJZZ) * (RHO - VMJZZ)
C
C CALC GAS ACCELERATION
C
      XLTLA = BIGD / (RHO * (ZHL * ZHJZZ) + (VMJ22 * ZHJZZ) +
      1       RHOA * (ZHL / 2.0))
C     IF(ZTZZZ .EQ. 308.)WRITE(5,*)' LITTLE A = ',XLTLA     !@#
C
C CALC VENT VELOCITY AND THEN THE DISTANCE CEILING JET RISES IN THE VENT
C
      IF(ZTZZZ .EQ. 308.)WRITE(5,*)' EN REL RATE =',TEO           !@#
      USUBC = 0.365 * UF(TEO)
      IF(ZTZZZ .EQ. 308.) WRITE(5,*)' USUBC = ',USUBC !@#
C
      A = ZLVZH(IV) / USUBC
      AA = A * A
      ZHJZU(IV) = (XLTLA / 2.) * AA
C
C COMPARE CEILING JET THICKNESS AND DISTANCE IT RISES THRU' THE VENT.
C THEN CALC APPROPRIATE CVMFR
C
      IF(ZHJZU(IV) .LE. ZHJZZ) THEN
            CVFB2A = (XLTLA * VMJZZ VAREA(IV) * ZLVZH(IV))
      1                (2. * USUBC)
            CVF2 = CVFB2A
            RETURN
      ELSE
            UCWGL DSQRT(((USUBC * USUBC) + (2. * (CH * CH) * BIGD))
      1           VMJZZ)
            XLSBVP = ZLVZH(IV) - (UCWGL* DSORT((2. * ZHJZZ / XLTLA))
C     IF (ZTZZZ .EQ. 306.)WRITE(5,*)' LSUBVP = ',XLSBVP     !@#
            XLTLR = RHO / RHOA
```

```
            XLTLX = 1. + (XLTLR * (RSUBA * RSUBA))
C     IF(ZTZZZ .EQ. 306.)WRITE(5,*)' LTLCHI = ',XLTLX       !@#
C
            CVFB2B = (ZBVZH(IV) * VMJZZ * UCWGL * ZHJ2Z) +
     1              (CH * ZBVZH(IV) * XLSBVP * RHOA
     2              DSQRT(2. * G * ZHL * XLTLR * (1. - XLTLR) / XLTLX))
            CVF2 = CVFB2B
            RETURN
      END IF
      RETURN
C
      END
```

```
C ******************************************************************************
C
      SUBROUTINE CVMF01(G,TMU,TMD,TEPR,TEO,TMO,RHOD,RHO,RHOA,NOO,ZRF,
     1                  ZHR,ZHL,ZTZZ,ZKAZZ,ZKLZ,ZPR,PI,MAXV,KKV,
     2                  CVMDOT)
C
C ******************************************************************************
C
C CALLED BY VENT
C
C EQUATIONS BY H.E. MITLER
C
C CODED BY D. BELLER
C
C THIS ROUTINE IS INTENDED TO BE AN IMPROVED VERSION OF HFLOW. IT IS
C ESSENTIALLY A CONTROLLING ROUTINE WHICH DIRECTS THE CALCULATION FLOW
C REGARDING CEILING VENT MASS FLOW RATES.
C
C GOOD FOR ONE ROOM CONTAINING UP TO FIVE OBJECTS, ONLY!
C
C OUTPUT IS: CVMDOT = CEILING VENT MASS FLOW RATE: CVMFR
C
C INPUT IS:
C     G     = ACCELERATION OF GRAVITY
C     TMU   = "UPPER" VENT MASS FLOW RATES
C     TMD   = "LOWER"  "    "     "    "
C     TEPR  = RADIENT ENERGY LOST BY THE FLAMES
C     TEO   = CHANGE IN ENERGY OF THE OBJECTS
C     TMO   =   "     "  MASS  "   "     "
C     RHOD  = LOWER LAYER DENSITY
C     RHO   = UPPER   "      "
C     RHOA  = AMBIENT DENSITY
C     NOO   = NUMBER OF OBJECTS
C     ZRF   = BURNING RADIUS OF OBJECTS
C     ZHR   = ROOM HEIGHT
C     ZHL   = UPPER LAYER DEPTH
```

```
C     ZTZZ  = TIME
C     ZKAZ  = AMBIENT TEMPERATURE
C     ZKLZ  = UPPER LAYER TEMP
C     ZPR   = PRESSURE AT FLOOR
C     Pi    = 3.14159…
C     MAXV  = NUMBER OF VENTS
C     KKV   = VENT INDEX
C
C LOCAL PARAMETERS ARE:
C     ZHI   = FLOOR-TO-INTERFACE DISTANCE ZHR - ZHL
C     ZHFZZ = HESKESTAD FLAME HEIGHT
C     NDXOBJ = OBJ INDEX: 0 = OBJECT'S FLAMES DON'T TOUCH CEILING
C                         1 =    "     FLAMES TOUCH CEILING
C     NDXRM = ROOM INDEX: 0 = NO OBJ'S FLAMES DON'T TOUCH CEILING
C                         1 = AT LEAST 1 OBJ'S FLAMES TOUCH CEILING
C     DOORMD = SUM OF HOT GAS FLOWS OUT DOORS/WINDOWS
C     PYMDOT = SUM OF OBJECT PYROLYSIS RATES
C     VAREA = VENT AREAS
C     ASUBI = TOTAL AREA OF OPEN DOORS/WINDOWS
C     ASUBV = CEILING VENTS
C     RSUBA = (CH * ASUBV) (CD ASUBI)
C     VBETA = (DOORMD - PYMDOT) (CD * ASUBI)
C     INITC4 = INITIALIZATION SWITCH
C     IFLCNT = COUNTER TRACKING NUMBER OF OBJECTS WHOSE FLAMES
C           TOUCH THE CEILING: IF = 0, THEN NONE DO; OTHERWISE
C           THIS EQUALS THE NUMBER THAT DO
C
C PARAMETERS FROM COMMON:
C     H     = PLUME SOURCE-TO-CEILING DISTANCE
C     ZBVZ*,ZLVZ* = VENT DIMENSIONS
C     ZHOZZ = OBJECT HEIGHT
C     IOPEN = FLAG FOR VENTS: 0 = OPEN
C                             1 = CLOSED TO OPEN ON TIME CONVNT
C                             2 = CLOSED TO OPEN ON TEMP CONVNT
C     CONVNT = VENT OPENING CONTROL: TIME OR TEMP
C     IHVNT = HORZ (CLNG OR FLR V'S) VENT FLAG: 0 = NO, 1 = YES
```

```
C     ICLVNT = CEILING VENT FLAG: 0 = NO, 1 = YES
C     ISTAT = OBJECT STATUS: 5 = FLAMING
C     CD,CH = VENT FLOW COEFFICIENTS: DOORS,CV'S
C
      IMPLICIT REAL*8 (A-H,O-Z)
C
      INCLUDE 'BD:CVMFR.CMN'
      INCLUDE 'BD:HVNTEB.CMN'
      INCLUDE 'BD:CVENT.CMN'
      INCLUDE 'BD:OBJECT.CMN'
      INCLUDE 'BD:ECCHTX.CMN'
      INCLUDE 'BD:CONTRL.CMN' !@#
C
      DIMENSION TMU(10),TMD(10)
      DIMENSION TMO(5),TEPR(5),TEO(S),ZRF(5)
C
      DATA NDXRM,NDXOBJ / 6*0 /
      DATA INITC4 / 0 /
C
      NOBJ = NOO
      IV = KKV
      XXV = MAXV
C
C CALL PLUME SOURCE-TO-CEILING DISTANCE OF OBJECT ONE ONLY!!!
C
      IF (INITC4 .NE. 0) GO TO 3
      INITC4 = INITC4 + 1
C
      H = ZHR - ZHOZZ(1)
C     IF(IT.EQ.1)WRITE(5,*)' ZHR= ',ZHR,' ZHOZZ(1)= ',ZHOZZ(1)
C     IF(IT.EQ.1)WRITE(5,*)' IN CVMFO1 H= ',H   !@#
C
3     CONTINUE
C
C CALC VENT AREAS FOR THIS TIME STEP
```

```
      CALL VENTA(MAXV)
C
C CALC TOTAL PYROLYSIS RATE
C
      PYMDOT = 0.0
      DO 10 10 = 1, NOBJ
            IF (ISTAT(IO) .NE. 5) GO TO 10
            PYMDOT = DABS(TMO(IO)) + PYMDOT
10    CONTINUE
C
C CALC TOTAL GAS FLOW OUT DOORS/WINDOWS
C
      DOORMD = 0.0
      DO 30 J I, MAXV
            IF(IHVNT(J) .EQ. 1) GO TO 30
            IF(TMU(J) .LE. 0.0) GO TO 30
            IF(IOPEN(J) .EQ. 0) THEN
                  GO TO 20
            END IF
            IF (IOPEN(J) .EQ. 1) THEN
                  IF(ZTZZ .GE. CONVNT(J)) GO TO 20
                  GO TO 30
            ELSE
                  IF(ZKLZ .GE. CONVNT(J)) GO TO 20
                  GO TO 30
            END IF
20          CONTINUE
            DOORMD = DOORMD + TMU(J)
30    CONTINUE
C
C CALC RSUBA AND VBETA
C
      DENOM = CD * ASUBI
      IF (DENOM .EQ. 0.)DENOM = CD
C
      RSUBA = (CH * ASUBV) / DENOM
```

```
      VBETA = (DOORMD - PYMDOT) / DENOM
C
C CALC FLAME HEIGHT AND COMPARE W/ ZHR - OBJ HEIGHT = H TO SET
C NDXRM AND NDXOBJ
C
      DO 40 10 = 1, NOBJ
            IF (ISTAT(IO) .EQ. 5) THEN
C CALC HESKESTAD FLAME HEIGHT, BUT FIRST CONVERT TO KW
                  QCDOT = DABS(TEO(IO) / 1000.)
                  ZHFZZ(IO) = 0.23 * (QCDOT**0.4) -
      1                                  (1.02 (2. * ZRF(IO)))
                  IF(ZHFZZ(I0) .LT. O.O)ZHFZZ(IO) = ZHFZZP(IO)
                  IF(ZHFZZ(IO) .GE. H) THEN
                        NDXRM = 1
                        NDXOBJ(IO) = 1
                  ELSE
C DETERMINE NUMBER OF OBJECTS WHOSE FLAMES DO NOT TOUCH THE CEILING:
C NDXRM = 0 WHEN IFLCNT = 0
                        NDXOBJ(IO) = 0
                        IFLCNT = 0
                        DO 50 JO = 1, NOBJ
                              IFLCNT = IFLCNT + NDXOBJ(JO)
50                            IF ((NOBJ - IFLCNT) .EQ. NOBJ) NDXRM = 0
                  END IF
            END IF
40    CONTINUE
C
C CALL CVMFR ROUTINE ACCORDING TO NDXRM
C
      ZHI = ZHR - ZHL
C     IF(IT.EQ.1)WRITE(5,*)' NDXRM= 1,NDXRM     !@#
      IF(NDXRM .EQ. 0) THEN
            CALL CVA001(G,RHO,RHOA,RHOD,ZHL,ZHI,CH,IV,CVMFR)
C     IF(IT.EQ.1)WRITE(5,*)' CVMFR(CVAOO1)= ',CVMFR   !@#
            CVMDOT = CVMFR
            RETURN
```

```
      ELSE
            CALL CVB001(TEPR,TEO,G,RHO,RHOD,RHOA,ZHL,ZKLZ,ZHI,ZPR,ZHR,
      1           ZKA,IV,PI,NOO,MXV,CVMFR)
C     IF(IT.EQ.1)WRITE(5,*)' CVMFR(CVB001)= ',CVMFR   !@#
            CVMDOT = CVMFR
            RETURN
      END IF
      RETURN
      END
```

```
C ***************************************************************************
C
      FUNCTION UF(QDOT)
C
C ***************************************************************************
C
C CALLED BY CVB101 AND CVB201
C
C EQUATION BY H.E. MITLER
C
C CODING BY D. BELLER, FALL86
C
C THIS FUNCTION CALCS THE VELOCITY COMPONENT ATTRIBUTABLE TO THE FLAMES
C OF A FIRE BENEATH A CEILING VENT
C
C INPUT IS: ODOT = ENERGY RELEASE RATE OF OBJECT BENEATH THE VENT (W)
C
      IMPLICIT REAL*8 (A-H,O-Z)
C
C CONVERT ODOT TO KILOWATTS
C
      QDOTKW = DABS(QDOT) / 1000.
C
      UF = 0.824 * (QDOTKW**0.2)
C
      RETURN
      END
```

```
C
C
      FUNCTION UV(G,HH,HHDD,DNSTY,DNSTYA,DNSTYD,RA,VS)
C
C
C
C CALLED BY CVA001 AND CVB101
C
C EQUATION BY H.E. MITLER
C
C CODED BY D. BELLER, FALL S6
C
C THIS FUNCTION CALCS THE VENTED GAS VELOCITY FOR CEILING VENTS OF
C ENCLOSURES WITH SMALL FIRES AND FOR CEILING VENTS NEAR THE AXIS OF
C LARGE FIRES.
C
C INPUT IS:
C     G     = ACCELERATION OF GRAVITY
C     HE    = UPPER LAYER DEPTH
C     HHDD  = FLOOR-TO-LAYER INTERFACE
C     DNSTY = UPPER LAYER DENSITY
C     DNSTYD = LOWER  "      "
C     DNSTYA = AMBIENT       "
C     RA    = RSUBA AS DEFINED IN ROUTINE CVMFO1
C     VB    = VBETA "     "     "    "      "
C
C LOCAL PARAMETERS ARE:
C     A,B,C,D = CONVENIENCE PARAMETERS
C
            IMPLICIT REAL*8 (A-H,O-Z)
C
            A =(2. * G) / DNSTY
            B = HE * (DNSTYA - DNSTY)
            C = HHDD * (DNSTYA - DNSTYD)
            D = DNSTY * DNSTYA * (RA * RA)
```

```
      UV = (DSORT(A * (B + C) * ((DNSTYA * DNSTYA) + D)) -
     9     (VB * RA)) / (DNSTYA + (DNSTY * (RA * RA)))
C
      RETURN
      END
```